Double-layered Wound Dressing Based on Electrospun Antimicrobial Polymer

By

Nicole Whiting

Thesis presented in partial fulfilment of the requirements for the

degree of Master of Science (Polymer Science)

at

Stellenbosch University

Supervisor: Prof. Bert Klumperman

University of Stellenbosch

Department of Chemistry and Polymer Science

Faculty of Science

March 2017

Declaration

By submitting this thesis electronically, I declare that the entirety of the work contained therein is my own original work, that I am the sole author thereof (unless to the extent explicitly stated otherwise), that reproduction and publication by Stellenbosch University will not infringe any third party rights and that I have not previously in its entirety or in part submitted it for obtaining any qualification.

Nicole Whiting March 2017

To my parents and loved ones

Abstract

The design and production of novel wound dressings that address resistance of microorganisms to antimicrobial agents, has attracted considerable attention. The ability to produce polymers with specific characteristics for specific applications offers a wide variety of options for application in the biomedical field, especially polymers that exhibit antimicrobial behaviour.

This thesis is thus committed to the design, synthesis and characterisation of a bi-layered wound dressing, as well as antimicrobial evaluation of the final product. The bi-layered wound dressing consists of a component that maintains a favourable moist wound environment and a second component that addresses microbial infection. For the component that maintains the favourable moist wound environment two hydrogels will be created and electrospun. For this study the hydrogels were chosen to be sodium alginate, a hydrogel already in use for wound dressings, as well as a hydrogel from poly(styrene-*alt*-maleic anhydride) (SMA). For the antimicrobial component, quaternary ammonium salts were synthesised, as these are known to have antimicrobial properties. SMA is a biocompatible and commercially available copolymer that can easily undergo chemical modification through the highly reactive maleic anhydride residues and therefore is an attractive polymer for the production of hydrogels and antimicrobial polymers. SMA was synthesised by conventional free radical chemistry, followed by modification to yield a hydrogel as well as modification of SMA to yield two quaternary ammonium salts, exhibiting antimicrobial activity.

SMA was electrospun and treated with a heat-activated crosslinking agent, namely diethylene glycol, to yield a nanofibrous hydrogel. A second nanofibrous hydrogel was also created from a natural polymer, namely sodium alginate. SMA was also treated with 3-(*N*,*N*-dimethylamino)propyl-1-amine (DMAPA), a compound with both a primary and tertiary amine, to yield poly(styrene maleimide) (SMI). SMI was then treated with two alkyl halides (1-bromooctane and 1-bromododecane) to yield quaternary ammonium compounds (qSMI) that shows antimicrobial activity. The quarternised SMI is then also electrospun to yield an antimicrobial nanofibrous layer and heat treated to render the fibres insoluble in water and organic solvents. The bi-layered wound dressing is produced by electrospinning one layer on top of the other in the case of the SMA hydrogel, followed by heat treatment to render the fibres insoluble. In the case of the alginate hydrogel, qSMI is electrospun and heat treated, followed by electrospinning of alginate on top of the qSMI layer.

The individual electrospun fibre mats as well as the bi-layered system are subjected to antimicrobial evaluation by means of confocal fluorescence microscopy as well as zone inhibition on agar plates. The organisms used for the antimicrobial evaluation were *Staphylococcus aureus*, a Gram-positive bacterium, and *Pseudomonas aeruginosa*, a Gram-negative bacterium. Confocal imaging and zone inhibition revealed that qSMI containing the C12 aliphatic side chain showed a greater antimicrobial activity towards *S. aureus* as compared to C8. In the case of *P. aeruginosa* it was not clear which of the C8 or C12 containing qSMI fibres showed greater antimicrobial activity, however confocal imaging and zone inhibition revealed that both showed antimicrobial activity towards *P. aeruginosa*.

Opsomming

Die ontwerp en vervaardiging van oorspronklike wondbedekkings wat die weerstand van mikro-organismes tot antimikrobiese middele aanspreek geniet aansienlike navorsingsaandag. Die vermoë om polimere met spesifieke eienskappe vir spesifieke toepassings te vervaardig bied `n wye verskeidenheid opsies vir aanwending in die biomediese veld, veral vir polimere wat antimikrobiese eienskappe het.

Hierdie tesis is gerig op die ontwerp, sintese en karakterisering van `n dubbellaag wondbedekking en die ondersoek van die antimikrobiese eienskappe van die eindproduk. Die dubbellaag wondbeddekking bestaan uit `n komponent wat `n gunstige vogtige wondomgewing handhaaf en `n tweede komponent wat mikrobiese infeksie aanspreek. Vir hierdie studie is twee jel matrikse gekies om die gunstige vogtige wondomgewing te handhaaf, naamlik natrium alginaat, `n jel matriks wat reeds as wondbedekking gebruik word, en poli(stireen-*alt*-malaïene anhidried) (SMA) as die tweede jel matriks. SMA is `n biologies-versoenbare kommersieël beskikbare kopolimeer wat maklik chemiese modifikasie ondergaan deur sy hoogs reaktiewe maleïene anhidried groepe en is dus `n aantreklike polimeer vir die vervaardiging van jel matrikse en antimikrobiese polimere. SMA is deur konvensionele vrye radikaal chemie gesintetiseer, gevolg deur wysiging om `n jel matriks te vervaardig, sowel as wysiging van SMA om `n kwaternêre ammonium sout wat antimikrobiese aktiwiteit toon, te vervaardig.

SMA vesels is voorberei en behandel met `n hitte geaktiveerde bindingsagent, naamlik di-etileenglikol, om `n nano-veselagtige jel matriks te vorm. `n Tweede nano-veselagtige jel matriks is uit `n natuurlike polimeer, naamlik natrium alginaat, vervaardig. SMA is ook met 3-(*N*,*N*-dimetielamino)propiel-1-amien (DMAPA), `n molekule met beide `n primêre en tersiêre amien, behandel om poli(stireen maleïmied) (SMI) te vervaardig. SMI is gevolglik met twee alkielhaliede (1-bromo-oktaan en 1-bromododekaan) behandel om kwaternêre ammonium molekules (qSMI) wat antimikrobiese aktiwiteit toon, te vervaardig. Vesels is dan ook uit die qSMI vervaardig om `n nano-veselagtige laag te maak wat dan met hitte behandel is om die vesels onoplosbaar te maak in water en ander organiese oplosmiddels. Die dubbellaag wondbedekking word vervaardig deur een vesellaag op die ander te spin in die geval van die SMA jel matriks, gevolg deur hitte behandeling om die vesels onoplosbaar te maak. In die geval van die natrium alginaat jel matriks is die qSMI laag eerste vervaardig, met hitte behandel, gevolg deur vesel vervaardiging van die alginaat bo-op die qSMI-laag.

Die onderskeie veselagtige matte en die dubbellaag sisteem is dan aan antimikrobiese evaluering blootgestel deur middel van konfokale fluoressensie mikroskopie, sowel as sone inhibisie op agar plate. Die organismes wat ondersoek is, is *Staphylococcus aureus*, `n Gram-positiewe bakterium, en *Pseudomonas aeruginosa*, `n Gram-negatiewe bakterium. Konfokale besigtiging en sone inhibisie het aangedui dat qSMI met die C12 alifatiese syketting `n groter antimikrobiese effek op *S. aureus* het in vergelyking met die C8 syketting. Vir *P. aeruginosa* was dit nie duidelik watter van die C8 of C12 syketting qSMI vesels beter antimikrobiese aktiwiteit getoon word nie, maar konfokale besigtiging en sone inhibisie het wel getoon dat beide antimikrobiese aktiwiteit teen *P. aeruginosa* besit.

Table of Contents

List of Figures

List of Schemes

List of Tables

List of Equations

Abbreviations

Abbreviation	Meaning
DMAEMA	2-(*N*,*N*-dimethylamino)ethyl methacrylate
AIBN	2,2'- Azo-bis (isobutyronitrile)
DMAPA	3-(*N*,*N*- dimethylamino)-1- propylamine
AIDS	Acquired Immunodeficiency Syndrome
ATRP	Atom Transfer Radical Polymerisation
ATR- FTIR	Attenuated Total Reflectance Fourier Transform Infrared
DNA	Deoxyribonucleic Acid
Acetone-d_6	Deuterated Acetone
DMSO-d_6	Deuterated Dimethyl sulfoxide
DEG	Diethylene Glycol
h	Hour
LB	Luria-Bertani
MAnh	Maleic Anhydride
MRSA	Methicilin-resistant *Staphylococcus aureus*
MEK	Methyl Ethyl Ketone
min	Minutes
DMF	*N*,*N*- Dimethylformamide
DMAc	*N*,*N*-dimethylacetamide
N_2	Nitrogen
NNRTI	Nonnucleoside Reverse Transcriptase Inhibitors
NMR	Nuclear Magnetic Resonance
NRTI	Nucleoside Reverse Transcriptase Inhibitors
OD	Optical Density
ppm	Parts Per Million
PBS	Phosphate Buffered Saline
SMI-qC_{12}	Poly (styrene- [(*N*-dodecyl)-*N'*, *N'*-dimethyl-3-propyl maileimide]) copolymer
SMI-qC_8	Poly (styrene- [(*N*-octyl)-*N'*, *N'*-dimethyl-3-propyl maileimide]) copolymer
SMI	Poly (styrene-[*N*-3-(*N'*, *N'*- dimethylamino) propyl maleimide]) copolymer
SMA	Poly (styrene-*alt*-maleic anhydride) copolymer
PEO	Poly(ethylene oxide)
PVP	Poly(*N*-vinylpyrrolidone)
^{1}H-NMR	Proton Nuclear Magnetic Resonance Spectroscopy
qSMI	Quaternised SMI
RNA	Ribonucleic Acid
SEM	Scanning Electron Microscopy
SEC	Size Exclusion Chromatography
NaOH	Sodium Hydroxide
St	Styrene
SSI	Surgical Site Infection

THF	Tetrahydrofuran
TEA	Triethylamine
USA	United States of America

Symbols

Symbols	Meaning
d	Distance polymer jet needs to travel
Đ	Dispersity
E	Electric field strength
kV	Kilovolts
M	Molar concentration
md	Dry Mass
M_n	Number average molecular weight
mw	Wet Mass
R	Absorption Ratio
V	Voltage difference between electrodes

Chapter 1: Prologue

1.1. Introduction

The emergence of microbes with resistance to antimicrobial agents is of great concern to all of us. It is especially problematic in a medical setting as surgical site infections (SSIs) has been reported as the most common healthcare-associated infection for 2010 in the USA and therefore demands the prevention of microbial infection in this setting. Research into novel antimicrobial dressings and antimicrobial polymeric materials has notably increased in order to provide alternatives to antimicrobial agents that already show resistance. This may include the incorporation of known antimicrobial agents or the inclusion of naturally occurring antimicrobial substances into fibrous or other polymeric materials. Common agents already incorporated into wound dressings include silver, iodine and antiseptic agents like polyhexanide. Some disadvantages are however associated with current approaches, like diminishing effectiveness over time seen in continuous release of low molecular weight antibacterial agents from antibacterial matrices. Some antimicrobial agents may also be cytotoxic to human cells.

The ability of scientists to create polymers for specific applications thus allows for the design of wound dressings that may address more than one area of interest. Historically wound management consisted of a natural or synthetic wound dressing like gauze or cotton wool. These maintained a dry wound environment that was found to be less favourable for wound healing due to wounds dressed with gauze or cotton wool being more susceptible to microbial invasion, painful upon removal as these dressings often adhere to the wound and may thus cause trauma to the wound bed when removed. Today modern wound dressings are designed to maintain a more favourable moist wound environment that minimises microbial infection, increases healing rates, reduces pain and ease of overall healthcare.

Electrospinning is a simple and cost-effective technique that can be used to produce polymer nanofibres or composites. Nanofibres produced by electrospinning have a high surface to volume ratio, an advantage that enables the use of nanofibres in biomedical applications like wound dressings. Post-spinning modification of nanofibres is also possible, further increasing the attraction of the electrospinning technique for use in wound dressing applications.

1.2. The aim and objectives of this work

The aim of this study was to develop a bi-layered wound dressing, utilising the single needle electrospinning technique, which contains a non-leaching permanently antimicrobial polymer layer as well as a second hydrogel layer that will be able to maintain a moist wound environment.

The main objectives of the study can be summarised as follows:

a) To synthesise the SMA copolymer by conventional free radical chemistry.
b) To modify SMA by reaction with a primary amine to yield the SMI precursor and subsequent reaction with a alkylhalide to yield a quaternary ammonium (qSMI).
c) To create and electrospin a hydrogel as well as the qSMI to yield the bi-layered system.
d) Microbial evaluation of the qSMI antimicrobial polymers as well as the bi-layered system.

1.3. Thesis layout

Chapter 1 - Prologue

Chapter 1 gives a brief insight into the need for development of wound dressings that are able to address microbial invasion as well as maintain favourable conditions for wound healing. The aim and objectives of the study are also presented.

Chapter 2 - Literature review

A comprehensive literature review of the types of wound dressings that is available for medical use, as well as antimicrobial agents is presented.

Chapter 3 - Synthesis, characterisation and modification of SMA

Chapter 3 describes the methods employed to synthesise SMA. Subsequent modification and characterisation of the relevant polymers are also discussed.

Chapter 4 - Electrospinning and hydrogel formation

Chapter 4 is dedicated to the formation of two hydrogels in fibrous form, one from SMA and one from sodium alginate. The electrospinning of qSMI and the production of the bi-layered system is also presented.

Chapter 5 - Antimicrobial evaluation

Chapter 5 presents the evaluation of the antimicrobial activity of all electrospun fibres using confocal fluorescence imaging as well as the zone inhibition method.

Chapter 6 - Epilogue

Chapter 6 describes conclusions and recommendations for future work.

Chapter 2: Literature review

2.1. Introduction

We all remember scraping a knee playing in a tree or falling with your bicycle as a child and your mother dressing your wound with some gauze or cotton wool and a bandage. During 2010 in the USA it has been reported that an estimated 16 million operative procedures were performed in acute care hospitals[1], of which surgical site infections (SSIs) were the most common healthcare-associated infections, accounting for 31% of all healthcare-associated infections among hospitalised patients[1]. Though most of these are minor skin infections, more serious cases of SSIs are associated with a mortality rate of 3%, and 75% of SSI-associated deaths are directly attributable to the SSI. This is due to microbes becoming more and more resistant to antibiotics, like the commonly known Methicillin-resistant *Staphylococcus aureus* or MRSA. Surgical site infections also occur in 2-5% of all surgical procedures and in 5-12% of caesarean deliveries[2].

According to Statistics South Africa[3], the number of deaths due to complications from surgery (which includes secondary infections) was reported to be between 4-8% of all deaths in 2013. Figure 2.1 shows a graphical representation of the causes of deaths in South Africa during 2013.

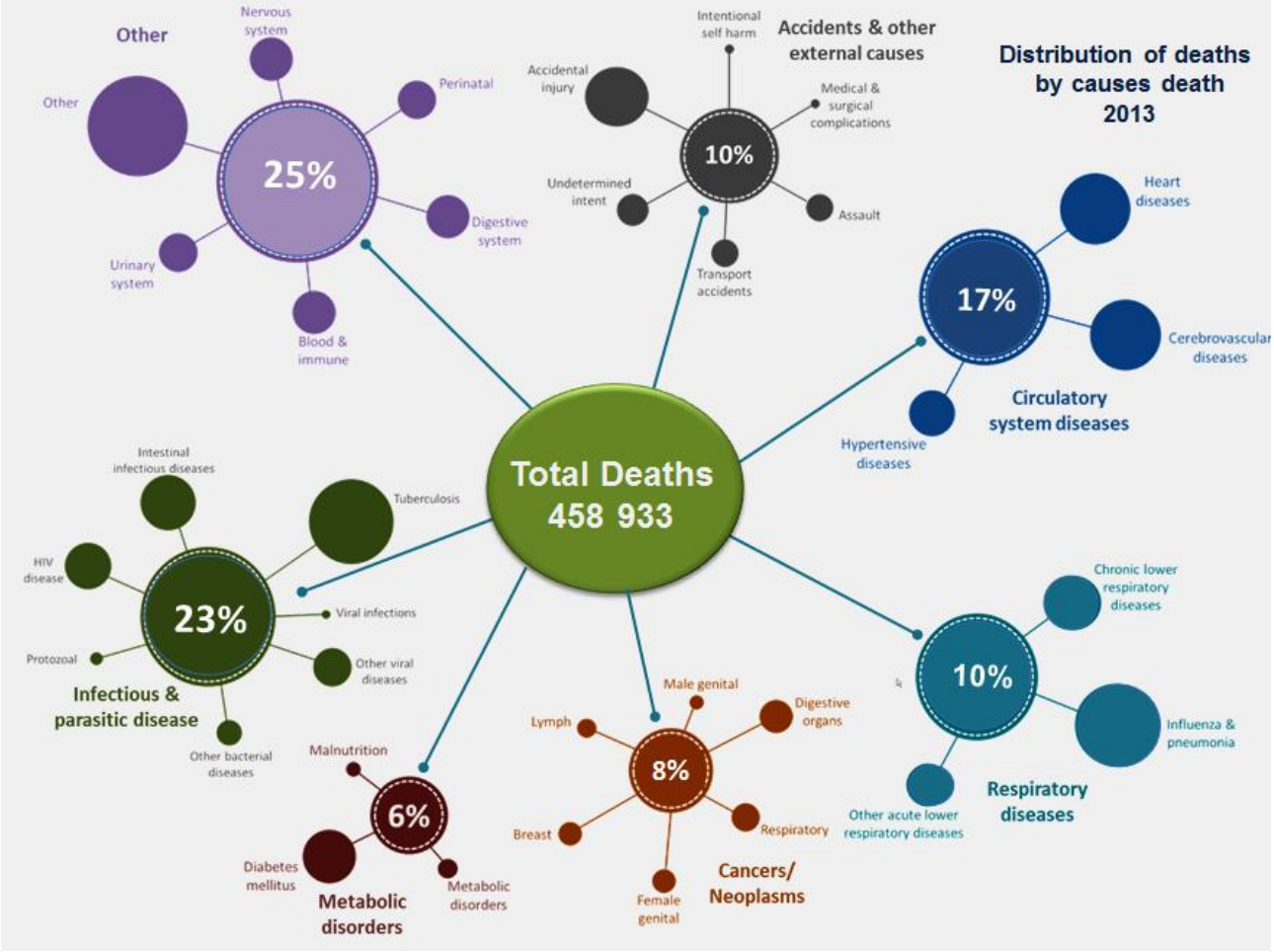

Figure 2.1: Graphical representation of total deaths and causes of death in South Africa in the year 2013[3]

Post-operative care is thus important in terms of early detection of post-operative complications, hygiene and overall ease of wound care.

2.2. Wound dressings

Wound dressings form an integral part of the global medical and pharmaceutical industries. Historically, wound management was associated with the use of natural or synthetic materials such as gauze, cotton wool and lint as wound dressings. The primary function of these wound dressings was to keep the wound dry, allowing evaporation of the wound exudate and preventing pathogenic bacteria to enter the wound[4]. The use of gauze, cotton wool and lint as wound dressings are not of common practice today as some disadvantages are associated with their use, including[5]:

- the inability of these materials to prevent microbial invasion
- leads to trauma at the time of removal as these dressings adhere to the surface of the wound
- it has low absorption ability leading to the accumulation of wound exudates which then become favourable environments for microbial attack
- they do not allow proper permeability of gases
- are only useful for minor wounds
- and provide a dry wound environment.

More recently it has been found that a moist wound environment has been associated with increased healing rates, improved cosmesis, reduced pain, less infection and ease of overall health care[6].

A wound dressing or combination of dressings is considered ideal if it ensures optimal healing by meeting the following requirements[5, 7-10]:

a) able to maintain a moist wound environment around the wound, preventing wound drying
b) removes excess wound exudate, preventing saturation of the dressing to its outer surface
c) permits thermal insulation
d) controls pH
e) allows gaseous diffusion
f) conforms to the wound surface
g) ability to facilitate debridement if so required
h) minimizes scar formation
i) provides mechanical protection
j) is impermeable to extraneous bacteria and does not contaminate the wound with foreign particles
k) is non-fibre shedding
l) non-toxic and non-allergenic
m) is non- adherent, comfortable and conforming as well as easy to remove
n) minimises pain from the wound
o) is cost-effective and cosmetically acceptable
p) stimulates growth factors
q) biocompatible

Classification of wound dressing can be done in numerous ways; depending on the function of the dressing on the wound (for example debridement, antibacterial, occlusive, absorbent, adherence)[11], the type of material used for the production of the dressing (for example hydrocolloid, alginate, collagen)[12] as well as the physical form of the dressing (ointment, film, foam, gel). Table 2.1 summarises the types of wound dressings and gives a description of each as from the paper by Zahedi *et al*[13].

Table 2.1: Wound dressing types and their description from Zahedi *et al*[13]

Dressing type	Product name	Description
Passive	Gauze	Gauze is manufactured as bandages, sponges, tubular bandages, and stocking. Guaze may adhere to the wounds and disrupt the wound bed when removed, causing trauma to the wound bed. Therefore, these are suitable for minor wounds.
	Tulle	Greasy gauzes consisting of Tulle gauze and petroleum jelly does not stick to the wound surface and is suitable for a flat and shallow wound with minimal to moderate exudates.
Interactive	Semi- permeable films	Semi-permeable, polyurethane membrane which has acrylic adhesive. These are transparent allowing easy wound check and are also suitable for shallow wounds with low exudate.
	Semi- permeable foams	Soft, open cell, hydrophobic, polyurethane foam sheet 6-8 mm thick. These dressings are designed to absorb large amounts of exudate and are therefore not suitable for low exuding wounds as they will cause dryness and scabbing.
	Amorphous hydrogels	Amorphous gels are not crosslinked. They are used for necrotic or sloughy wound beds to rehydrate and remove dead tissue. They are not used for moderate to heavily exuding wounds.
Bioactive	Hydrocolloids	These are semi-permeable polyurethane films in the form of solid wafers; contain hydroactive particles such as sodium carboxymethyl cellulose that swells with exudate or forms a gel. Depending on the hydrocolloid dressing chosen they can be used in wounds with light to heavy exudate, sloughing, granulating wounds.
	Alginates	Calcium alginate which consists of an absorbent fibrous fleece with sodium and calcium salts of alginic acid (ratio 80:20). They are good for exuding wounds and helps in debridement of sloughing wounds. They are not used on low exuding wounds as this will cause dryness and scabbing. These dressing should be changes daily.
	Collagens	Collagens are dressings which come in pads, gels or particles and promote deposition of newly formed collagen in wound bed. They absorb exudate and provide a moist wound environment.
	Hydrofibres	Hydrofibres are soft nonwoven pad or ribbon dressings made from sodium carboxymethyl cellulose fibres. They absorb exudates and provide a moist environment in a deep wound that needs packing.

The more modern wound dressings have been developed with their essential characteristic being to retain and create a moist wound environment. These are mainly classified according to the materials used to produce the dressings and a few of the more common dressings are discussed below.

2.2.1. Hydrocolloid dressings

Hydrocolloid dressings are bioactive wound dressings that describe a number of wound management products obtained from a combination of colloidal materials (gel forming agents like carboxymethyl cellulose, gelatin and pectin) in combination with materials such as elastomers and adhesives. These are bonded to a carrier of semi-permeable film or foam sheet in order to produce a flat, occlusive, adhesive dressing that will form a gel on the wound surface and promote moist wound healing[10]. Typically, they occur in the form of thin films, sheets or composite dressings in combination with materials such as

alginate[4]. Hydrocolloid dressings are among the most commonly used dressings in practice[4] due to their ability to adhere to both moist and dry wound sites. When intact, these dressings are impermeable to water vapour, but when the wound exudate has been absorbed it forms a soft coherent gel[10] that covers the wound and promotes moist wound healing[4, 10]. This is especially useful for the rehydration of dry necrotic eschar[10]making these dressings suitable for light to moderately exuding wounds.

Generally the occlusive nature of the hydrocolloid dressings is beneficial however, it can be disadvantageous to use in the case of infected wounds that require a certain amount of oxygen for rapid healing[4]. The use of hydrocolloid dressings in infected wounds is thus questionable due to the hypoxic and excessively moist wound environment that may cause autolysis of necrotic tissue, increasing the risk of infection[8]. The fibrous nature of these dressings may also act in a disadvantageous manner as some fibres can be deposited into the wound. The fibres will have to be removed during dressing change which can be painful[4]. Hydrocolloid dressings may also produce a distinctive odour in some cases due to the product breakdown[7]. This may also be mistaken for infection[10].

2.2.2. Alginate dressings

Alginate or alginic acid is one of the most extensively researched and applied natural polymers in tissue engineering and drug delivery systems. Its abundance in nature as a structural component found in a family of marine brown algae (Phaeophyceae) [8, 10] and as capsular polysaccharides in some soil bacteria makes it an attractive polymer for research. This polysaccharide is comprised of mannuronic (M-residues) and guluronic (G-residues) acid residues which are covalently linked in alternating or random sequences[8] as seen in Figure 2.2.

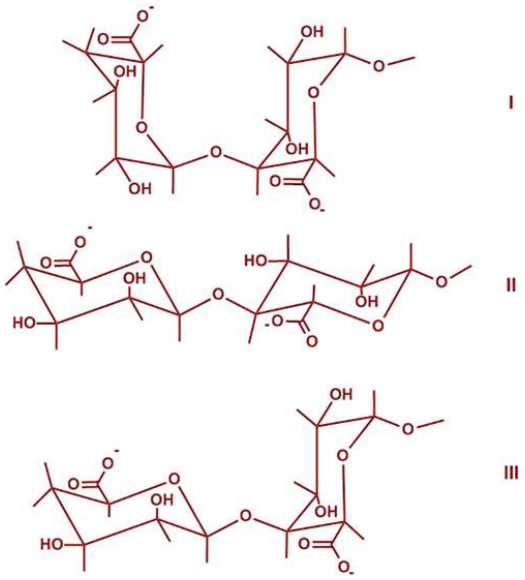

Figure 2.2: Chemical structure of the repeating units found in alginates: (I) L-guluronic acid (G); (II) D-mannuronic acid (M); (III) alternating L-guluronic and D-mannuronic acids (GM)[14]

Alginates have the ability to form reversible hydrogels: the product of ionic interactions of alginate with divalent cations like Ca^{2+}, Mg^{2+}, Ba^{2+} and Mn^{2+}. Ionic interaction causes crosslinking of the G-residues of adjacent alginate chains[8]. The major reason for alginate's appeal as a wound dressing is due to the ability of crosslinked alginate to form gels when in contact with wound exudates[4]. Alginate also has high absorption ability through hydrophilic gel formation, thereby limiting wound secretions and minimising microbial contamination[4]. Depending on the amount of mannuronate or guluronic acid present in the alginate dressing different types of gels may form upon hydration: dressings rich in mannuronate will form soft flexible gels,

whilst dressings rich in guluronic acid will form a firmer gel. The relative amount of mannurinate and guluronic acid also influences the amount of exudate that will be absorbed[10] by the wound dressing.

Alginate partially dissolves on contact with the wound fluid, forming a hydrophilic gel. This is a result from the exchange of sodium ions present in the wound fluid with the calcium ions present in the dressing[10]. The exchange creates a slow degrading gel that maintains an optimum wound environment in terms of moisture content and healing temperature[4]. The gel formed from alginate dressings high in mannuronic acid can be removed simply by washing with a saline solution, whilst those dressings high in guluronic acid tend to keep their structural integrity and may be removed in one piece[10].

Alginate dressings are useful in the case of moderate to heavily exuding wounds, but should be used with a secondary dressing, like a hydrocolloid or foam, to prevent drying out of the dressing[7]. One of the other advantages in the use of alginate dressings is that they can be used in infected or non-infected wounds, the latter requiring a non-occlusive secondary dressing[7]. The use of alginate dressings is however limited to exuding wounds as they require moisture (obtained from the wound exudate) in order to function effectively. As the primary function of alginate dressings is to maintain a moist wound environment by forming a gel from the wound exudate, the use of alginate dressings on dry wounds or wounds covered with hard necrotic tissue could dehydrate the wound and inevitably delay healing[4]. The dressing may also adhere to the wound bed, causing damage to the healing tissue and pain upon removal[10].

2.2.3. Hydrogel dressings

Hydrogel dressings are insoluble, swellable hydrophilic materials made from natural[5] as well as synthetic polymers[4], mostly used for the maintenance of highly moist wound environments[8] as they possess excellent tissue compatibility and have most of the characteristics needed in an ideal wound dressing[5]. The ability of these crosslinked materials to entrap large amounts of water (70-90 %)[4] and maintain a moist wound environment required for an ideal dressing[5] heeds their attraction as wound dressings. Crosslinking, whether it is covalent or non-covalent, allows the control of swelling capacity, maintenance of the conformational structure and the reversible swelling or shrinking in pH specific aqueous environments and ionic strength values[8]. Hydrogel dressings are able to transmit moisture vapour and oxygen, however bacterial and fluid permeability is dependent on the secondary dressing used in combination with the hydrogel[10]. Hydrogels can be applied as an amorphous gel or in the form of an elastic, solid sheet or film[4] and are useful in the case of wounds with minimal to moderate exudate[7].

The transparent nature of hydrogels allows one to monitor the wound without removal of the dressing. The flexible nature of hydrogel sheet dressings allows one to cut them to better fit around a wound[4]. The sheet dressings also do not require a secondary dressing as the transmission of water vapour through the dressing is controlled by a semi-permeable polymer film backing[4]. The poor mechanical properties of hydrogel dressings after swelling constitute their main disadvantage[5]. This makes them difficult to handle and has been noted to affect patient compliance[4]. The poor mechanical properties of hydrogels can be overcome by incorporating composite materials like where a textile material is coated with a polymer solution[5]. Another drawback is the accumulation of fluids around the wound which can lead to maceration of the skin and bacterial proliferation, producing a foul smell in infected wounds[4] and leads to healing problems[8].

2.2.4. Foam dressings

Developed as an alternative to hydrocolloid dressings[8], foam dressings consists of either a porous polyurethane foam or film[4, 7, 10] or can also be a silicone based foam[4, 7, 10]. They are highly absorbent due to their porous nature and thus capable of handling high volumes of wound exudate[7], like in the case of moderate to heavily exuding wounds[4, 8, 10]. The capacity of wound exudate that can be absorbed by foam

dressings is dependent on the polymeric material used for the foam, foam thickness[4, 8], pore size[4] and texture[4]. Polyurethane foams consist of up to three layers, including a hydrophilic surface that is in contact with the wound, a hydrophobic backing[10] and an occlusive polymeric layer to prevent bacterial contamination and loss of fluids[4]. Silicone foams on the other hand, consist of a silicone elastomer prepared from two liquids mixed together to form an expanding foam to fit the wound shape and form a soft, open-cell foam dressing[10].

Foam dressings are semipermeable[7], provide thermal insulation[7], highly absorbent[8], coushioning[8], protective[8], facilitate uniform dispersion of the exudate throughout the absorbent layer[10], prevent leakage[10] and can conform to body surfaces[8]. Silicone foams have the added advantage of protecting the surrounding wound area from further damage[10] as the silicone foam fits into the wound shape. The absorbent and protective nature of foam dressings also allow for them to be left on the wound for up to seven days[8].

Foam dressings are not suitable for use in the case of dry epithelising wounds or scars as their ability to achieve an optimum moist wound healing environment is reliant on wound exudates[4].

2.2.5. Antimicrobial dressings

The application of antibiotics and antibacterial agents helps with prevention or combat of infections, like in the case of diabetic foot ulcers, surgical and accident wounds as infection rate may be high due to reduced immune resistance response as a result from extreme trauma[4]. In cases like these the use of a dressing that contains and maintains a continuous release of antimicrobial agents at the wound site may be beneficial. They thus promote healing by providing continual antimicrobial action and also maintain a favourable moist wound environment[6].

Often systemic administration of antimicrobial agents result in toxic reactions such as cumulative cell and organ toxicity of aminoglycosides in the ears and kidneys[4] due to high antibiotic doses needed to achieve sufficient systemic efficiency. Delivering antibiotics directly to the infected area may therefore be more beneficial in order to avoid complications (like organ toxicity) due to systemic administration[4]. In essence, using antimicrobial dressings that can deliver antimicrobial agents directly to the wounds may provide better tissue compatibility, reduced occurrence of bacterial resistance and reduced interference with wound healing[4]. The risk of systemic toxicity may also be lowered as lower doses of antibiotics are applied within dressings. Additionally, localised antibiotic delivery may overcome ineffective systemic antibiotic therapy due to poor blood circulation at the extremities, like in the case of diabetic foot ulcers[4].

The main goal when using antimicrobial dressings should always be the provision of an optimum wound environment to speed up healing. When selecting a suitable antimicrobial agent, the following should be considered: specificity and efficacy of the agent, cytotoxicity to human cells, potential to select resistant strains and allerginicity[7]. The more common antimicrobial agents currently used in antimicrobial dressings include products containing iodine, silver and antiseptic agents like polyhexanide[7].

Iodine is clinically commonly used in one of two forms, as povidone-iodine (an iodophor) and cadexomer iodine. Povidone-iodine is formed by the complexation of iodine with poly(*N*-vinylpyrrolidone) (PVP), an iodophor produced as impregnated tulle[10]. Cadexomer iodine is also formed by the complexation of iodine with a polymeric cadexomer[10] starch vehicle to form a topical gel or paste[6]. When the wound exudate us absorbed by the cadexomer moiety, slow release of low concentrations of free iodine takes place, effectively reducing bacterial contamination in the wound and positively affects the healing process as compared to conventional treatments[6]. Caution should be taken if a patient has thyroid disease as systemic uptake of iodine is possible[10]. The thyroid function of patients should therefore be monitored when treated with iodine containing dressings[10].

Silver, in ionic or nanocrystalline form, has been used as an antimicrobial agent for many years, particularly in the treatment of burns in the form of silver sulfadiazine cream[10]. The incorporation of silver into semiocclusive dressings like foams, hydrocolloids, alginates and hydrofibers[6] has broadened its use in other types of wounds that are colonised or infected[10]. As these products come into contact with or absorb wound exudate they release silver cations into the wound[6].

2.3. Antimicrobial agents

Long before a proper understanding of the mode of action of antimicrobial agents, disinfectants and antiseptics were commonly used. This is due to the simple observation that the spoiling of meat and rotting of wood was curbed by certain substances. The term "antiseptic" was first used in 1750 to describe substances that prevent decay[15]. Eventually this idea would be applied to the treatment of wounds. It was not however until the nineteenth century that the use of antiseptics became general practice as a man named Lister would eventually bring about the use of antiseptics in surgical practice by 1870[15]. He would use a 2.5% solution of phenol for dressing wounds and a 5% solution of phenol to sterilise surgical equipment, also applying phenol vigorously during surgery. He would later use a phenol spray to produce a sterile environment for surgical operations to be carried out[15]. This was a great step forward for surgery as wounds would regularly become infected and a high mortality rate reigned. This antiseptic era in surgery gave rise to the aseptic era, where the focus now is to avoid bacterial contamination rather than killing bacteria. The infection of surgical wounds is still a constant risk and antiseptics are still used as a second line of defence.

2.3.1. Antifungal agents

During the past two decades resistance to antibacterial and antifungal agents has grown significantly. The gravity of antimicrobial resistance is great in terms of the implications it has on morbidity, mortality and health care costs. Considerable attention has thus been spent to have a detailed understanding of antimicrobial resistance mechanisms, improved methods to detect resistance, innovative antimicrobial treatment of infections caused by resistant organisms, as well as simple methods to prevent the increase and spread of resistance[16]. An understanding of antimicrobial resistance by all types of microbes are important, however antibiotic resistance in bacteria have enjoyed considerable research attention for several reasons: a) the bulk of community-acquired and nosocomial infections are as a result of bacterial infections; b) the large and ever increasing number of antibacterial classes offers a more diverse range of resistance mechanisms to study; and c) the ability to move bacterial resistance determinants into well-characterised bacterial strains facilitates the detailed study of molecular mechanisms of resistance in bacterial species[16].

For a period of almost 40 years, the only drug available for the treatment of serious fungal infections was amphotericin B[16, 17]. Unfortunately, this drug was known to cause significant nephrotoxicity[16]. It wasn't until the late 1980s and early 1990s that other drugs were approved, namely the imidazoles and triazoles. The imidazoles and triazoles introduced a safe and effective treatment of local and systemic fungal infections[16]. The triazoles, particularly fluconazole, have been used extensively for the treatment of fungal infections due to their high safety profile. Unfortunately, due to the extensive use of fluconazole reports of antifungal resistance are also increasing, thus necessitating to the need for a better understanding of resistance to antifungal agents. Resistance to antifungal agents has been less focussed on than antibacterial resistance for several reasons, the most important probably due to fungal diseases not being recognised as important pathogens until relatively recently. The annual death rate due to fungal infections for the period 1950-1970 was relatively steady, however, since 1970 the death rate increased[16] as changes in medical practices also came about. Changes in medical practices that contributed to the increase in death rate as a result of fungal infections include widespread use of immunosuppressant therapies, frequently using broad-spectrum antibacterial agents unselectively, common use of indwelling intravenous devices and the advent of chronic immunosuppressive viral infections like acquired immunodeficiency syndrome (AIDS)[16]. The increasing

severity and frequency of fungal infections is of great concern, particularly in patients with impaired immunity.

Many fungal infections are caused by opportunistic pathogens that are already present in or on the body or acquired from the environment and can be classified into a) allergic reactions to fungal proteins, b) toxic reactions to toxins present in certain fungi and c) infections or mycoses[18]. Aside from patients suffering from AIDS, invasive fungal infections and dermatomycoses are common in individuals that are more susceptible to infection such as neonates, cancer patients receiving chemotherapy, organ transplant patients and burn patients. The risk of fungal infection increases with treatment with corticosteroids and antibiotics, diabetes, lesions of the epidermis and dermis, malnutrition, neutropenia and surgery[18].

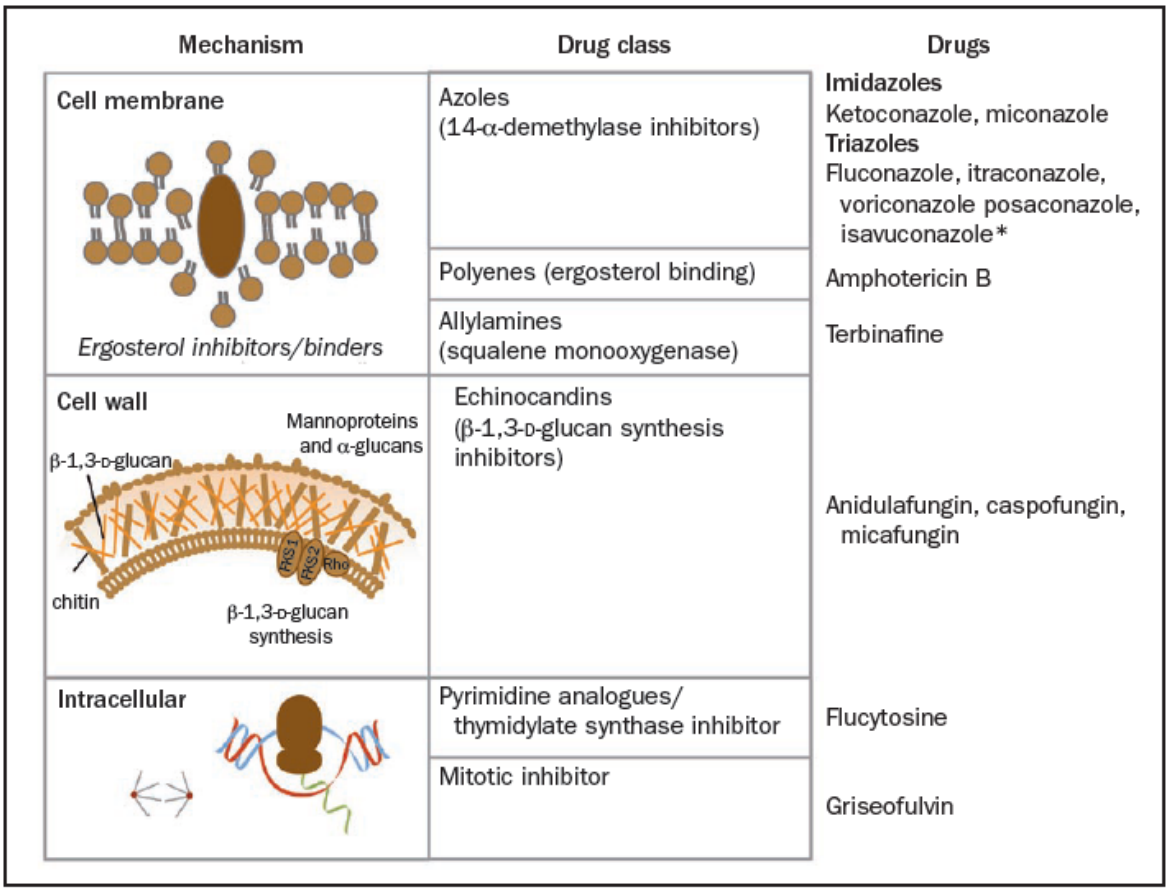

Figure 2.3: Targets for antifungal therapy[17]

The complex nature of fungal cells allow for multiple targets for antifungal therapy (Figure 2.3)[17]. One of these targets is fungal ergosterol synthesis inhibitors, like the azoles[17-19]. Ergosterol, the major component of the fungal cell membrane, is a bioregulator of membrane fluidity, asymmetry and integrity. It plays a hormone-like role in fungal cells, stimulating growth. Squalene epoxidase, an enzyme, together with squalene cyclase converts squalene to lanosterol. When lanesterol is inhibited it prevents the conversion of lanesterol to ergosterol.

Ergosterol disruptors like polyenes antibiotics form a complex with ergosterol to disrupt the fungal plasma membrane, resulting in increased membrane permeability[19], the leakage of the cytoplasmic contents like sodium, potassium and hydrogen ions[21], inevitably causing death of the fungal cell. Polyenes, like amphotericin B, are fungicidal in nature and have the broadest spectrum of antifungal activity of clinically available agents. Amphotericin B has been the "golden standard" for fungal therapy since its introduction in

the 1950s[17, 19, 20]. This amphoteric polyene macrolide can form soluble salts in acidic as well as basic environments[20].

Another target for antifungal therapy is glucan synthesis inhibitors. The glucan polysaccharide plays an essential role in maintaining the physical properties of the cell wall. The blockage of glucan synthase ultimately causes lysis of fungal cells, as less glucose is incorporated into the glucan polymer[18].

Another important polysaccharide within the cell wall is chitin. Chitin plays an integral role in determining the shape of the cell, even though a small percentage of chitin is present in the fungal cell wall (less than 1%), covalently linked to glucan in the cell wall, but well separated from the glucan. This essential polymer is absent in humans and therefore chitin synthase is an attractive target in the discovery of new antifugal agents[18].

Another option for antifungal therapy is nucleic acid synthesis inhibitors, like flucytosine[19]. Initially developed as an anticancer drug, today it is used with Amphotericin B. It works as an antifungal agent by its conversion into 5-fluorouracil within the target cells which is incorporated into ribonucleic acid (RNA). This causes premature chain termination and further inhibits the synthesis of deoxyribonucleic acid (DNA) [18]. Sordadins, which are absent from mammalian cells and the electron transport chain, are selective inhibitors of fungal protein synthesis by blocking the function of fungal translation. Lastly, the inhibition of microtubules synthesis also serves as an antifungal target. Microtubules are polymers consisting of α- and β-tubulin dimers, forming a highly organised cellular skeleton in all eukaryotic cells[18]. A detailed classification of antifungal agents in use today is summarised in Table 2.2.

The known cytotoxicity of Amphotericin B has led to the development of more targeted topical fungal treatment[21]. Topical burn wound agents available as wound dressings include silver-coated dressings like silver sulfadiazine dressings, chlorhexidine acetate dressings and nystatin dressings[22]. Attempts into the development of Amphotericin B as a topical agent has also been investigated by Sanchez *et al*[21], where nanoparticle encapsulated Amphotericin B was incorporated into a silane-based hydrogel nanoparticle platform for controlled drug release. Their system showed significant reduction in metabolic activity of the fungal biofilm ranging from 80-95 % reduction in viability.

Conventional systemic or topical antifungal therapy in oral candidiasis often results in increased cytotoxicity. Cossu *et al*[23] has therefore investigated the production of starch stabilised Pickering emulsions as delivery vehicles for the controlled release of antifungal agents. They produced Pickering emulsions of thymol, a natural phenolic compound that shows antifungal activity, as well as Amphotericin B. Calcium alginate films containing starch Pickering emulsions of thymol or Amphotericin B were then produced. Both showed antifungal activity, with Amphotericin B requiring as little as 10 μg/mL for growth zone inhibition and thymol requiring 9000 μg/mL or higher for growth inhibition.

Study into electrospun mats containing cyclodextrin polymers to act as wound dressings that show tunable release of incorporated fluconazole that form inclusion complexes was conducted by Costoya *et al*[24]. Before treatment of the cyclodextrin mats with hexamethyldisiloxane, burst release of fluconazole took place within 30 min. Hexamethyldisiloxane coated fibers on the other hand released roughly 50 % of the fluconazole drug in the first 2 hours and showed a more sustained drug release up to 24 hours. Both the coated and uncoated mats showed activity against *Candida albicans*.

A comparative study of a silver-coated dressing containing silver sulfadiazine, a chlorhexidine acetate dressing and a nystatin dressing was done on rat burn wounds. Acar *et al*[22] found that nystatin dressings were the most effective against C. albicans-contaminated burn wounds and in the prevention of further infection into muscle tissue or systemic infection. The silver-coated dressing is a choice of treatment for fungal burn wound infection with an added antibacterial effect and it has the added benefit of requiring less frequent dressing changes.

Table 2.2: Classification of antifungal agents[18]

Class	Agent	Mechanism of action	Indication	Toxicity
First generation triazole	Fluconazole	A	Active against *Candida* spp.	Gastrointestinal intolerance
	Itraconazole	A	Anti- *Aspergillu*s activity	Fluid retention, left ventricular dysfunction, gastrointestinal intolerance
	Ketoconazole	A	Candidiasis, coccidioidomycosis, blastomycosis, histoplasmosis, paracoccidioidomycosis and cutaneous dermatophytic infections	Gastrointestinal, hepatitis
Second generation triazole	Voriconazole	A	Invasive aspergillosis	Elevation of transaminases and visual disturbances, rash and gastrointestinal symptoms
	Posoconazole	A	Prophylxis of invasive aspergillosis and *Candida* infection	Nausea, vomiting, headache, abdominal pain and diarrhea
	Ravuconazole	A	Active against a wide range of fungi, including *Candida* spp., *C. neoformans* and other yeast species	Gastrointestinal
Echinocardin	Caspofungin	B	Potent activity against *Aspergillus* spp., *Oesophageal candidiasis*	Headache, fever, nausea, rash, phlebitis
	Micafungin	B	Treatment of *Oesophageal candidiasis*	Nausea, vomiting, headache, diarrhea, phlebitis and leukopenia
	Anidulafungin	B	Active against *Candida* spp., *Oesophageal candidiasis*	Hypotension, vomiting, constipation, nausea, fever, diarrhea, hypokalemia and elevated hepatic enzymes
Antibiotics	Nystatin	C	Superficial (mucosal) candida infections of the oropharynx, oesophagus and intestinal tract	Nephrotoxicity
	Amphotericin B	C	Broad- spectrum of antifungal activity	Nephrotoxicity, infusional toxicity, low blood potassium
	Griseofulvin	D	For the treatment of cutaneous mycoses	Liver toxicity
Nucleoside analogues	Flucytosine	E	Active against *Candida* and *Aspergillus* spp.	Bone marrow toxicity
Allylamine	Terbinafine	F	Used for fungal nail infections	Mild rash, nausea, loss of taste

A = interact with cytochrome p-450; inhibit C-14 demethylation of lanosterol, thereby causing ergosterol depletion and accumulation of aberrant sterols in the membrane, B = the $\Delta^7 - \Delta^8$ isomerase and the Δ^{14} reductase inhibition, C = glucan synthase inhibitors, D = interact with ergosterol, thereby disrupting the cytoplasmic membrane, E = inhibits thymidylate synthase and therby DNA synthesis, F = inhibit squalene epoxidase

2.3.2. Antibacterial agents

The battle between humans and microbes that cause infection and disease has been a continual one throughout history and one still not won today. The availability of penicillin in the 1940s meant that major strides into the development of antibacterial drugs were made. Unfortunately, the common use of antibiotics led to bacteria developing more and more sophisticated resistance mechanisms.

Antibacterial agents act by interfering with either the structure of bacteria or metabolic pathways in the bacteria[25]. Antimicrobial agents used for treatment of bacterial infections can be categorised according to the primary mechanism of action. Four major mechanisms (seen in Figure 2.4) have been identified to date, including 1) interference with the synthesis of the cell wall[25-27] 2) inhibition of protein synthesis[25-27], 3) interference with nucleic acid synthesis[25-27] and 4) inhibition of a metabolic pathway[25].

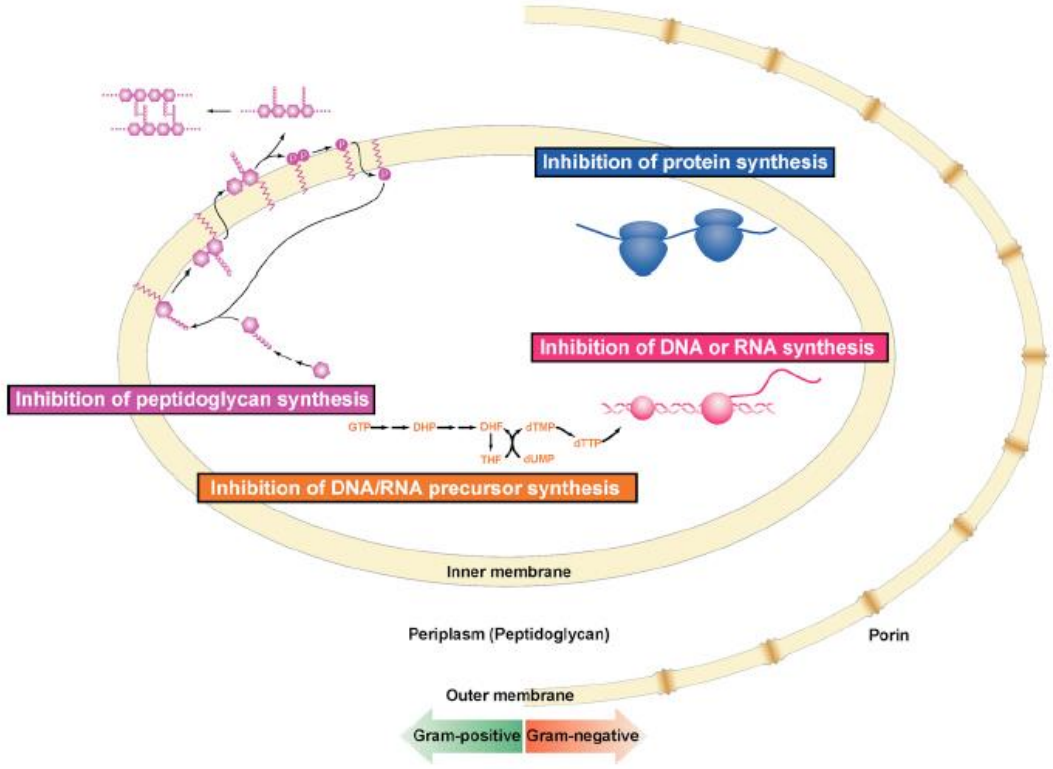

Figure 2.4: Major targets for antibacterial action[28]

The bacterial cell wall is unique in that it contains peptidoglycan[25-29] as structural component. It thus follows that this would be a sensitive site for selective attack[25-29]. Antibacterial drugs of the first class, namely those that inhibit bacterial cell wall synthesis include β-lactams, like the penicillins[25-29], cephalosporins[25-29], carbapenems[26] and monobactams[26], as well as glycopeptides[26] like vancomycin[25-29] and teicoplanin[25-28]. The β-lactams exhibit interference by interfering with the necessary enzymes for the synthesis of the peptidoglycan layer. The glycopeptides vancomycin and teicoplanin bind to the terminal D-alanine residues of the forming peptidoglycan chain, in so preventing the necessary crosslinking for a stable cell wall.

The purpose of proteins within the bacterial cell is several fold, including maintaining the shape and structural integrity of the cell or acting as enzymes that control the metabolic activity of cells[29]. Those drugs that inhibit protein synthesis include macrolides[25-28], aminoglycosides[25-29], tetracyclines[25-29], chloramphenicol[25-29], streptogramins and oxazolidinones. Bacterial and eukaryotic ribosomes are structurally different, therefore allowing antibacterial agents to take advantage of these structural differences in order to selectively inhibit bacterial growth. The different antibacterial agents that inhibit protein synthesis can either

bind to the 30S subunit of the ribosome (including macrolides, aminoglycosides and tetracyclines) or may bind to the 50S subunit of the ribosome (like chloramphenicol).

The genetic information of all living cells is contained by the chromosomes and the area in a chromosome that contains a particular character is known as a gene[29]. Genes control the structure of all enzymes and the rates at which they are produced. Interfering with the production of essential enzymes will thus have detrimental effects for the bacterial cell. Interference with nucleic acid synthesis is achieved by the fluoroquinolones[25-28] that disrupts DNA synthesis and causes fatal breaks in the double-strand DNA during replication. Other drugs utilising the mechanism of nucleic acid inhibition include the sulphonamides and trimethoprim which ultimately inhibit DNA synthesis by blocking the folic acid synthesis pathway.

Another possible mechanism that may be included is the disruption of a specific membrane structure[27]; however this mechanism of action is not well defined. It is suspected that polymyxins have allows greater permeability of the bacterial membrane and causes the bacterial contents to leak from the membrane[27]. Depolarisation of the membrane and eventual cell death may also take place, like in the case of the cyclic lipopeptide daptomycin that inserts its lipid tail into the bacterial cell membrane[23].

The inclusion of antibacterial agents in wound dressings is of common practice today, with numerous options already available[4] and studies into novel antibacterial dressings also on the rise. Topical antiseptic agents can also be used with more traditional wound dressings, like gauze, to prepare an antibacterial wound dressing. Common topical agents used include iodine-releasing agents, chlorine-releasing agents, hydrogen peroxide, chlorhexidine, silver-releasing agents and acetic acid[4]. Numerous wound dressings containing antibiotics are also available for use in infected wounds. The antibiotics already incorporated into wound dressings include minocycline, vancomycin, streptomycin, neomycin, chlorhexidine digluconate and ciprofloxacin[4].

Novel developments of antibacterial dressings have already brought interesting options to light. The work done by Namazi *et al*[30] focussed on the design of a carboxymethyl cellulose hydrogel that incorporated mesoporous silica MCM-41 as a nano drug carrier. They then loaded the nanocomposite hydrogel system with tetracycline and methylene blue as antibacterial agents and found that the antibacterial agents showed an extended release profile due to the incorporation of the silica particles.

Previous study has shown bacterial nanocellulose to be a possible suitable biomaterial that fulfils all requirements of an ideal modern wound dressing, the only drawback being its inactivity in terms of antimicrobial behaviour. Moritz *et al*[31] has therefore functionalised bacterial nanocellulose with an antiseptic drug, namely octenidine. Their system showed a biphasic release profile of octenidine, with rapid release in the first 8 hours, followed by a more sustained release up to 96 hours. Their wound dressing system also showed antimicrobial activity against *Staphylococcus aureus*. Their product also proved to be stable, releasable and biologically active over a period of 6 months, presenting a wound dressing that is ready to use. Other investigations include a sponge-like nano Ag/ZnO-loaded chitosan composite dressing with high porosity and swelling that also showed enhanced blood clotting and antibacterial activity[32]. Singh *et al*[33] created hydrogel films based on acacia gum and carbopol meant for the slow release of the antibiotic drug gentamicin. In another study, He *et al*[34] produced fibrous membranes of polyvinylidene fluoride loaded with enrofloxacin that also displayed a rapid release of the antibacterial drug within the first 12 hours, followed by sustained release for 3 days. Their product showed good antibacterial properties. The possibilities for novel wound dressings containing antibacterial agents are thus very diverse.

2.3.3. Antiviral agents

The virus, a simplistic living organism, consists of genetic material contained in a protein capsule known as a capsomer[35]. Although viruses lack a metabolic system, viruses are formidable adversaries in the human body

for several reasons. First of all, they have the ability to use their host's cell processes for metabolism and replication[35]. They remain latent for years, with no antiviral drug currently available that can eliminate this viral latency[35]. Thirdly, their genetic material can change over time and this increases the risk of drug resistance[35]. Lastly, some viruses have the ability to penetrate into the central nervous system[35]. This is problematic as drugs and immune cells are often unable to reach these infections. Due to the parasitic nature of viruses, the use of a pharmaceutical agent that will kill or inhibit a virus is most likely to cause injury to the host cell.

Currently, the aim of antiviral agents is to interfere with some part of the viral reproductive cycle[35]. The viral replication process that leads to disease symptoms have been described in six steps, namely adsorption, penetration, uncoating, replication, maturation and new viruses[35]. A virus attaches itself to a host cell (absortion) and enters the host cell by the process of endocytosis (penetration). The virus enters the cell wall of the host cell through an opening formed for the virus to enter. The opening closes again and traps the virus inside the cell. Once inside the host cell, the virus can now start the uncoating process where the virus opens its capsule or protein coat to expose its genetic material, ready for protein synthesis. The synthesised proteins are then used as either capsomers or enzymes that catalyse viral multiplication. Viral DNA is incorporated into the host cell's chromosomes by an enzyme known as integrase. The host cell therefore produces new viral nucleic acid that is the template for protein synthesis. The viral protein is then hydrolysed into smaller subunits by a protease enzyme. During the maturation stage, capsomers and newly produced nucleic acids are assembled to yield a new virus. The final step is the release of the newly formed virus that ultimately leads to the destruction of the host cell. It is at this stage that disease symptoms occur[35].

Like mentioned before, antiviral agents interfere with some part of the reproductive cycle described above. Interference can be classified according to which stage of the replication cycle they affect[35]. They are a) uncoating inhibitors, b) nucleic acid synthesis inhibitors, c) nucleoside reverse transcriptase inhibitors, d) non-nucleoside reverse transcriptase inhibitors and e) protease inhibitors.

Uncoating inhibitors binds to a viral protein capsule and concentrate in lysosomes[35]. Lysosomes exist as separate particles that contain hydrolytic enzymes that can break down proteins and certain carbohydrates within their limiting membrane. An increase in concentration of the antiviral agent within the lysosomes increases the lysosomal pH and ultimately interferes with membrane fusion, inhibiting the uncoating process of the virus. Antiviral agents that adopt this mechanism are amantadine[35-37] and rimantadine[35-37] used in the treatment of influenza A.

Nucleic acid synthesis inhibitors interfere with the synthesis of viral DNA or RNA[35]. For most of these antiviral agents to become active, they have to undergo phosphorylation (a process where they are changed to phosphates) by viral kinases. Once phosphorylation of the drug occurs it cannot cross the viral cell membranes, causing it to accumulate at high concentrations within the infected cells. High concentrations of the phosphorylated drug inhibit DNA or RNA polymerases, terminate the DNA chain or suppress viral messenger RNA. Antiviral agents that inhibit viral activity according to this mechanism include: acyclovir used for the treatment of herpes virus[35-37], ganciclovir and foscarnet used for the treatment of cytomegalovirus retinitis[35, 36], and ribavirin used for the treatment of respiratory syncytial virus and Lassa fever[35-37].

Nucleoside reverse transcriptase inhibitors (NRTI) exhibit a similar mechanism of action to the nucleic acid synthesis inhibitors described above[35]. These antiviral agents are phosphorylated by cellular kinases, forming phosphates that can inhibit viral reverse transcriptase and terminators of the viral DNA chain. This classification of antiviral agent is currently approved for the use in HIV treatment as HIV infection includes a component of reverse transcriptase. Examples of some of the described drugs include didanosine, lamivudine, stuvadine, zalcitabine and zidovudine[35-37]. Lamivudine is also an appropriate drug to use for treatment of hepatitis B[35-37].

Nonnucleoside reverse transcriptase inhibitors (NNRTI) bind to HIV reverse transcriptase, disrupting the catalytic site to block viral reproduction[35]. These agents are less toxic than the NRTI as they do not inhibit human DNA polymerase. Unfortunately rapid drug resistance occurs and therefore they are administered in combination with other drugs. Examples of NNRTI are nevirapine and delavirdine[35-37].

Protease inhibitors inhibit proteolytic enzymes needed for the production of viruses in the cells[35]. Protease inhibitors, like saquinavir, ritonavir and indinavir act synergistically with reverse transcriptase inhibitors against HIV[35-37].

Wound dressings for antiviral applications are not as common as for antifungal or antibacterial applications. Silver sulfadiazine containing wound dressings have however shown some antiviral activity[38, 39].

2.3.4. Antiseptic agents

The use of antiseptic agents is a common occurrence in our everyday life-from antibacterial soaps to waterless hand sanitizers. This common use of antiseptics in everyday objects has cause for great concern as this helps along the increase of resistance of microorganisms.

Common antiseptic agents used include aldehydes (like formaldhyde and gluteraldehyde)[40]. Aldehydes may be occupationally hazardous, even at low concentrations[2]. Futhermore guanidines (like chlorhexidine, polyhexamethylene guanidine and polyhexamethylene biguanidine), benzalkonium compounds, ethylene oxide, triclosan, halogens (like sodium hypochlorite, tosylchloramide, iodophors and polyvinylpyrrolidone/ povidone and povidone-iodine) and phenolic compounds (like phenol and thymol/ methyl salicylate)[40] are also commonly used antiseptics.

Surgical site infections (SSI) are also common occurrence, with 2-5 % of all surgical procedures resulting in SSI and 5-12 % of caesarean deliveries resulting in SSI[2]. Caesarean delivery of babies is considered the most common surgical procedure among American women, accounting for 32.7 % of 3.9 million births in 2013[2]. Surgical site infection of course is costly and may impact mother-infant bonding, breastfeeding and cause extra stress for the new mother.

Considering the skin is a major source of pathogens that cause SSI, effective preoperative skin treatment with antiseptic agents may decrease SSI. In a study comparing a chlorhexidine-alcohol combination with an iodine-alcohol combination found that the chlorhexidine-alcohol significantly lowered the risk of SSI after caesarean delivery when used as preoperative skin treatment[2].

The regular use of antiseptics, like triclosan and triclocarban, in health care practices has also been identified as a cause for concern by the FDA. Research suggested that higher levels of absorption and systemic exposure of antiseptic agents than what was previously believed[41] takes place. In a study regarding 181 pregnant women, triclosan was found in the urine of all women and was found in about half of the tested cord blood samples, indicating systemic exposure to triclosan. Researchers also found butyl paraben, another type of antiseptic commonly used in health care, in urine and cord blood[41]. Interestingly, a follow-up study found that the presence of some antimicrobial agents in maternal urinary and cord blood were associated with birth outcomes like lower gestational age at birth and birth weight as well as length. The possible disruption to foetal development and hormone function by triclosan and other antimicrobial compounds, is thus concerning in terms of the long term effects of these agents in health care workers who are pregnant or breastfeeding as the effects of frequent use are unclear[41].

Waterless hand sanitizers usually contain isopropanol, ethanol or benzalkonium chloride as the active ingredient[41]. Studies have shown that high levels of skin absorption and systemic exposure of these agents takes place as waterless hand sanitizers are frequently used and not washed off (actually they are only effective when left on the skin). Medical personnel are required to use hand sanitizers before and after

contact with patients and always after removing examination gloves. They therefore use waterless hand sanitizers more often than prescribed and this may increase their exposure to potentially harmful ingredients[41]. As the use of hand sanitizers form an integral part in effective infection prevention, this could result in medical personnel applying a sanitizing product up to 100 times per day, which well exceeds the normal day to day use.

2.4. Antimicrobial polymeric materials

Microbial contamination is of great concern in numerous areas, including medical devices, healthcare products, food packaging, food storage and household sanitation[42]. Bacterial contamination which may lead to serious implant-associated infections[42] is of great concern in medical disciplines that utilise biomaterials, like for catheters and implants. Controlling microbial growth is thus one of the fundamental survival techniques for all higher species. A great variety of defence mechanisms against microbes have been developed in nature itself by plants, animals and even microbes. These mechanisms however often do not function efficiently in human society, meaning that microbial infections are high in the list of "killers". Resistant microbial strains further hinder treatment, as well as the number of antibiotic-immune patients increasing faster than the development of useable antibiotics[43].

Antimicrobial polymers as an alternative to existing biocides are of great importance. Although the working mechanism of a large number of structurally different polymers is not fully understood, some of them are known for their low potential of developing resistant microbial strains[43].

Microbial cells have the ability to attach to artificial surfaces in a moist environment and can thus survive and proliferate as artificial materials commonly lack a defence mechanism against microbial growth[42]. As the number of cells increases on the surface the cells start to form a biofilm of a polysaccharide matrix containing embedded cells[43]. These biofilms allow microbes to survive under harsh environmental conditions and make the cells up to 1000 times less susceptible to most antibiotics and biocides[43]. The toxins excreted from these biofilms make them pathogenic[43]. Antibiotic genes may also be spread within the biofilm, increasing the formation of multi-resistant bacterial strains[43]. Man-made materials can also be degraded by microbial biofilms, necessitating the control of microbial growth on surfaces.

The ideal antimicrobial polymer should[42]:

a) be easy and inexpensive to synthesise
b) be stable in long-term usage and storage at the temperature of its intended use
c) be insoluble in water for a water-disinfection application
d) not decompose to and/or emit toxic products
e) not be toxic or irritating to those handling it
f) have the possibility tobe regenerated upon loss of activity
g) be biocidal to a broad spectrum of pathogenic microorganisms in brief times of contact.

A possible way to address the problem of microbial surface contamination is to keep the environment sterile[42] by using disinfectants like hypochlorite, hydrogen peroxide and other reactive oxygen species, silver salts, quaternary ammonium compounds, alcohols or the commonly used triclosan[43, 44]. The problem with this method is that the sterile state does not last long and frequent use of disinfectants poses great environmental problems as the use of disinfectants have shown to support the formation of microbial resistance, e.g. MRSA which causes more deaths than HIV in the USA[43].

Another way to combat microbial surface contamination is to prepare antimicrobial surfaces that prevent growth of biofilms[43] as an alternative way to inhibit the spread of microbial infections. These surfaces can either repel microbes, meaning they cannot attach to the surface or they can kill microbes in the vicinity. To kill microbes in the vicinity the surfaces may be loaded with biocides like silver, antimicrobial ammonium

compounds, antibiotics, active chlorine or triclosan[43]. Although efficient, they eventually exhaust and the released biocides cause great environmental problems as microbial resistance may take place.

Alternatively surfaces that can produce biocides catalytically by means of an externally applied chemical, electrical or optical energy, is an interesting option[43]. Also the design of surfaces that kill microbes on contact is a possible alternative. These surfaces in principle do not release biocides or exhaust and can be realised by tethering antimicrobial polymers.

Literature reveals three general types of antimicrobial polymers: polymeric biocides, biocidal polymers and biocide-releasing polymers[42]. The general working of these are depicted below in Figure 2.5.

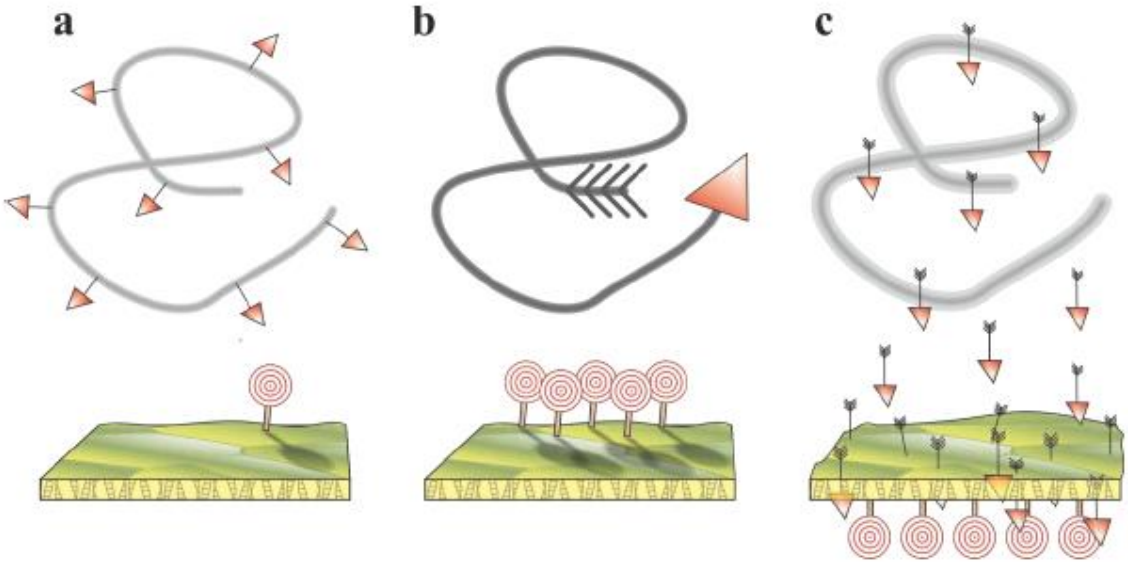

Figure 2.5: General working principles of antimicrobial polymers: (a) polymeric biocides; (b) biocidal polymers; (c) biocide-releasing polymers[42]

Polymeric biocides are based on the concept that the biocidal groups that are attached to the polymer act in a similar way as the analogous low molecular weight compounds; that means the repeating unit is a biocide[43]. Due to sterical hindrance caused by the polymeric backbone, one expects polymeric biocides to be less active than their low molecular weight counterpart. Polymeric biocides are thus polymers of bioactive repeating units, i.e. polymers of interconnected biocides which act similarly to the monomers. The insoluble nature of the majority of polymers in water means that the polymerisation of biocidal monomers often does not lead to the formation of active antimicrobial polymers or polymerisation of a biocide leads to inability to reach the target by the biocidal functional group.

In biocidal polymers the entire macromolecule embodies the working of the antimicrobial agent, not necessarily requiring antimicrobial repeating units. Since the surface of microbial cells generally carry a net negative charge[43, 44] due to their membrane proteins, polycations are attracted to the surface and if they have a proportionate amphiphillic character they have the ability to disrupt the outer membrane as well as the cytoplasmic membrane and can cause lysis of the bacterial cells[42]. To date this has been the established mode of action of polycationic antimicrobial polymers, like polycationic polymers containing quaternary ammonium and phosphonium, tertiary sulfonium and guanidinium functions[43].

Biocide-releasing macromolecules were first prepared by Vogl and Tirell who were able to polymerise salicylic acid that unfortunately did not result in polymers with antimicrobial properties. They were however able to demonstrate that the degradation of the polyester brought about the release of salicylic acid in a controlled fashion[43]. Biocide-releasing polymers do not actually act through the polymer itself, but instead

act as a carrier for biocides that can be transferred to the microbial cells for attack. These polymeric systems are usually the most active systems of these described, since they have the ability to release the carried biocides close to the cell in high local concentrations.

Antimicrobial surfaces can also be produced by attaching antimicrobial polymers to different surfaces[43] through multiple techniques including chemical grafting, layer-by-layer deposition and plasma polymerisation[43]. At first, elaborate techniques were employed to covalently attach antimicrobial polymers to surfaces, like glass. An example of this is surface-grafted poly-4-vinyl-N-hexylpyridinium followed by modification of a glass slide with aminosilane and acryloyl chloride. The acrylated slide was then copolymerised with 4-vinylpyridine and finally alkylated with hexylbromide. This procedure is rather elaborate, requiring many chemical steps and the use of organic solvents[43]. This technique may be useful for laboratory preparation, but will not be feasible for industrial application. Quaternary ammonium compounds have also been successfully attached to porous glass beads by using 3-chloropropyltrimethoxysilane as coupling agent[45]. The glass beads were covered with the alkoxysilane followed by quarternisation of the immobilised chloropropyl residues with various *N*,*N*-dimethylalkylamines with alkyl groups between C_2 and C_{18}. The antibacterial behaviour of the glass beads were determined by passing bacterial cell suspensions through a column packed with the surface treated glass beads. Unquaternised surfaces did not show much antibacterial behaviour, whilst the surface treated glass beads functionalised with alkyl groups greater than C_8 showed more substantial antibacterial activity as compared to the antibacterial behaviour of those with shorter alkyl groups.

Surface-attached non-releasing polymers could be made by the incorporation of polymeric additives for polyurethane and acrylate coatings that migrate to the surface of the coating during the preparation of the coating[43]. The first approach utilises soft blocks of 1,3-propylene oxide with alkylammonium groups as crosslinked soft segments, whilst the second approach uses macromonomers based on polyoxazolines with biocidal quaternary ammonium end groups, copolymerised with the acrylate monomers and crosslinking agents.

Another useful approach in the development of antimicrobial surfaces is utilising controlled radical polymerisation techniques to attach organic molecules capable of initiating polymerisation from the surface of the material. One example is the work done by Lee *et al*[46] where they prepared non-leaching antibacterial glass and paper surfaces by means of controlled radical polymerisation. The surface was modified by the polymerisation of the tertiary amine-containing monomer 2-(*N*,*N*-dimethylamino)ethyl methacrylate (DMAEMA) in a "grafting from" fashion by means of atom transfer radical polymerisation (ATRP). The antimicrobial character on the polymer-modified surfaces is then achieved by quarternisation of the amino groups of PDMAEMA brushes with an alkyl halide.

It also logically follows that one would try to polymerise a known antimicrobial agent that can be chemically modified into a derivative that may undergo polymerisation and retain its bioactive functional groups. Another possibility is the modification of the polymer backbone or its functional pendant groups (like hydroxyl, carboxyl or amino groups) by reaction with a complementary reactive antimicrobial agent. Benzalkonium chloride derivatives show a broad spectrum of antimicrobial activity. Styrene derivatives are ideal to create polycationic molecules that will retain the cationic character obtained from the quarternised group of the benzalkonium chloride derivatives. Another polymeric candidate is polymers containing biguanidines, like polyhexamethylene biguanidine, used as antimicrobial agent in contact lens disinfectant[47].

Many other antimicrobial polymers have been synthesised and evaluated for antimicrobial behaviour. Some of these include cationic polymers containing biguanide, phosphonium salts, quaternary pyridinium salts and quaternary ammonium salts as active functional groups[48].

2.5. Conclusions

The ever increasing development of microbial resistance against common antimicrobial agents in use today necessitates the development of alternatives to known antimicrobial drugs and techniques used in the treatment of patients as well as techniques utilised in medical practice for safe and sterile equipment, devices and medical procedures. Incorporating known antimicrobial materials in different forms, like the nanoparticle encapsulated Amphotericin B, is a rather interesting development into new or better wound dressings that address problems like the associated nephrotoxicity of Amphotericin B. Development of antimicrobial polymers also prove to be a widely applicable technique for the introduction of new antimicrobial agents as well as products stemming from the polymer. The advantage of developing antimicrobial polymers stems from the ability to tailor polymers for a specific end purpose and utilising them in different physical forms, like films, fibres, coatings and emulsions.

The ability to tailor polymers for a specific end purpose allows one to better obtain the conditions described for an ideal wound dressing. The discovery that moist wound environments improve healing also steers the development of modern wound dressings into the development of products like hydrogels. The necessary antimicrobial character needed to address infection may therefore be achieved by using an antimicrobial polymer or incorporating known antimicrobial agents into the favoured modern dressing (like a hydrogel).

2.6. References

1. Surgical Site Infection (SSI) Event http://www.cdc.gov/nhsn/PDFs/pscmanual/9pscssicurrent.pdf (accessed 5 December 2016)
2. Tuuli, M. G.; Liu, J.; Stout, M. J.; Martin, S.; Cahill, A. G.; Odibo, A. O.; Colditz, G. A.; Macones, G. A. *N. Engl. J. Med.* **2016**, *374*, 647–655.
3. Causes of Death 2013 http://www.statssa.gov.za/?page_id=737&id=3
4. Boateng, J.; Catanzano, O. *J. Pharm. Sci.* **2015**, *104*, 3653–3680.
5. Gupta, B.; Agarwal, R.; Alam, M. S. *Indian J. Fibre Text. Res.* **2010**, *35*, 174–187.
6. Ovington, L. G. *Clin. Dermatol.* **2007**, *25*, 33–38.
7. Vowden, K.; Vowden, P. *Surg.* **2014**, *32*, 462–467.
8. Moura, L. I. F.; Dias, A. M. A.; Carvalho, E.; de Sousa, H. C. *Acta Biomater.* **2013**, *9*, 7093–7114.
9. Abdelrahman, T.; Newton, H. *Surg.* **2011**, *29*, 491–495.
10. Jones, V.; Grey, J. E.; Harding, K. G.*British Med J.* **2006**, *332*, 777–780.
11. Sai K, P.; Babu, M. *Burns*, **2000**, *26*, 54–62.
12. Queen, D.; Orsted, H.; Sanada, H.; Sussman, G. *Int Wound J*, **2004**, *1*, 59-77.
13. Zahedi, P.; Rezaeian, I.; Ranaei-Siadat, S.-O.; Jafari, S.-H.; Supaphol, P. *Polym. Adv. Technol.* **2010,** *21*, 77-95.
14. Visinescu, D.; Patrinoiu, G.; Tirsoaga, A.; Carp, O. *Environmental Chemistry for a Sustainable World*; Springer Netherlands, **2012**.
15. Franklin, T. J.; Snow, G. A. *Biochemistry of Antimicrobial Action*; Chapman and Hall Ltd.:London, **1978**.
16. Ghannoum, M. A.; Rice, L. B. *Clin Microbiol Rev*, **1999**, *12*, 501–517.
17. Lewis, R. E. *Mayo Clin Proc.*, **2011**, *86*, 805–817.
18. Kathiravan, M. K.; Salake, A. B.; Chothe, A. S.; Dudhe, P. B.; Watode, R. P.; Mukta, M. S.; Gadhwe, S. *Bioorg. Med. Chem.* **2012**, *20*, 5678–5698.
19. Ashley, E. S. D.; Lewis, R.; Lewis, J. S.; Martin, C.; Andes, D. *Clinical Infectious Diseases*. **2006**, *43*, S28-39.
20. Orosz, S. E.; Frazier, D. L. *Journal of Avian Medicine and Surgery*. **1995**, *9*, 8–18.
21. Mann, J.; Crabbe, M. J. C.; *Bacteria and Antibacterial Agents*; Spektrum Academic Publishers: Oxford, **1996**.
22. Sanchez, D. A.; Schairer, D.; Tuckman-vernon, C.; Chouake, J.; Kutner, A.; Makdisi, J.; Friedman, J. M.; Nosanchuk, J. D.; Friedman, A. J. *Nanomedicine Nanotechnology, Biol. Med.* **2014**, *10*, 269–277.
23. Acar, A.; Uygur, F.; Evinc, R.; Ersin, U.*Burns*. **2011**, *37*, 882–885.
24. Cossu, A.; Wang, M. S.; Chaudhari, A.; Nitin, N. *Int. J. Pharm.* **2015**, *493*, 233–242.
25. Costoya, A.; Montini, F.; Llovo, J.; Concheiro, A.; Abraham, G. A.; Alvarez-lorenzo, C. *Int. J. Pharm.* **2016**, *513*, 518–527.
26. Tenover, F. C. *The American Journal of Medicine.* **2006**, *119*, S3-10
27. Walsh, C. *Nature*. **2000**, *406*,775-781.
28. Walsh, C.; *Antibiotics*; ASM Press: Washington, **2003**
29. Hammond, S. M.; Lambert, P. A.; *Antibiotics and Antimicrobial Action*; Edward Arnold (Publishers) Ltd: London, **1978**
30. Namazi, H.; Rakhshaei, R.; Hamishehkar, H.; Samadi, H. *Int. J. Biol. Macromol.* **2016**, *85*, 327–334.
31. Moritz, S.; Wiegand, C.; Wesarg, F.; Hessler, N.; Müller, F. A.; Kralisch, D.; Hipler, U.; Fischer, D. *Int. J. Pharm.* **2014**, *471*, 45–55.
32. Lu, Z.; Gao, J.; He, Q.; Wu, J.; Liang, D.; Yang, H.; Chen, R. *Carbohydr. Polym.* **2017**, *156*, 460–469.

33. Singh, B.; Sharma, S.; Dhiman, A. *Int. J. Pharm.* **2013**, *457*, 82–91.
34. He, T.; Wang, J.; Huang, P.; Zeng, B.; Li, H.; Cao, Q.; Zhang, S.; Luo, Z.; Deng, D. Y. B.; Zhang, H.; Zhou, W. *Colloids Surfaces B Biointerfaces* **2015**, *130*, 278–286.
35. Burpo, R. H. *JOGNN*. **2000**, *29*, 181–190.
36. De Clercq, E. *Journal of Clinical Virology*. **2001**, *22*, 73–89.
37. De Clercq, E. *Journal of Clinical Virology*. **2004**, *30*, 115–133.
38. Rai, M.; Yadav, A.; Gade, A. *Biotechnol. Adv.* **2009**, *27*, 76–83.
39. Qin, Y. *Int. Wound J*.**2005**, *2*, 172-176.
40. Lachenmeier, *Side Eff. Drugs Annu.* **2015**, *37*, 273–279.
41. Nania, P.; *AORN J*., **2016**, *104*, 13–14.
42. Kenawy, E. R.; Worley, S. D.; Broughton, R.; *Biomacromolecules* **2007**, *8*, 1359–1384.
43. Siedenbiedel, F.; Tiller, J. C. Polymers. **2012**, *4*, 46–71.
44. Timofeeva, L.; Kleshcheva, N. *Appl Microbiol Biotechnol*. **2011**, *89*, 475–492.
45. Nakagawa, Y.; Hayashi, H.; Tawaratani, T.; Kourai, H.; Horie, T.; Shibasaki, I. *Appl. Environ.Microbiol.* **1984**, 47, 513-518.
46. Lee, S. B.; Koepsel, R. R.; Morley, S. W.; Matyjaszewski, K.; Sun, Y.; Russell, A. *J.Biomacromolecules* **2004**, 5, 877-882.
47. Zhang, Y.; Jiang, J.; Chen, Y. *Polymer* **1999**, *40*, 6189-6198.
48. Tashiro, T. *Macromolecular Materials and Engineering* **2001**, 286, 63-87.

Chapter 3: Synthesis, characterisation and modification of SMA

3.1. Introduction

Post-polymerisation modification of polymers to produce polymers with specific properties for a specific application is of common practice in recent years. In this study, the alternating polymer poly(styrene-*alt*-maleic anhydride) (SMA) is selected as base polymer that will be modified after polymerisation and later used to produce nanofibres of SMA as well as nanofibres of the modified SMA polymer via the single needle electrospinning process. SMA is a cheap, readily available, easily synthesised and thermoplastic polymer[1]. Chemical modification of SMA can be easily achieved as the maleic anhydride units present in SMA are easily accessible and rather reactive, allowing for relatively easy modification of the SMA polymer. Modification of a polymer before the electrospinning process favours the formation of covalent bonds between SMA and the modifying agent. A modifying agent containing a reactive group that will covalently attach to SMA via a ring-opening reaction of the maleic anhydride unit will thus be a good agent for the modification process. The maleic anhydride residues show reactivity towards water, alcohols and primary as well as secondary amines. One can thus synthesise nanofibers with tailored functionalities by simply selecting modifying agents containing amine or alcohol moieties in the modification process of SMA. Amines however exhibit a greater nucleophilic character as opposed to alcohols and are the agent of choice as the ring-opening reaction at the anhydride moiety requires strong nucleophilic anhydride-reactive agents.

The modification agents used in this case are selected in order to obtain a functionalised polymer that exhibits antimicrobial characteristics. A primary amine functional group from the modifying agent is available for the nucleophilic reaction with the reactive anhydride group. The anhydride group undergoes a ring-opening reaction within the five membered maleic anhydride moiety to yield an amide. Heat treatment is then used to obtain a stable five membered cyclic imide. Functional groups can also be introduced to the pending side chain of the imide simply by choice of the primary amine reacted with the maleic anhydride residues. If the functionality in the pending side chain contains a tertiary amine, it can be subjected to further reaction with an alkyl halide to yield a quaternised SMI (qSMI) polymer that contains a positively charged aliphatic quaternary ammonium group.

3.2. Results and discussion

This chapter describes the procedures and protocols used in the synthesis and characterisation of the alternating polymer poly(styrene-*alt*-maleic anhydride) (SMA). Furthermore, post-polymerisation modification of SMA with a primary amine to form poly(styrene-*alt*-(*N*-substituted-maleimide)) (SMI) and its derivatives is also described. The polymers synthesised and modified during the study were then used in the electrospinning process described in Chapter 4 to produce functionalised polymer nanofibers.

3.2.1. Synthesis of poly(styrene-*alt*-maleic anhydride) copolymer

An alternating copolymer of styrene and maleic anhydride (MAnh) was synthesised in a 1:1 molar ratio of styrene:maleic anhydride, using conventional free radical chemistry. The initiator was added in a 200:1 monomer:initiator ratio. The procedure was followed as described in the work done by Cloete *et al*[2].

In a 1000 mL round bottom flask equipped with a stirrer bar, styrene (30 g, 0.288 mol) was dissolved in 400 mL MEK, along with maleic anhydride (28.25 g, 0.288 mol) and AIBN (0.2365 g, 0.00144 mol). The reaction mixture was degassed with N_2 for at least 30 min and then reacted overnight under reflux at 60 °C.

The polymer was precipitated in isopropanol and dried under vacuum at 60 °C overnight to remove residual solvent and unreacted monomer.

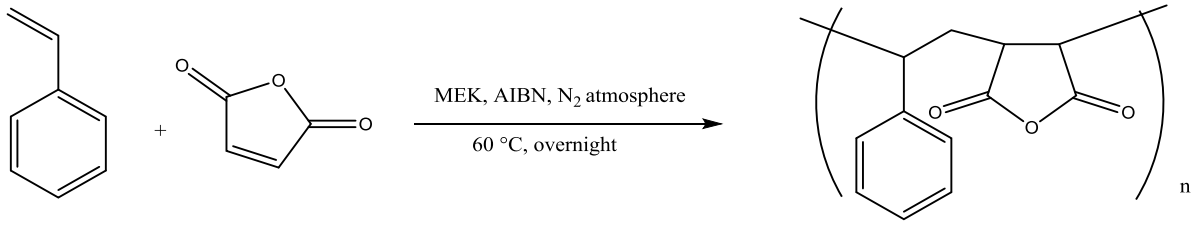

Scheme 3.1: Reaction scheme of the synthesis of poly(styrene-*alt*-maleic anhydride) via conventional free radical polymerisation.

Scheme 3.1 represents the schematic illustration of the reaction between the monomers to yield SMA (yield= 93.27 % [54.33 g], M_n= 222 856 g·mol^{-1}, *Đ*= 2.01). Molar mass (M_n) and dispersity (*Đ*) were determined by means of size exclusion chromatography (SEC) in a *N*,*N*-dimethylacetamide system (DMAc), calibrated with PMMA standards. Free radical polymerisation typically yields polymers with relatively high *Đ* values and is reflected in the *Đ* value of 2.01 obtained.

^{1}H-NMR (DMSO-d_6): δ (ppm) = 6.6-7.5 (s broad, 5H aromatic), 3.2-3.5 (s broad, 2H, -CH-CH-), 1.8-2.2 (s broad, 3H, -CH-CH_2-).

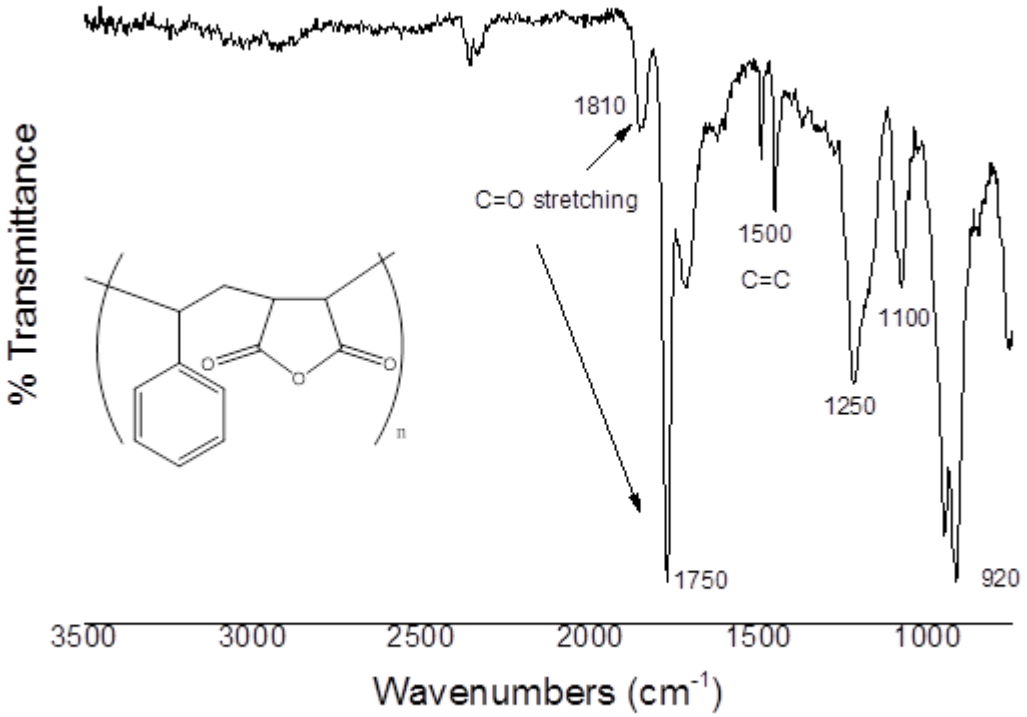

Figure 3.1: ATR-FTIR spectrum of SMA

In Figure 3.1 the characteristic carbonyl symmetric and asymmetric stretching vibrations of the maleic anhydride moiety can be seen at 1810 and 1750 cm^{-1}. The signals observed at 1605 cm^{-1} and 1500 cm^{-1} are due to the C=C stretching of the aromatic styrene ring and the C-H bending vibration of the aromatic ring. The bands observed at 1250 cm^{-1}, 1100 cm^{-1} and 920 cm^{-1} are assigned to the cyclic anhydride groups.

3.2.2. Modification of SMA with 3-(*N*,*N*-dimethylamino)propyl-1-amine to yield poly(styrene-alt-*N*-(3-(*N*',*N*'-dimethylamino)propyl)maleimide) (SMI)

Modification of the SMA polymer described in Section 3.2.1 took place at the cyclic anhydride moiety of the copolymer via a nucleophilic addition reaction using 3-(*N*,*N*-dimethylamino)propyl-1-amine (DMAPA), an *N*-alkylamine, containing a primary as well as a tertiary amine group. The reaction between the anhydride residues and a primary amine is rapid and straight forward. The addition reaction results in a ring-opened structure that contains a carboxylic acid and an amide group. The polymer underwent heat treatment and loss of water at the amide to yield a cyclic maleimide product. The modification reaction is shown below in Scheme 3.2.

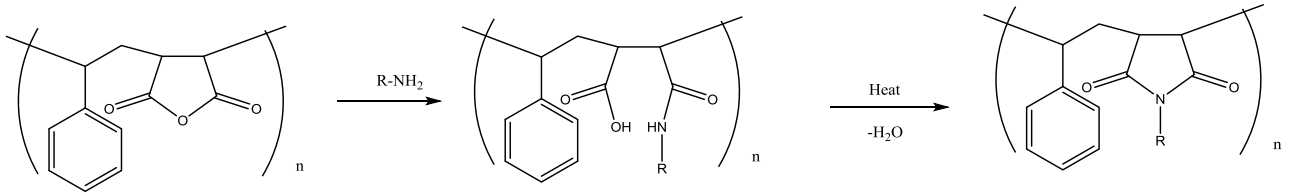

Scheme 3.2: SMA modification with primary amine and subsequent loss of water to yield SMI

Scheme 3.3 indicates the modification of SMA with DMAPA. In a 100 mL three-neck round bottom flask equipped with a magnetic stirrer bar, SMA (1.000 g, 0.004945 mol) (calculated MAnh fraction) was dissolved in 20 mL *N, N*-dimethylformamide (DMF). DMAPA (see Table 3.1 for amount of DMAPA used in each modification) in 10 mL DMF was added dropwise to the SMA over a period of 30 min. The white/ yellowish reaction mixture was left to stir for a further 2 hrs at room temperature, then gradually heated to 160 °C and left under reflux for 4-6 hrs[3] to yield the clear yellow ring closed maleimide product. The resulting polymer was precipitated in cold diethyl ether, isolated and dried under vacuum overnight. In the case of the 100% modified SMI polymer, DMAPA was added in a 1.25 molar excess relative to the anhydride.

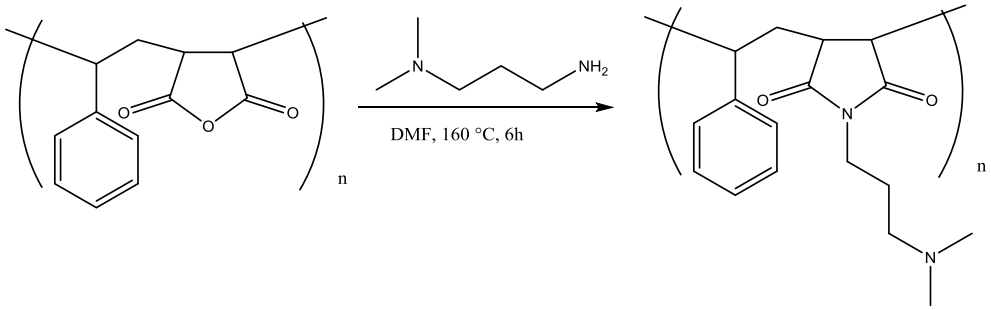

Scheme 3.3: Reaction scheme of SMA modification with DMAPA

Table 3.1: Modification of SMA with DMAPA

% Modification	DMAPA (g)	mmol	Yield (g)
30	0.1516	1.484	1.027
40	0.2021	1.978	1.068
50	0.2527	2.473	1.121
60	0.3032	2.967	1.113
70	0.3537	3.462	1.143
80	0.4043	3.956	1.203
90	0.4548	4.451	1.319

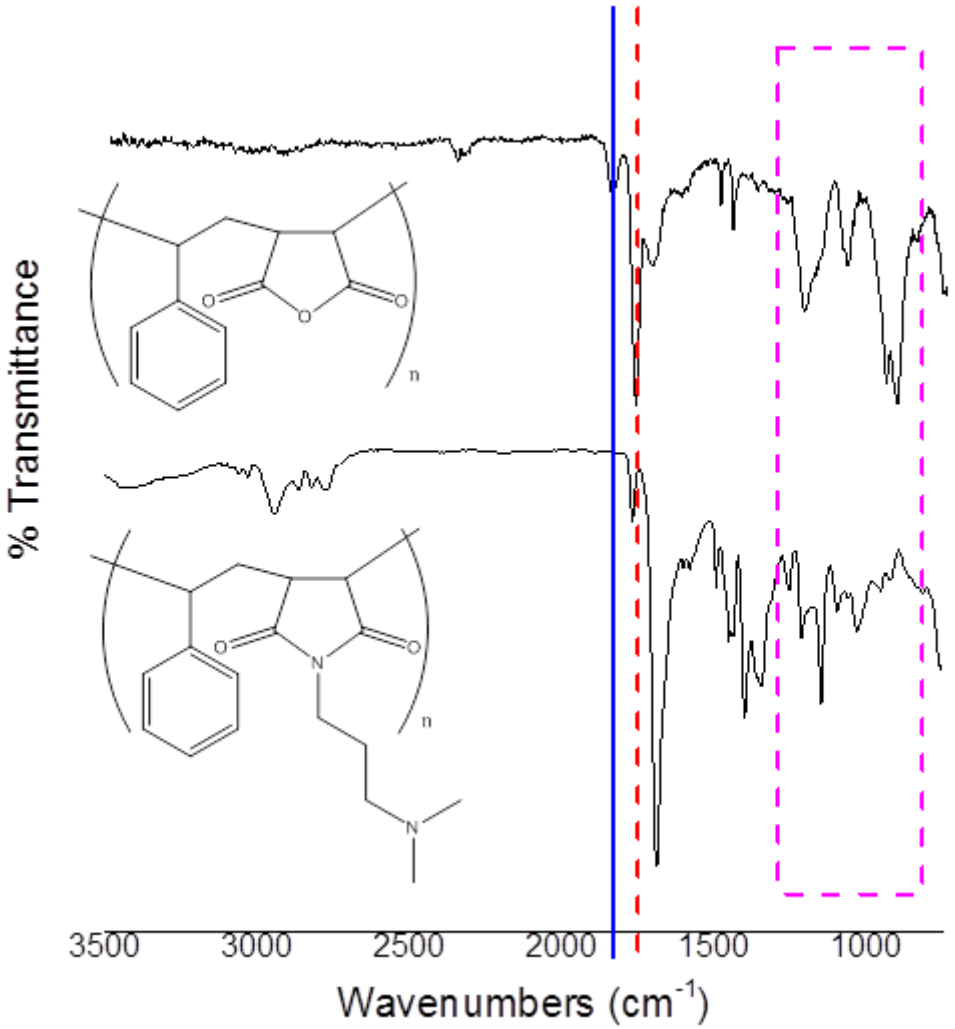

Figure 3.2: Stacked ATR-FTIR spectra of SMA and SMI

The imidisation of the SMA can be confirmed from the shift of the C=O carbonyl anhydride peaks to a lower wavenumber as indicated by the blue and red lines in Figure 3.2. These peaks are characteristic of the

symmetric and asymmetric stretch vibrations of the C=O bond within the imide groups. The presence of the tertiary amine groups can also be observed in the changes of the anhydride bands indicated in the magenta box.

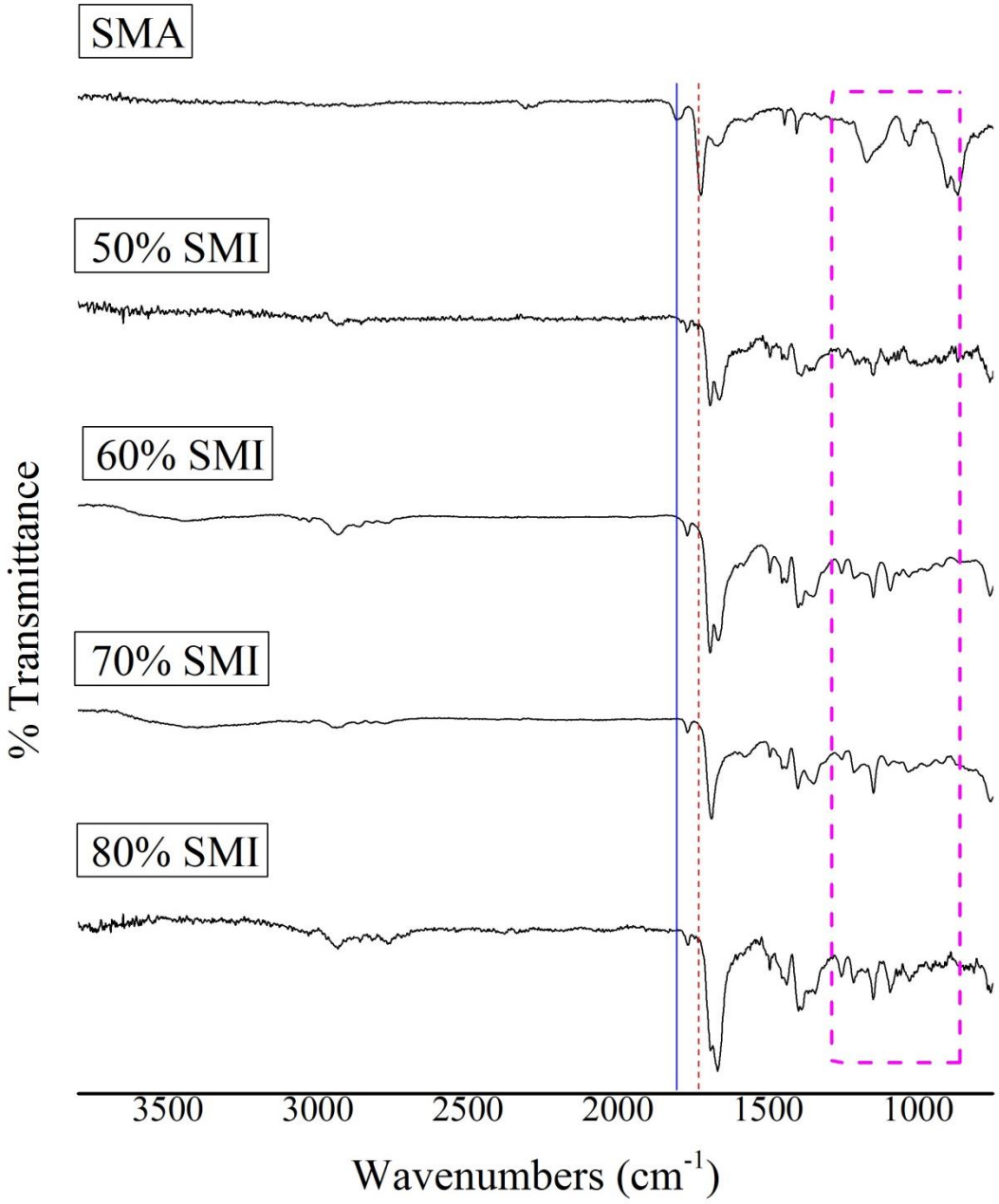

Figure 3.3: Stacked ATR-FTIR spectra of partially imidised SMI

In Figure 3.3, like in Figure 3.2, we also notice a shift in the C=O peaks of the carbonyl anhydride units to a lower wavenumber as indicated by the blue and red lines. The intensity of the C=O peaks of the imide functionality seems to increase as the percentage of imidisation also increases. An increase in intensity of the tertiary amine signal, indicated by the magenta box, can also be observed.

During the partial modification of SMA with DMAPA as described above and indicated in Table 3.1, the formation of a white solid was observed. For modifications below 70 % (i.e. 30-60 %) it was observed that aggregation or clumping takes place after 30 min of DMAPA addition. The aggregated solid was still present after heating to 160 °C and stirring for 6 hrs. A colour change from white to yellow of the aggregate was also observed. Modifications above 70 % did not show any clumping or aggregation after 30 min of DMAPA addition. After heating to 160 °C for 6 hrs, the white solid observed at the point where DMAPA dripped into the SMA solution, was no longer present and colour change from white to clear yellow was observed. This was interesting as the crosslinking process of the SMI polymers could not be completely described as of yet.

3.2.2.1. Model study

A model study (Scheme 3.4) using a compound similar to the maleic anhydride unit was devised in order to try and explain this clumping phenomenon observed. The observed clumping may possibly be related to the crosslinking of SMI and its derivatives, like in the case of quaternised SMI (qSMI) fibres after they have been subjected to heat treatment. Heat treatment of qSMI fibres at 120 °C renders the fibres insoluble in water and organic solvents. The following model study may then be able to explain the clumping as well as shed some light on the crosslinking of qSMI fibres.

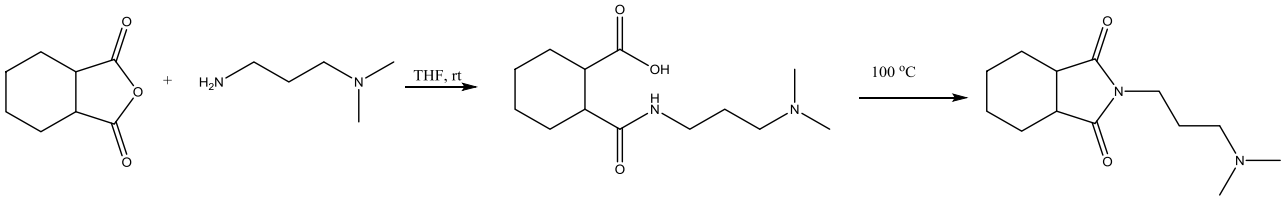

Scheme 3.4: Schematic representation of model study

The model compound used in this study was chosen to be 1,2-*cis*-cyclohexanedicarboxylic anhydride as it is similar to maleic anhydride and the most reactive site of the compound is the anhydride moiety. The model compound was reacted in a 1:1 ratio with DMAPA and characterised.

In a 50 mL round bottomed flask equipped with a stirrer bar 1,2-*cis*-cyclohexanedicarboxylic anhydride (2.000 g, 0.01297 mol) and DMAPA (1.326 g, 0.01297 mol) in 10 mL dry THF were added. The reaction was left to stir at room temperature overnight in order to ensure completion of the reaction. Upon completion of the reaction, a white solid was observed. The solvent was removed and the product heated to 100 °C under vacuum overnight to yield the ring closed product. The product (3.019 g) was analysed using NMR and ATR-FTIR.

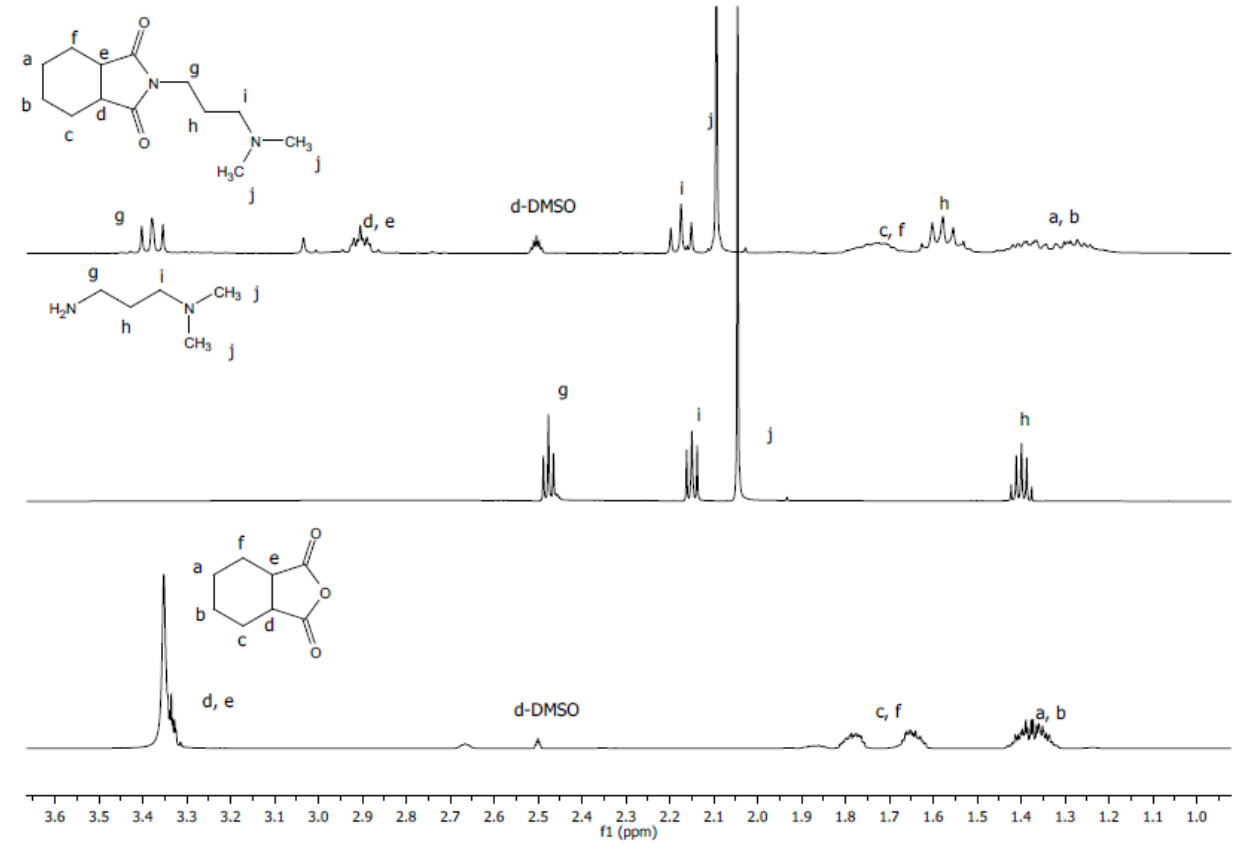

Figure 3.4: Stacked ^{1}H-NMR spectra of the model compound, DMAPA and the ring closed product

^{1}H-NMR of the starting materials could be successfully assigned as seen in Figure 3.4. The ^{1}H-NMR of the product could also be successfully assigned. The shift in ppm of peaks g, h and j to chemical shifts downfield in the product also confirms the success of the synthesised product. For protons c and f we notice one peak present in the ^{1}H-NMR of the product. This is due to the second peak overlapping with the peak observed for the protons labelled h. The large shift in ppm of g may be ascribed to the de-shielding effect caused by the presence if the imide moiety.

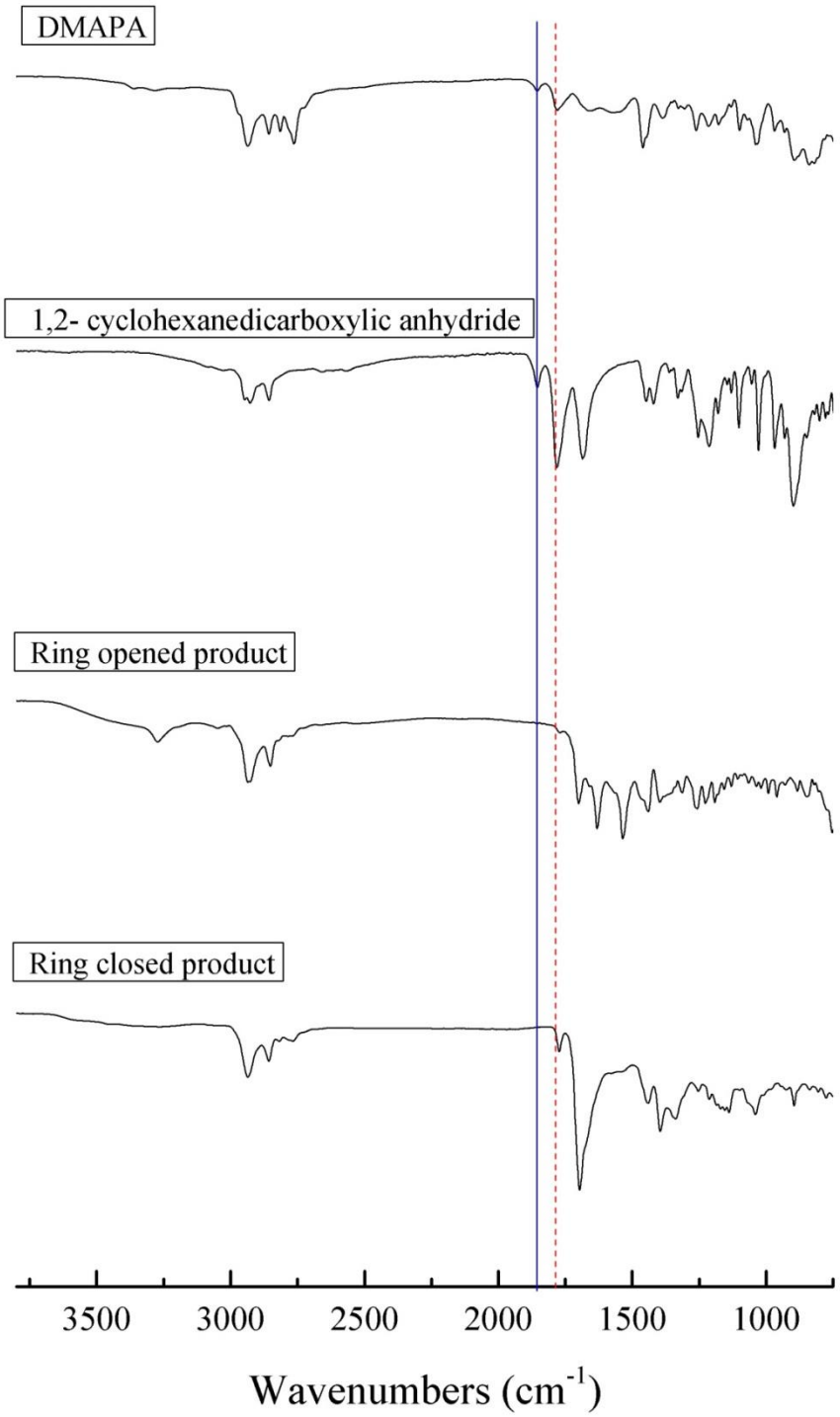

Figure 3.5: ATR-FTIR spectra of model compound, DMAPA, ring opened product and ring closed product

From the ATR-FTIR spectra in Figure 3.5 we notice that the C=O stretch observed at 1810 and 1780 cm^{-1} in the model compound shifted to 1780 and 1690 cm^{-1} in the product. This is characteristic of the formation of the imide bond observed in the product. We also notice the disappearance of the broad OH-stretch from the ring opened product at 3600-3050 cm^{-1} in the ring closed product.

Literature also revealed that it is possible for maleic anhydride to sometime react with tertiary amines[4, 5]. Depending on their overall structure, tertiary amines have the ability to undergo a variety of reactions. In 1942, Van Alphen[4] studied the reaction of triethylamine (TEA) with maleic anhydride (Scheme 3.5). He isolated a black impure substance that was water soluble and released TEA upon reaction with a base. Another group observed that above mentioned reaction was exothermic and initially noticed a clear yellow solution, but later isolated a dark brown solid. They rationalised their observations by stating that a charge-transfer complex (or π-complex) forms upon mixing the reagents, forming the yellow solution. The π-complex forms an intermediate σ-complex before collapsing to form the dark brown product. This is represented graphically in Scheme 3.5.

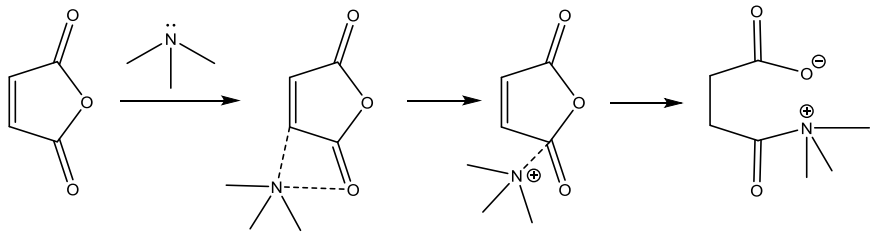

Scheme 3.5: Reaction of maleic anhydride with triethylamine forming suggested π- and σ-complexes

The model compound was then also reacted with TEA in order to confirm the possibility of an intramolecular reaction that may further explain the clumping observed or even crosslinking of qSMI fibres.

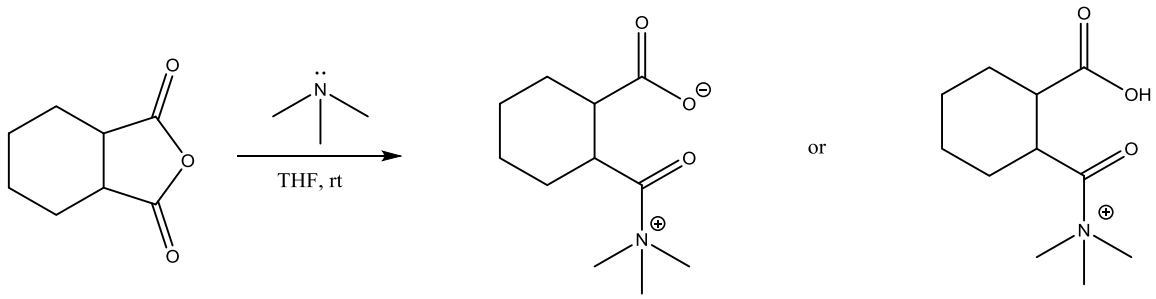

Scheme 3.6: Reaction of model compound with TEA

In a 50 mL round bottomed flask equipped with a magnetic stirrer bar, the model compound and TEA were reacted in a 1:1 ratio. TEA (1.313 g, 0.01297 mol) in 10 mL THF was added to the model compound (2.000 g, 0.01297 mol). The reaction was left to stir at room temperature overnight in order to ensure completion of the reaction. The solvent was removed and the amber coloured product (2.894 g) was dried under vacuum overnight as well. The product was then subjected to NMR and ATR-FTIR analyses.

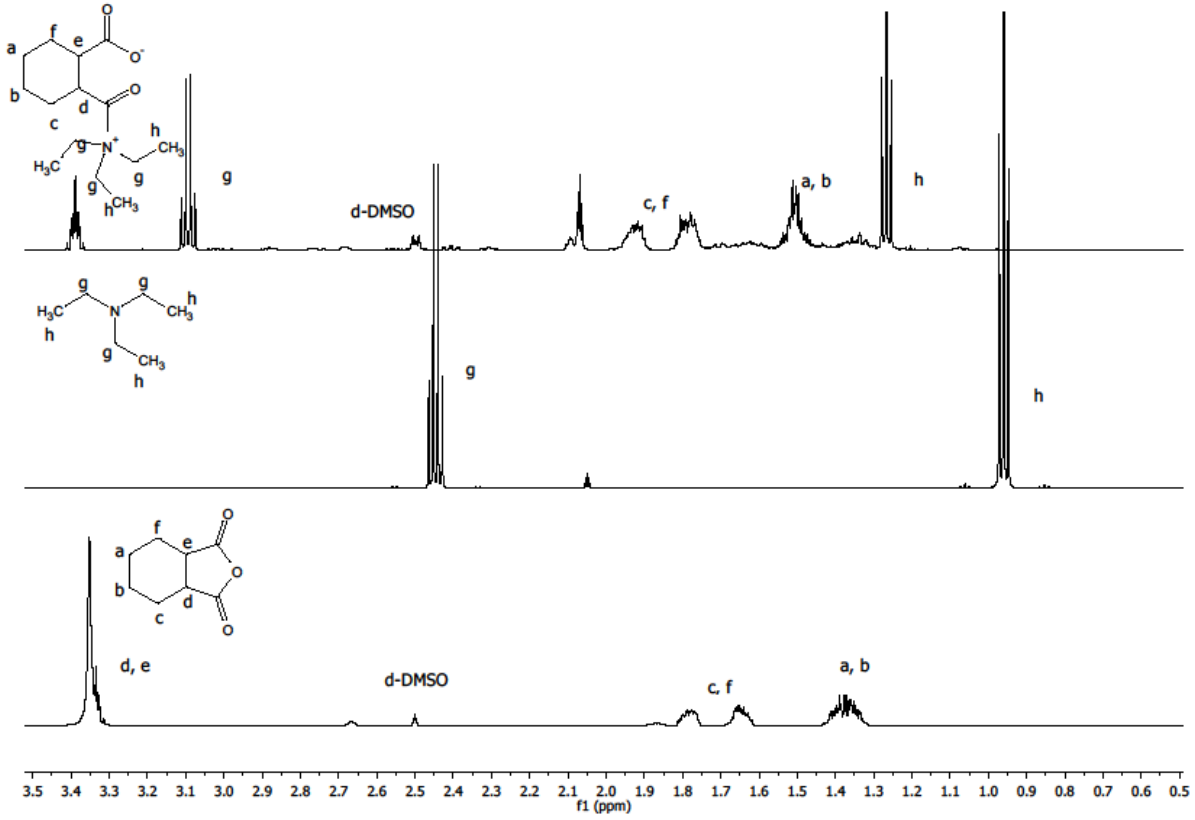

Figure 3.6: Stacked ^{1}H-NMR spectra of the model compound, TEA and their product

In Figure 3.6 the ^{1}H-NMR of the product revealed a shift in ppm to a more downfield value from the starting materials. All signals could be accounted for, thus confirming the successful reaction of the starting materials to yield the product.

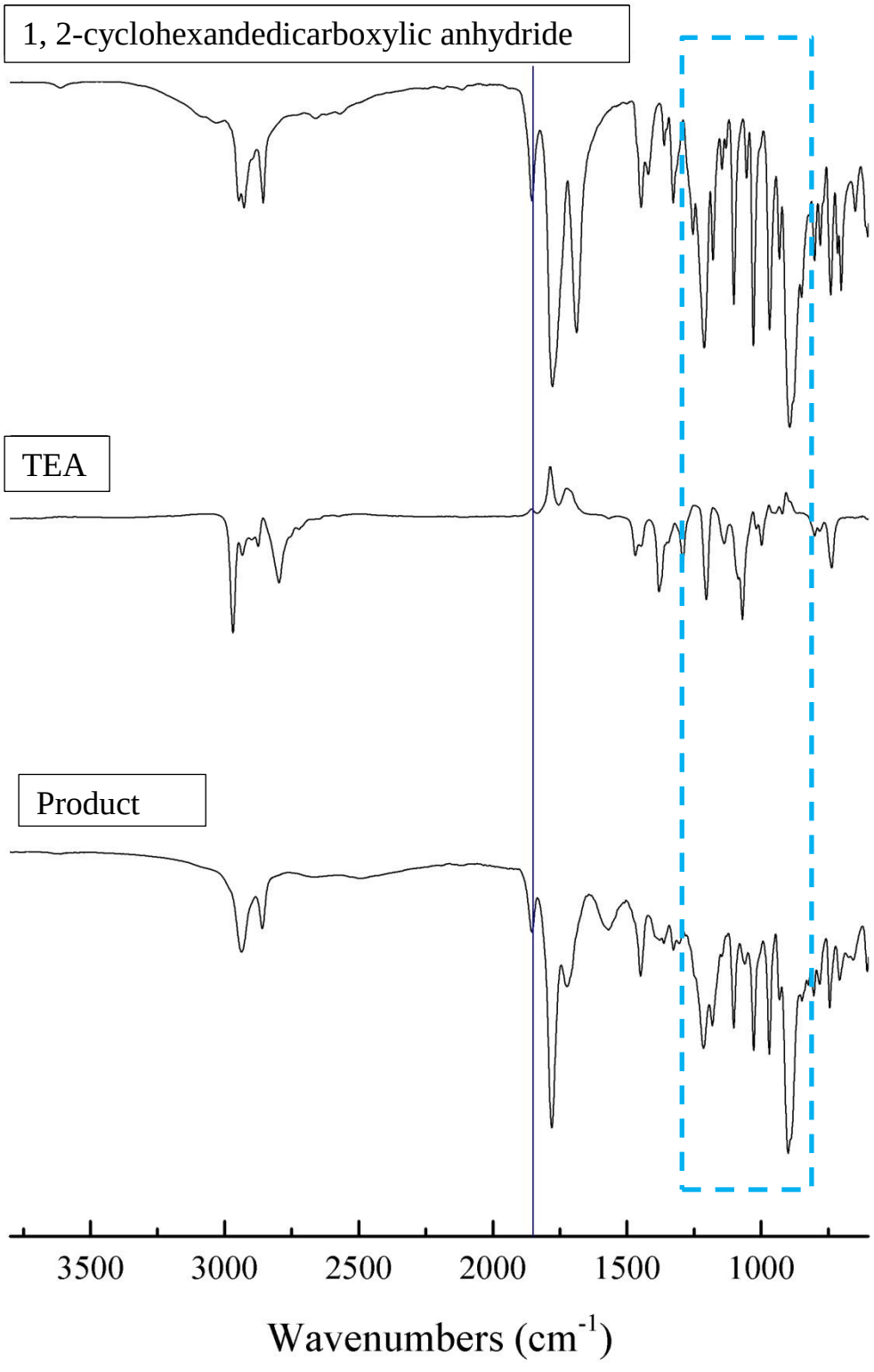

Figure 3.7: ATR-FTIR spectra of the model compound, TEA and the product of their reaction

In the ATR-FTIR spectrum depicted in Figure 3.7, we notice the change in the C=O peak at 1800 cm^{-1} and 1760 cm^{-1}. We also notice a change in the tertiary amine C-N stretching region indicated by the blue dashed box. This thus confirms that the reaction was successful.

3.2.3. Synthesis of functionalised SMI polymers

The work done by Bshena and co-workers[6] in 2008 utilised different alkylhalides as quaternisation agents in the modification of SMI, namely 1-bromobutane, 1-bromooctane and 1-bromododecane. Bshena found that aliphatic chains with more carbon atoms showed promising results towards antimicrobial efficiency. For this reason 1-bromooctane and 1-bromododecane were selected as modifying agents to compare.

SMI-qC_8 and SMI-qC_{12} were prepared by an addition substitution reaction of the SMI precursor with the above mentioned bromoalkanes. Scheme 3.5 illustrates the modification from SMA to the quaternised product.

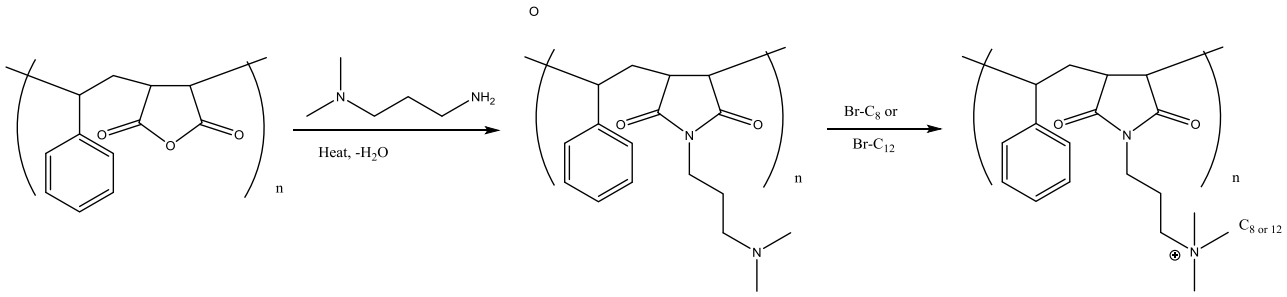

Scheme 3.7: Reaction scheme of modification of SMA to yield the SMI precursor and subsequent modification with alkyl halides to yield quaternised SMI

The modification procedures for both bromooctane and bromododecane are identical. The reaction procedure for bromooctane is described below.

In a round-bottomed flask with a condenser and magnetic stirrer bar, SMI (3.000 g, 10.4 mmol equivalents of MAnh) was dissolved in 100 mL DMF. Then 1-bromooctane (2.512 g, 13.01 mmol) was added dropwise and the reaction mixture stirred at 100 °C. The reaction was stopped after 30 hours. To ensure complete modification, 1-bromooctane was added in molar excess of 1.25 times relative to the maleimide moieties. Successful synthesis was confirmed by ATR-FTIR.

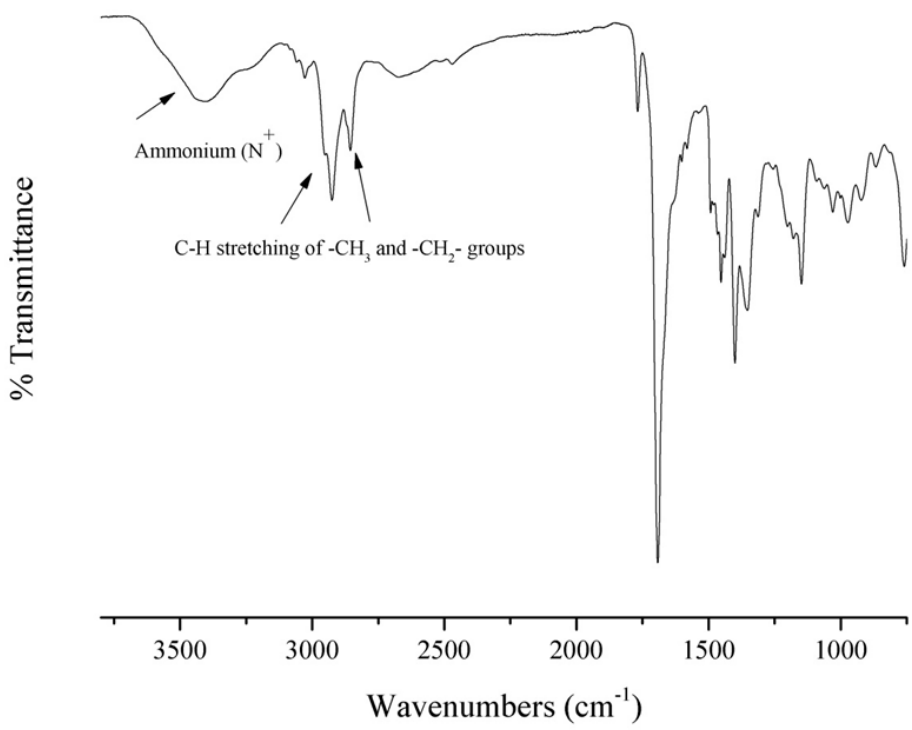

Figure 3.8: ATR-FTIR spectrum of SMI qC_8

From Figure 3.8 we notice the increase in the intensity of the C-H stretching of the $–CH_3$ and $–CH_2$ groups at 2850 and 2800 cm^{-1}. We also notice a broad band centered around 3400 cm^{-1}.The peaks observed due to C-H stretching as well as the appearance of the broad band attributed to the ammonium cation confirm the successful quaternistion of the tertiary amino groups of the SMI precursor.

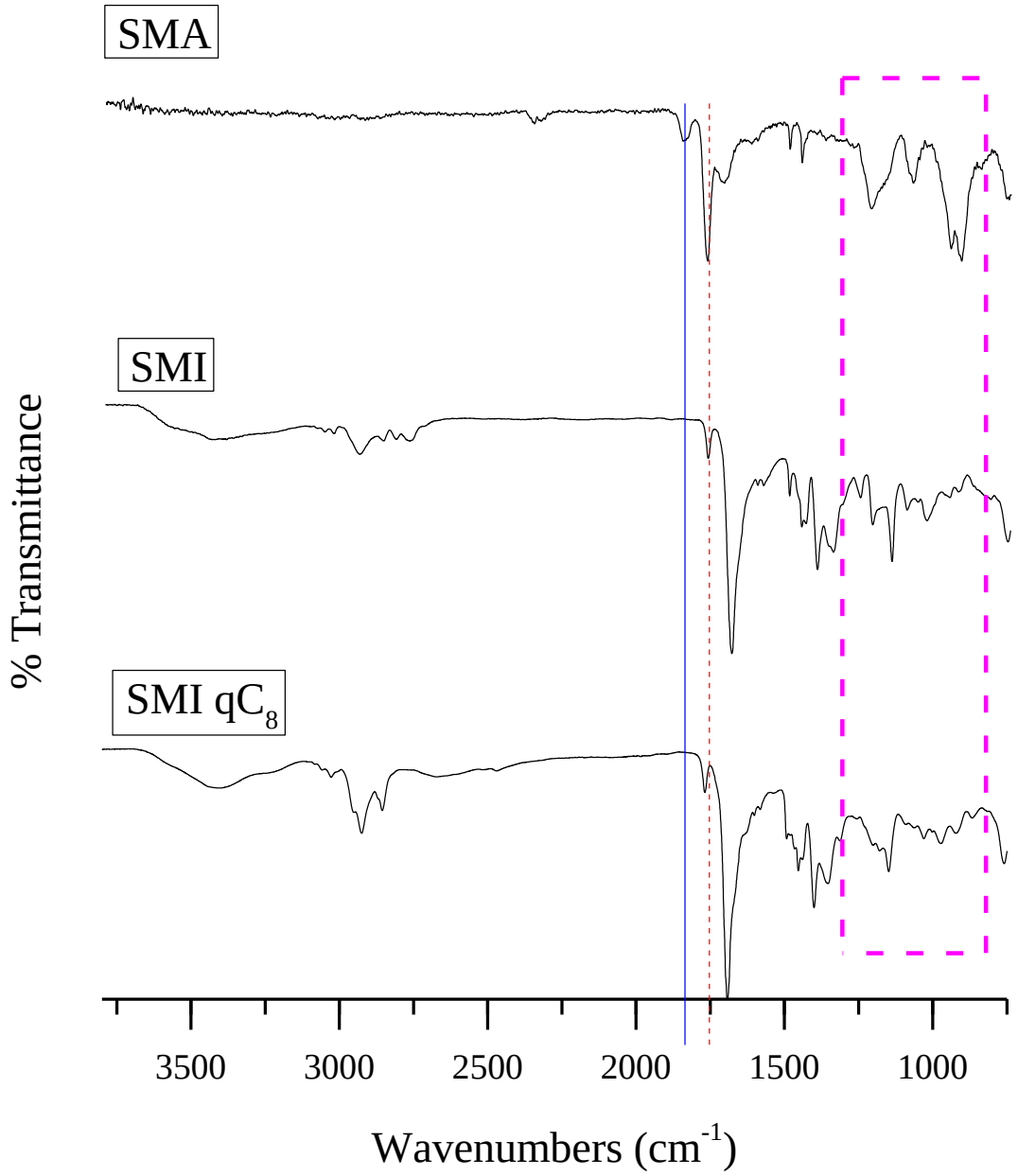

Figure 3.9: Stacked ATR-FTIR spectra of SMA, SMI and SMI-qC8

Like previously discussed, in Figure 3.9 we see the shift in wavenumbers of the C=O stretch due to imidisation as indicated by the blue and red lines, as well as the change in the tertiary amine region as indicated by the magenta box. This confirmed the successful synthesis to yield the quaternary ammonium product.

3.3. Conclusion

The conventional free radical synthesis of SMA was successful as could be confirmed using NMR and ATR-FTIR. SEC analysis showed that a polymer with a number average molar mass (M_n) of 222 856 g.mol^{-1} and dispersity ($Đ$) of 2.01 was obtained. The subsequent modification of the SMA to yield the quaternised polymers SMI-qC_8 and SMI-qC_{12} via an SMI intermediate could also be successfully confirmed by means of ATR-FTIR analysis. These polymers can thus be used for the electrospinning process described in Chapter 4.

A model study where the model compound, namely 1,2-cis-cyclohexanedicarboxylic anhydride, was reacted with DMAPA, (a compound containing both a primary and tertiary amine) and a tertiary amine (TEA) was developed as seen in Scheme 3.4 and Scheme 3.6. The model compound was successfully reacted with both compounds. The successful reaction of the model compound with TEA suggests that at lower modifications of SMA with DMAPA (30-60 %) intramolecular crosslinking reactions takes place with the tertiary amine group of DMAPA since the primary amine readily reacts with the anhydride moiety of SMA. This may also be a plausible explanation for the crosslinking process observed in quaternised SMI fibres when these fibres are subjected to heat treatment *in vacuo*, rendering these fibres insoluble in water and organic solvents.

3.4. Experimental

3.4.1. Experimental and characterisation details

The following chemicals and solvents were commercially obtained and used as received, without further purification, unless stated otherwise. Maleic anhydride 99% (Sigma-Aldrich), 3-(*N*,*N*-dimethylamino) propyl-1-amine 99% (Sigma-Aldrich), 1-bromooctane 98% (Sigma-Aldrich), 1-bromododecane 98% (Sigma-Aldrich), 1,2-*cis*-cyclohexanedicarboxylic anhydride 95% (Sigma-Aldrich), triethylamine 99% (Sigma-Aldrich), methyl ethyl ketone ≥99.7% (Sigma-Aldrich), isopropanol (Kimix), diethyl ether (Kimix), *N*,*N*-dimethylformamide (Kimix), deuterated dimethyl sulfoxide (Sigma-Aldrich, 99.9 atom % DMSO-d_6) and deuterated acetone (Sigma-Aldrich, 99.9 atom % Acetone-d_6) were used as received from the suppliers. Styrene monomer 99.5% (Fluka Chemicals) was purified by means of an aluminium oxide column and 2, 2^{I} -azo-bis (isobutyronitrile) (AIBN) (Riedel de Haen) was recrystallized from methanol and dried under vacuum before use.

3.4.1.1. Nuclear Magnetic Resonance (NMR)

The NMR analyses were done using Varian Inova 300 MHz, 400 MHz and 600 MHz NMR spectrometers. The interpretation of the obtained spectra was done using MestReNova (Version 6.0.2-5475) computer software. Sample preparations were done in deuterated DMSO and deuterated acetone.

3.4.1.2. Attenuated total reflectance Fourier Transform Infrared (ATR-FTIR) spectroscopy

A Nicolet FTIR (Nexus model) FTIR spectrometer from Thermo-Fischer was used to record infrared spectra. The FTIR was equipped with a Smart Golden Gate ATR accessory and a diamond/ZnSe internal reflection crystal. All samples are solids and did not require any sample preparation. The spectrum of each sample was recorded from 4000 cm^{-1} to 600 cm^{-1} with a spectral resolution of 8 cm^{-1} and 64 scans per run. Data acquisition was done using Omnic software and Origin software used for data processing.

3.4.1.3. Size Exclusion Chromatography (SEC)

Size exclusion chromatography (SEC) was used in order to determine molar mass and dispersity (*Đ*). The SEC analysis was done on a dimethyl acetamide (DMAc) system consisting of a Shimadzu LC-10AD pump, a Waters in-line degasser AF and a Waters 717plus autosampler. A Waters 2487 dual wavelength UV and a Waters 410 differential refractive index (DRI) is connected in series as detection systems. Dimethyl acetamide (DMAc, HPLC grade, stabilized with 0.05% BHT and 0.03% LiCl) is used as eluent at 40 °C and a flow rate of 1 mL/min. The system is calibrated using narrow poly(methyl methacrylate) (PMMA) standards ranging from 634 to 1.944×10^6 g/mol. The column set include a 50 × 8 mm guard column in series with three 300 × 8 mm, 10 μm particle size GRAM columns (two 3000 Å and a 100 Å) obtained from

Polymer Standards Service (PSS). Sample preparation entailed dissolving the polymer in BHT/LiCl stabilised DMAc to a maximum concentration of 2 mg/ mL and filtering before subjecting to analysis.

3.5. References

(1) Lee, S.; Ahn, T. A. E. O. A. N. *J. Appl Polym Sci*.**1999**, *71*, 1187–1196.

(2) Cloete, W. J.; Adriaanse, C.; Swart, P.; Klumperman, B. *Polym. Chem.* **2011**, *2*, 1479–1481.

(3) Liu, H.; Cao, K.; Huang, Y.; Yao, Z.; Li, B; Hu, G. *J. Appl Polym Sci*. **2006**, *100*, 2744-2749.

(4) Trivedi, B. C.; Culbertson, B. M. *Maleic Anhydride*; Plenum Press: New York, **1982**.

(5) Kluger, R.; Hunt, J. C. *J. Am. Chem. Soc.* **1984**, *106*, 5667-5670.

(6) Bshena, O. E. S. *Synthesis of Permanent Non-Leaching Antimicrobial Polymer Nanofibers*. PhD Thesis, Stellenbosch University, South Africa. **2012**.

Chapter 4: Electrospinning and hydrogel formation

4. Abstract

This chapter describes the electrospinning process in detail as well as the application of the single needle electrospinning technique to create non-woven nanofibrous mats from SMA, sodium alginate and the quaternised SMI polymers described in Chapter 3.

4.1. Electrospinning

The electrospinning technique has been known for almost a century[1]. The principle is based on a polymer solution or polymer melt being spun into fibres by electrostatic forces[1]. The electrospinning process has gained a lot of attention due to growing interest in nanotechnology and its applications[2-6]. The process is versatile in terms of creating a wide variety of fibres and also allows the fabrication of continuous polymer nanofibres in the submicron and nanometre range (between 50-500 nm in diameter)[7]. The electrospinning technique can also produce thin fibres with a variety of cross-sectional shapes, like branched fibres, flat ribbons and ribbons with other shapes[8].

Electrospinning is an ever evolving simple, cost effective and promising technique which facilitates the production of multi-functional nanofibres from numerous polymers, polymer blends, polymer composites and ceramics[9, 10]. Modification of polymer nanofibres through electrospinning is of great interest due to the unique properties obtained from the process when fibre diameter is decreased from micrometres to nanometres. The smaller fibre diameter leads to properties like smaller pore size, high surface area, flexibility in surface functionality, high specific surface area to volume ratio, uniform fibres, porosity, increased mechanical strength and high aspect ratios[2,11-13]. The aforementioned properties make for attractive options for numerous applications of polymer nanofibres, including food packaging, nanocatalysts, tissue scaffolds, protective clothing and textiles, filtration media, nanofibrous structures, storage cells for hydrogen fuel cells, optical electronics, reinforcements of nano-composites and drug delivery[2, 14].

Another favourable attraction of the electrospinning technique is the feasibility to modify not only the morphology of the nanofibres and internal bulk content, but also their surface structure. Post-spinning modification by chemical or physical vapour deposition is also possible. Another interesting modification can be made by controlling secondary structures of the nanofibres in order to obtain nanofibres with core or sheath structures, hollow interiors or a porous structure[15].

4.1.1. The single needle electrospinning process

In the single needle electrospinning process, a single blunted needle is attached to a syringe filled with a polymer solution or polymer melt. A high voltage supply is attached to the needle tip. By attaching the positive end of the high voltage power supply to the needle tip, it may act as a positive electrode. At a distance set by the user; a collector plate that is covered in aluminium is placed and acts as the negative electrode when the negative end of the same high voltage power supply is attached to the collector plate. A syringe pump regulates the flow rate of the polymer solution, pushing a droplet of the polymer solution through the needle tip. Two opposing forces now act on the droplet: the first the contractive surface tension of the polymer solution and the second is the same charge electrostatic repulsive forces that are introduced by the high voltage power supply[14]. Similar charges are induced in the polymer solution by means of the attached electrode. These charges now flow through the solution, accumulating on the surface of the solution droplet released at the needle tip and increase the charge density at the surface. Electrostatic repulsion takes

place, the force promoting the expansion of the surface area of the droplet, whilst the force from the surface tension will promote a reduction in the surface area of the droplet.

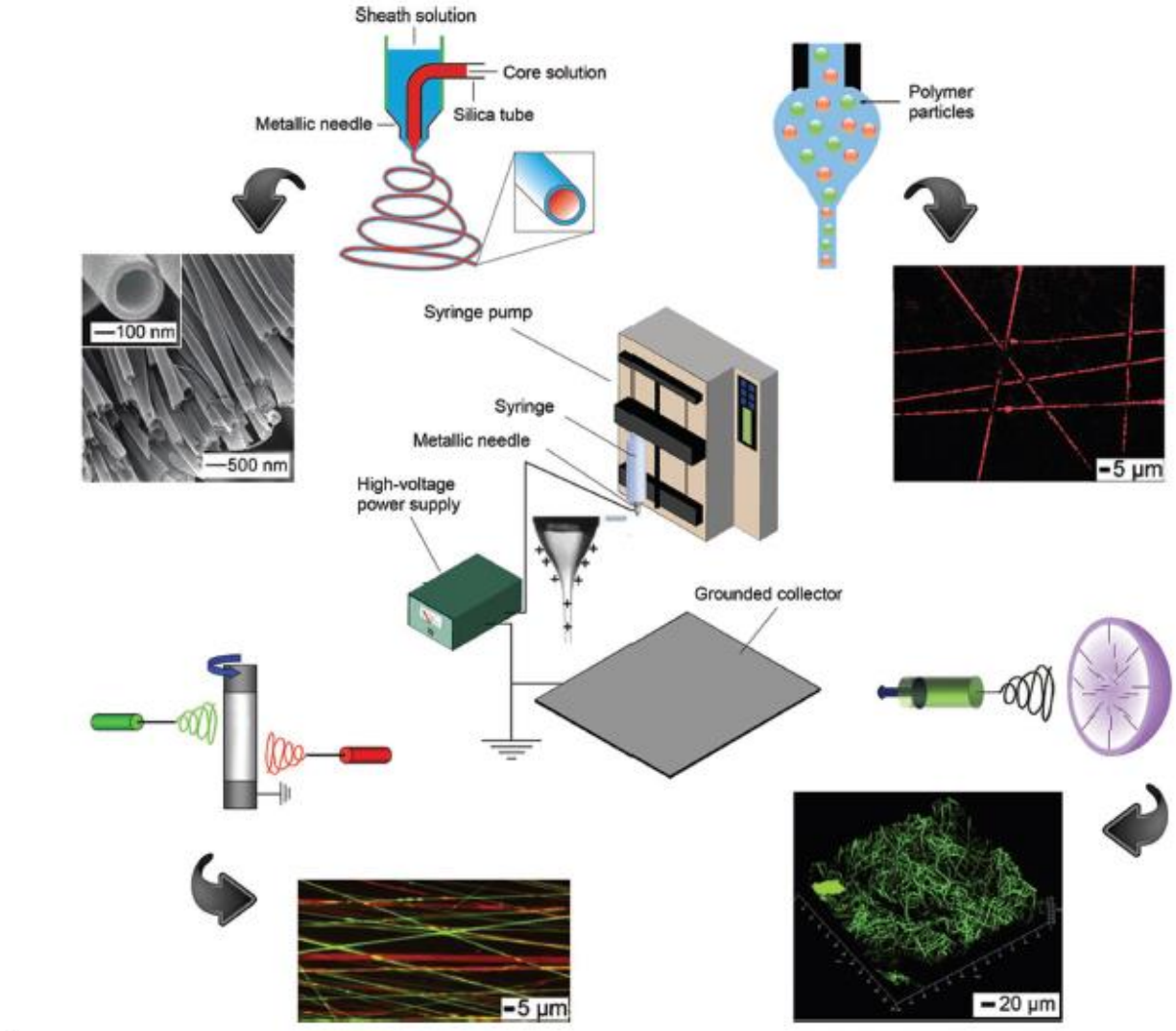

Figure 4.1: Illustration of variations in the single needle electrospinning process[16]

In Figure 4.1 in the middle we see the typical electrospinning setup. Top left shows a schematic of a co-axial spinneret with accompanying SEM images of the corresponding hollow nanofibres. In the top right corner the electrospinning of a polymer solution containing polymer particles is shown along with a fluorescence image that shows encapsulation of the polymer particles in the fibres. The image in the bottom left corner shows electrospinning with duel spinnerets and an accompanying fluorescence image showing a non-woven mat containing two different types of polymeric nanofibres. Lastly in the bottom right corner electrospinning with a hemispherical bowl collector and a confocal fluorescence image that illustrates the typical cotton-ball like scaffold of fibres.

As the electric field is increased, a critical value is reached where the electrostatic repulsive force overcomes the surface tension and a charged polymer jet is ejected from the tip of the Taylor cone[2]. A stable and straight jet is present right after ejection of the jet. The region of bending instability is reached after the jet passes this stable and straight segment[17, 18]. The charged jet is repelled from itself and undergoes whipping, due to the same charge of the ions contained in the polymer jet. The charged jet coils onto itself with each coil growing in radius. Secondary bending takes place as the charge repulsion along the fibre increases. This whipping action eventually stretches and elongates the charged jet, decreasing fibre diameter to produce fibres on

nanometre scale.[17, 19, 20]. During this process the solvent evaporates, solidifying the fibres and dry fibres accumulate on the collector plate.

Figure 4.1 shows a few ways how the electrospinning technique can be varied to produce different kinds of fibres. The ease of which one can produce nanofibres using single needle electrospinning is a desirable advantage of the electrospinning technique. Unfortunately single needle electrospinning does not yield large quantities of fibres, complicating production on a larger scale.[21]. This means that on an industrial scale as it has a slow production rate, making it economically unsustainable and unsuitable for industrial application. Due to the unsuitability for industrial application, research into upscaling the production process has been done and ball electrospinning was developed in order to increase production rate.

4.1.2. Parameters affecting the electrospinning process

A number of parameters and processing variables that interact differently and simultaneously influence the electrospinning process[2,15,17,23]. They are:

1. Electrospinning conditions described by the system or operational parameters, namely electric field strength, solution feed rate and distance between the capillary (needle or ball) and target (collector).
2. Solution parameters such as shear and elongation viscosity, conductivity, surface tension, dielectric constant of the solution, molar mass and distribution of the polymer as well as the architecture of the polymer (whether the polymer is linear or branched).
3. External parameters like environmental conditions of the electrospinning setup, including ambient temperature, the temperature of the solutions and the relative humidity.

A change in one of the parameters may affect one or more of the other parameters. A good example of this effect can de described in terms of chain entanglement necessary for electrospinning. In order for fibres to form, an acceptable number of chain entanglements are necessary. Entanglements are dependent on the molar mass and/or the concentration of the polymer solution. The molar mass and concentration of the polymer should be sufficiently high for fibre formation; however it cannot be so high that the relevant viscosity of the solution prevents polymer jets being formed by the electric field. The electric field and the surface tension should be low enough for a polymer jet formation and ejection. The viscosity should also be of such a nature that it prevents the collapsing of the jet into droplets to form beads-on-a-string type fibres due to incomplete solvent evaporation[2, 24]. Almost any polymer can thus be electrospun by simply changing the electrospinning process conditions and solutions parameters listed above[25].

4.1.3. Electrospinning process parameters that affect fibre diameter

Solvent evaporation and solidification of the polymer jets are important for the formation of nanofibres. The diameter of the fibres is primarily dependent on the size of the jets and the polymer solution itself[2]. Fibre diameter is greatly affected by the applied electric field strength, the distance between the capillary and target, and the flow rate. The solution parameters that affect fibre diameter are viscosity and solution conductivity[17,26]. The applied voltage and distance between the needle tip and collector plate determine the electric field exerted on and experienced by the polymer jet. The extent of whipping and elongation experienced by the polymer jet is mostly affected by the aforementioned parameters and thus has a direct influence on fibre diameter.

4.1.3.1. Electric field

An electric field, generated by a high voltage supply, is required between the needle tip of the syringe filled with the polymer solution and the collector plate in order for the electrospinning process to proceed. The electric field is thus a parameter that significantly affects fibre diameter. The electric field is a function of the

voltage applied as well as the distance from the needle tip to the collector. This relationship is defined by the following equation where E= electric field strength measured in kV/cm, V= Voltage difference between electrodes measured in kV and d= Distance between electrodes measured in cm:

$$E = \frac{V}{d}$$

Equation 4.1: Electric field strength equation

As mentioned before, a polymer jet is only ejected from the surface of the polymer droplet once the electrostatic forces overcome the surface tension of the solution[27]. The charged polymer jet then undergoes a process of whipping and elongation in the bending instability region as a result of electrostatic repulsion within the jet. It is during this process of whipping and elongation that the fibre diameter decreases until the solvent has evaporated and dry fibres collect on the collector plate[28]. If the applied electric field is increased, more charges will accumulate at the surface of the polymer droplet. The greater number of charges present on the surface of the droplet means that the newly ejected jet will be able to undergo more whipping and stretching, resulting in finer fibres[4, 29-31]. The higher the charge density carried by the jet surface, the less beading takes place[26]. Beading is greatly affected by the applied electrical field[32]. Increasing the concentration of the polymer solution means that the electric field will also have to increase in order to create a polymer jet[24].

4.1.3.2. Distance between the needle/ball and target

The distance between the needle tip and the collector directly influences the electric field strength as seen in Equation 4.1. A greater distance between the needle/ball and the target results in smaller fibre diameters as the jet has more traveling time and undergoes whipping and stretching to a greater extent[4, 24, 33]. If a high electric field is applied but the distance to the collector is small, thicker fibres may form as a result of more fluid ejected in a jet and shorter travelling time. This means that the jet does not have sufficient time to whip and stretch[2] and solvent evaporation does not take place efficiently, resulting in wet fibres or even a film on the collector plate. An effective spinning distance is thus important in order to allow for whipping and elongation to take place and to ensure the drying of fibres before they reach the collector plate.

4.1.3.3. Flow rate of the solution

The flow rate of the polymer solution through the needle is controlled by a syringe pump. Variation in the flow rate brings about variation in the fibre diameter[34]. Larger fibre diameter can be observed when a larger flow rate is maintained. This is due to the greater amount of the polymer solution that can be drawn from the needle tip[4, 34]. A too high flow rate results in dripping of the polymer solution from the needle tip. This means that the available charge cannot carry away the excess polymer solution fast enough[31]. In the case of a too low flow rate, the Taylor cone disappears as not enough solution is available for the deformation process, resulting in a discontinuous jet. An optimal flow rate is thus important in order to maintain a stable Taylor cone.

4.1.3.4. Viscosity

Viscosity, or the resistance of a solution to flow, is dependent on the molar mass and concentration of the polymer and is a primary parameter affecting fibre diameter[29]. An increase in the molar mass and concentration allows for more chain entanglements, and also increases the viscosity. In a solution where the viscosity is too low electrospraying will take place as too little chain entanglements are present to stabilise the jet. Instead the jet will break up into droplets[29]. On the other hand, a solution with too high viscosity will

also be difficult to electrospin as the jet will be difficult to induce. The greater viscosity means that more chain entanglements are present, hindering the flow of the solution as well as deformation in the Taylor cone region[2,26,31,33]. One can thus say that higher viscosity decreases the pathway of the jet and this means that less whipping and stretching will take place, resulting in larger fibre diameters.

4.1.3.5. Surface tension

The surface tension parameter plays an integral role in the jet initiation and bending instability processes. In order for stable Taylor cone formation and subsequent jetting to take place, the electric field charge needs to be of such a nature that it can overcome the surface tension of the spinning solution, if not, the surface tension will be the dominant force and fibre formation may not occur[4].

4.1.3.6. Electrical conductivity

The ability of a solution to transfer charges through its molecules, solvent molecules, additives or impurities within the solution defines its electrical conductivity. Once the polymer jet is ejected, whipping and stretching of the polymer jet is caused by the repulsion between charges of the same kind. The conductivity of a solution is thus important as the distribution of charges is necessary for the successful formation of the polymer jet and the whip and stretch process[29]. A higher electrical conductivity in a solution means that a larger number of charges may be distributed in the solution. This will result in the whipping and stretching process taking place to a greater extent and ultimately producing fibres with a smaller diameter. It also follows that a solution that does not exhibit electrical conductivity cannot be electrospun as the necessary charge transfer cannot take place among the molecules. The electrical conductivity of a solution can however be increased by adding a salt, increasing the temperature or using different solvents or solvent combinations in the solution. Full dissociation of the salt within the solvent means that both positively and negatively charged ions are present within the solution. The ions may move independently, each with the ability to partially carry the charge. The addition of a salt thus allows the solution to better carry the charges and in turn increases the electrical conductivity of the solution[2].

4.2. Electrospinning of SMA and subsequent hydrogel formation

Electrospinning of SMA required the determination of the optimum conditions for the production of uniform nanofibres. The conditions that needed to be optimised include the voltage applied, the distance from the needle tip to the collector plate, feed rate of the polymer solution, the concentration of the solution and the solvent system used. The solvent system should first of all have the ability to properly dissolve the polymer. Secondly, other considerations taken into account when selecting a proper solvent system include toxicity and the dielectric constant of the solvents. Once the optimum conditions were determined, SMA could be electrospun in order to create a hydrogel.

4.2.1. SMA crosslinked with different crosslinking agents

In a typical procedure for the preparation of water-absorbing SMA nanofibres, a solution containing 10 wt % SMA with diethylene glycol (DEG) as a crosslinker in a 10 % molar ratio to the SMA, was spun from a 1:2 DMF/acetone solution.

Table 4.1: Electrospinning conditions of SMA

Collector distance (cm)	Voltage (kV)	Flowrate (mL/min)
15	15	0.012

The resulting electrospun nanofibrous membrane was put in an oven at 100 °C for 2 h to allow for crosslinking of the fibres. Crosslinking was therefore done after electrospinning. The crosslinked SMA nanofibrous membrane was hydrolysed in a 1.5 M NaOH/ethanol solution for 24 h at room temperature. This was then followed by washing with ethanol and drying *in vacuo* at 50 °C for 10 h. The resultant nanofibrous mat was soft and pliable. Scheme 4.1 below represents a graphical representation of crosslinking with DEG. The primary alcohol group of DEG can react with the anhydride residue of SMA to produce the product represented in Scheme 4.1. Notice that the product has a primary alcohol available for reaction with another anhydride unit at the end of the glycol chain.

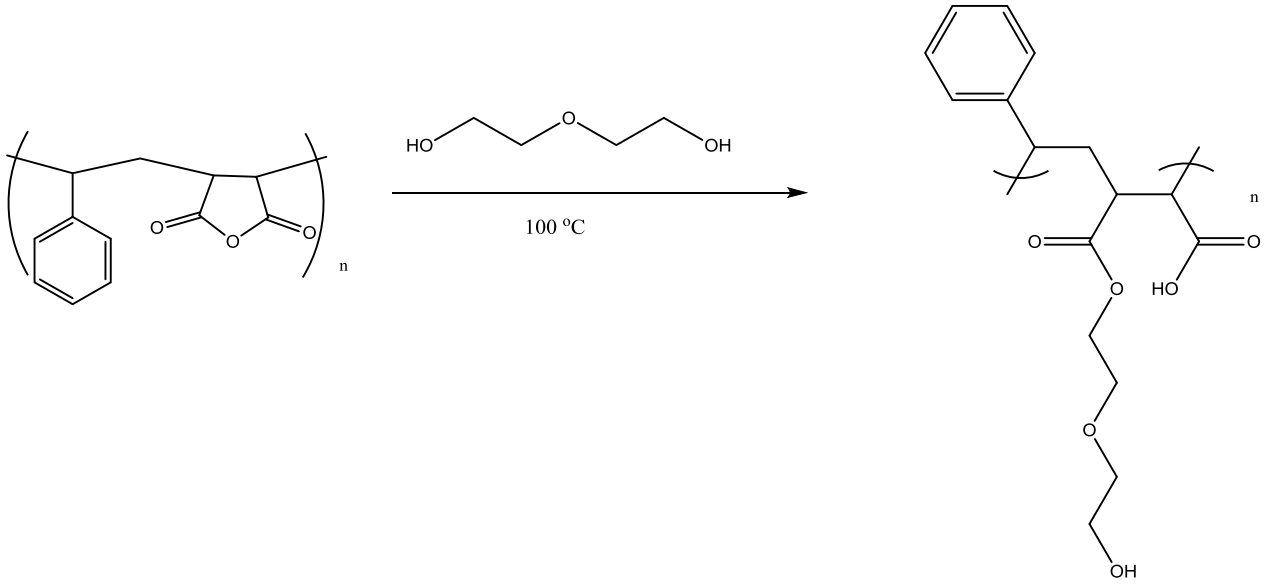

Scheme 4.1: SMA crosslinked with DEG

Using this technique to crosslink SMA also has its drawbacks as it is difficult to quantify the level of crosslinking that take place between the SMA fibres. Even though a 10 molar percentage of the crosslinker was added, one cannot definitively say that a 10 % crosslinking density exists within the fibre matrix. This is due to the possibility of the crosslinker evaporating with the solvent as well as incomplete or intermolecular reaction.

Other crosslinking agents were also considered. SMA was also crosslinked with ethylene diamine (Scheme 4.2). Using this crosslinker meant that the crosslinking procedure described above had to be modified, as addition of the crosslinker to the spinning solution increased the viscosity of the solution, making it difficult or even impossible to spin. This meant that crosslinking was already taking place before electrospinning was complete. This can be expected due to the rapid reaction that takes place between the anhydride moiety of SMA and a primary amine. In a typical procedure for the preparation of water-absorbing SMA nanofibres, a 10 wt% SMA solution was prepared in a 1:2 DMF/acetone solution. After the completion of the spinning process, the obtained fibres were dipped into an isopropanol solution containing 10 molar percentage of the crosslinker to anhydride units. The fibre mats prepared in this manner shrunk and was very brittle upon drying, making it difficult to work with, in the context of a wound dressing.

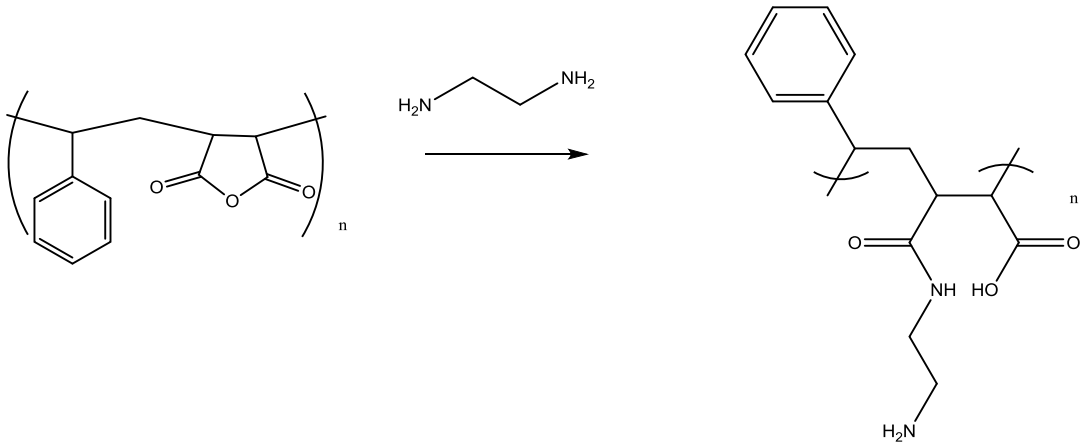

Scheme 4.2: SMA crosslinked with ethylene diamine

From the crosslinking agents already used, it seemed that another crosslinking agent that combined the properties of the other two crosslinking agents would be a good choice to achieve crosslinking that may be quantifiable. This crosslinker would therefore rapidly react with the anhydride units, like for the primary amine and require a heat dependent reaction to complete the crosslinking process, like observed for the primary alcohol when using DEG as crosslinking agent. SMA was thus reacted with 10 molar percent of 2-amino-2-methyl-1-propanol as seen in Scheme 4.3, an agent that contains both a primary amine as well as a primary alcohol. During the reaction process however, the SMA crosslinked and was not soluble in water or organic solvents. This meant that the same electrospinning procedure as for DEG as crosslinker could not be followed. The dipping method could be used, but that still means that the crosslinking density could not be quantified.

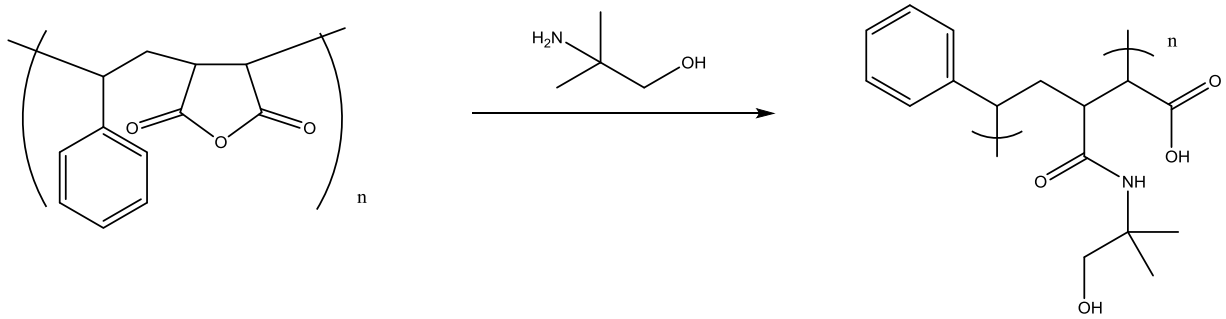

Scheme 4.3: SMA crosslinked with 2-amino-2methyl-1-propanol

SMA crosslinked with DEG was thus used as the hydrogel mat for further studies as it was the easiest to produce and still had soft and pliable characteristics after crosslinking and hydrolysis.

4.3. Electrospinning of sodium alginate and subsequent hydrogel formation

The optimum voltage, needle tip to collector plate distance, feed rate and concentration of alginate was determined in order to electrospin sodium alginate.

Sodium alginate, poly(ethylene oxide) (PEO) and Triton-X 100 (a surfactant) were dissolved in distilled water in different ratios. The optimum ratio of alginate:PEO:surfactant was found to be 4 wt %:4 wt %:2 wt % (with a total solids concentration of 10 wt %) in solution as this was the only solution that yielded uniform fibres.

Table 4.2: Electrospinning conditions of sodium alginate

Collector distance (cm)	Voltage (kV)	Flowrate (mL/min)
15	15	0.008

The nanofibrous mat was then ionically crosslinked by soaking the mat in ethanol for 1 minute, followed by soaking for 10 seconds in a 2 wt % calcium chloride solution in 1:5 ethanol/water. The crosslinked mat was lastly rinsed in water for 1 minute. The stability of the mats was then determined by soaking the mats in distilled water without agitation for up to one week at room temperature.

4.4. Water absorption studies

After the electrospinning and crosslinking of both the SMA and alginate nanofibrous mats, the water absorption of both was determined. Five 1×1 cm squares of each of the mats were cut out and the mats were submerged in a PBS buffer with pH of 7.4 as this mimics physiological conditions.

The squares were submerged in excess PBS buffer for up to 24 h at room temperature without agitation for absorption measurement. The mats were removed and free PBS on the surface was removed by placing on filter paper.

The absorption ratio can be calculated using the following equation:

$$R = \frac{m_w - m_d}{m_d}$$

Equation 4.2: Absorption ratio, where m_w is the mass of the wet mat and m_d is the mass of the dry mat

Table 4.3: Absorption ratios of five 1×1 cm strips of SMA after 24 hrs in PBS buffer

m_w (mg)	m_d (mg)	R
76.8	9.8	6.84
56.7	6.2	8.15
103.2	9.3	10.1
100.4	10.8	8.30
81.8	7.8	9.49
		Average= 8.57

Table 4.4: Absorption ratios of five 1×1 cm strips of alginate after 24 hrs in PBS buffer

m_w (mg)	m_d (mg)	R
212.0	8.5	23.9
175.6	10.7	15.4
400.9	11.9	33.7
643.6	10.7	59.1
775.6	12.8	59.6
		Average= 38.4

From Table 4.3we see that SMA can on average absorb over 800% its own weight in water, whilst Table 4.4 indicates that alginate can absorb over 3800% its own weight in water. The ability of SMA and alginate to absorb large quantities of moisture in its fibrous form may be tentatively ascribed to the large surface to volume ratio exhibited by nanofibres obtained from electrospinning. However, a better conclusion on the ability of SMA and alginate to absorb moisture can be drawn if the same material was subjected to water absorption studies in its different forms (e.g. film or a solid).

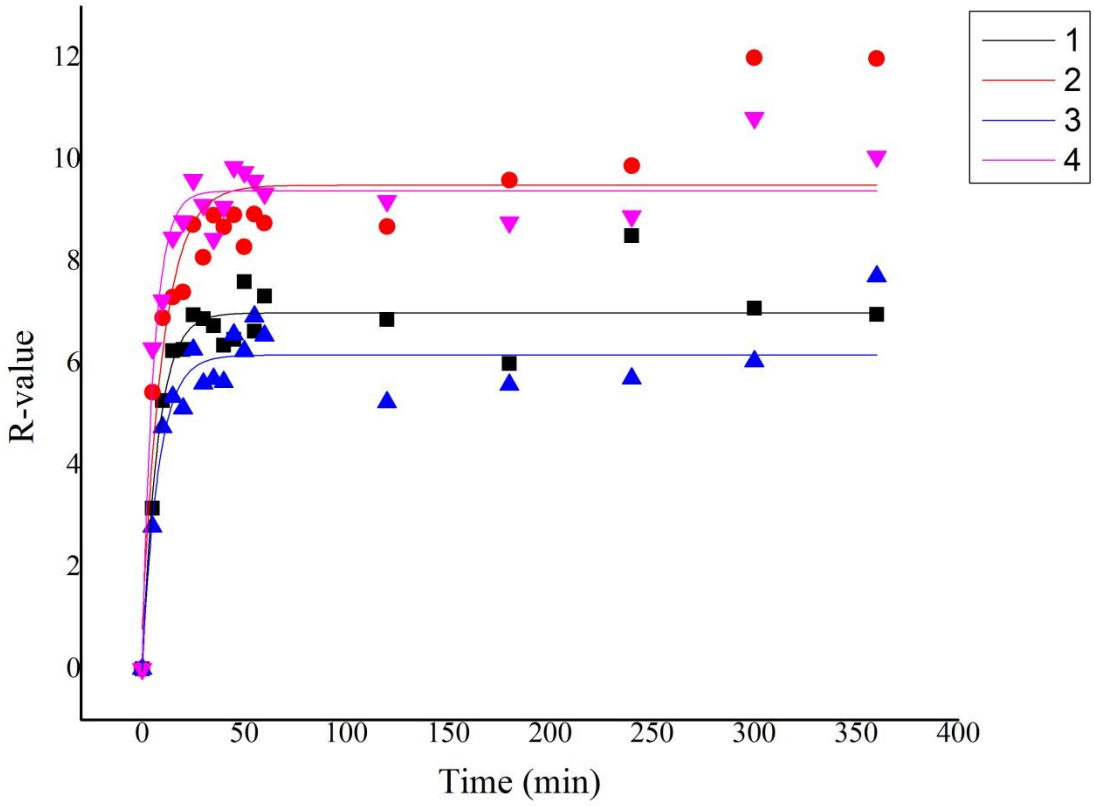

Figure 4.2: SMA water absorption of four 1×1 cm strips over time. 1 = 0.0225 g dry mass, 2 = 0.0151 g dry mass, 3 = 0.0219 g dry mass, 4 = 0.0144 g dry mass

In Figure 4.2 we see the absorption behaviour of SMA in PBS over time. Looking at the individual data points of Figure 4.2 it is difficult to draw a proper idea of the water absorption behaviour of SMA over time; however a general exponential growth curve is seen. Fitting the best curve through the data points, a better picture of water absorption comes to light: we see that all fibre mats show exponential uptake of water up to around 45 min, after which the uptake plateaus. From the masses of the dry fibre squares, we would expect samples 1 and 3 and samples 2 and 4 to exhibit roughly the same behaviour. This is true as can be seen in Figure 4.2 above. The plateauing of the curves can be ascribed to the fibres reaching an equilibrium state at which point no further water uptake is associated with the polymeric fibres. There however still lies the possibility for water to be trapped in the pores between the fibres. It is therefore possible to ascribe the deviation from the expected trend to the possible entrapment of water in the pores of the fibrous mat before the weighing process to determine the mass of water uptake, as the fibre mats are placed on filter paper to remove excess water. Another possible explanation for the deviation is that during the process of removing excess water on filter paper, some of the swollen hydrogel fibres (now very soft and gel-like) got stuck to the filter paper. This means possible loss of fibres or even addition of paper fibres upon removal to weigh.

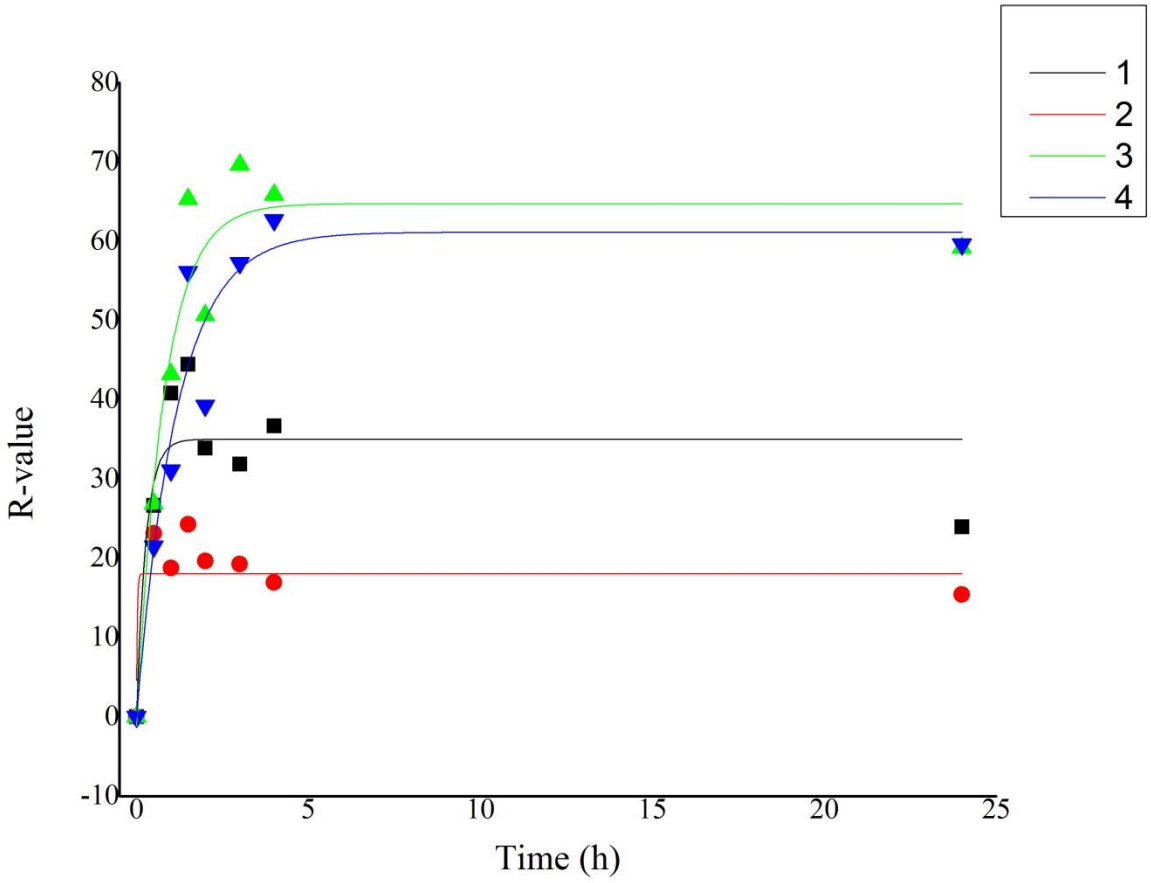

Figure 4.3: Water absorption of four 1×1 cm strips alginate over time. 1 = 0.0085 g dry mass, 2 = 0.0077 g dry mass, 3 = 0.0107 g dry mass, 4 = 0.0128 g dry mass

Figure 4.3 represents the water absorption behaviour of alginate over time. From Figure 4.3 we see that alginate follows the same general trend as seen for SMA in Figure 4.2. If we also draw the best fitted curve through the data points we see an exponential growth curve that plateaus around 3-4 hours of water uptake. The same reasoning as for the SMA hydrogel can be used in terms of the deviations seen: water trapped within the pores of the nanofibrous mats affect the weight of the fibre mat as well as the fibres sticking to the filter paper. In the case of the alginate hydrogel, the time between measurements were also extended. This is due to the soft nature of the wet hydrogel. Excessive handling of the alginate caused the hydrogel to slowly break apart. The time elapsed between measurements were thus extended to minimise damage caused when handling the wet fibrous mat with tweezers.

4.5. Electrospinning of qSMI

In a typical procedure for the preparation of qSMI fibres, 28 wt% SMI (for both SMI-qC_8 and SMI-qC_{12}) was spun from a 1:1 DMF:THF solution.

Table 4.5: Electrospinning conditions of qSMI

Collector distance (cm)	Voltage (kV)	Flowrate (mL/min)
15	15	0.011

The nanofibrous membrane was put in an oven at 120 °C overnight to allow crosslinking of the fibres. Heat treatment rendered the fibres insoluble in water as well as organic solvents.

The qSMI fibres were firstly spun onto the aluminium collector plate following the procedure described above and then heat treated at 120 °C overnight to render them insoluble. This was then followed by the electrospinning of an alginate solution containing alginate:PEO:Triton-X 100 in a ratio of 4 wt %:4 wt %:2 wt % on top of the qSMI fibres. In the second case, qSMI and SMA were spun one onto the other following the procedures described in Sections 4.2 and 4.5, followed by heat treatment at 120 °C to render both layers insoluble in water and organic solvents. In the case of the alginate and qSMI bi-layered systems, the choice to electrospin qSMI and heat treat the fibres, followed by electrospinning of alginate on top of the heat treated qSMI, stemmed from an earlier observation when both layers were electrospun onto one another before heat treatment as heat treatment burned the alginate fibres. Upon closer inspection, the SMA and qSMI fibres adhered to one another; however it was possible to pull the layers apart. The adhesion between these layers may simply be due to how the fibres collected onto the same collector plate, as no heat treatment took place between spinning, thus allowing for possible fusion of the layers. The ability to pull apart the fibre layers however may be ascribed to the brittle nature of SMA. The alginate and qSMI fibres also adhered to one another during the spinning process, but not to the same extent as in the case of SMA. This may be due to the difference in the production process.

4.6. Scanning Electron Microscopy (SEM) imaging

Scanning electron microscopy (SEM) was done on the electrospun fibres described in Sections 4.2, 4.3 and 4.5 in order to determine fibre morphology as well as fibre diameter.

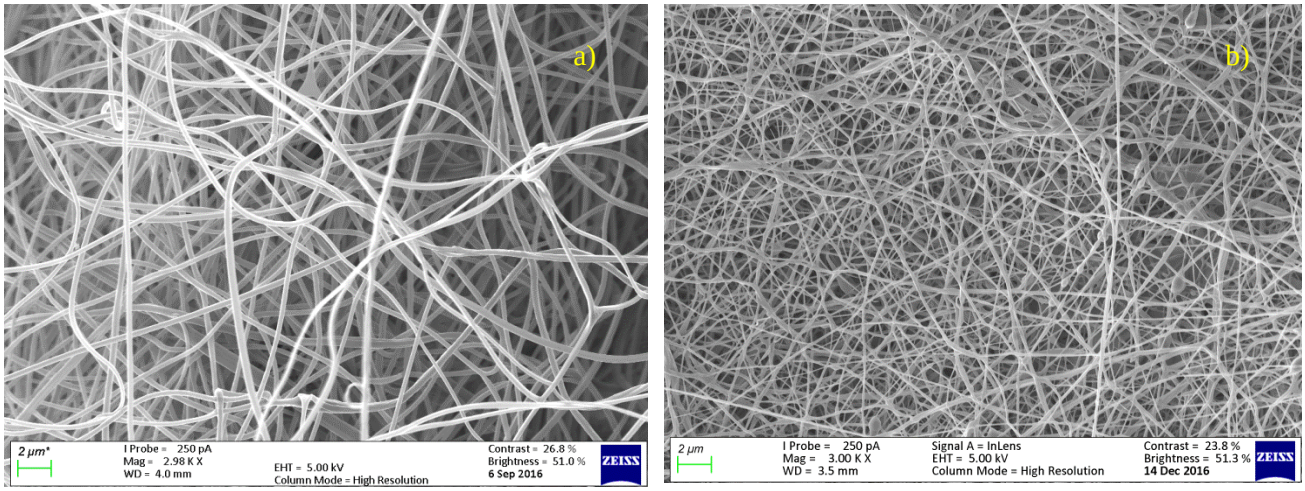

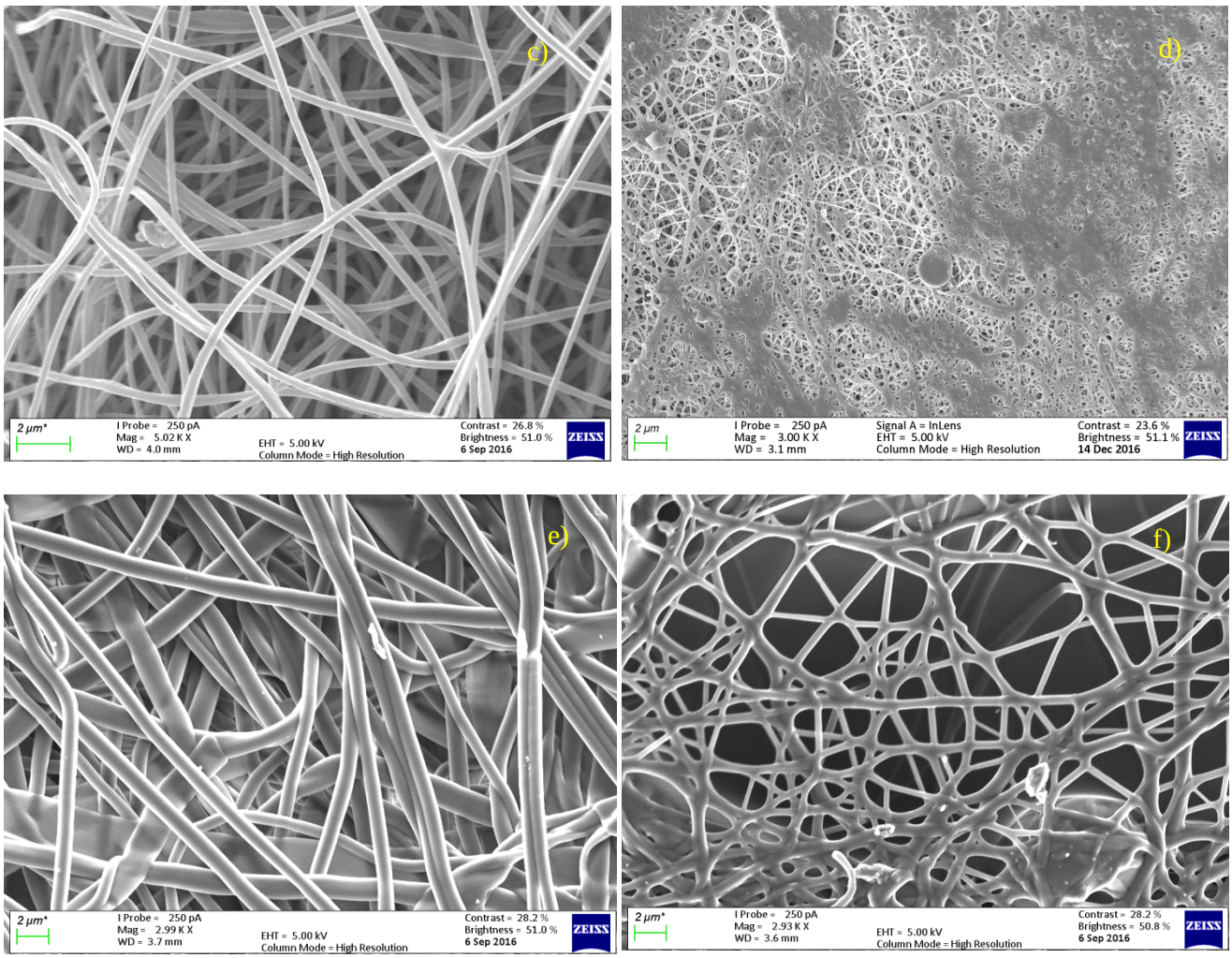

Figure 4.4: SEM imaging of fibre mats: a) SMA at 3000x magnification, b) uncrosslinked alginate at 3000x magnification, c) SMA at 5000x magnification, d) crosslinked alginate at 3000x magnification, e) SMI-qC_{12} at 3000x magnification and f) SMI-qC_8 at 3000x magnification

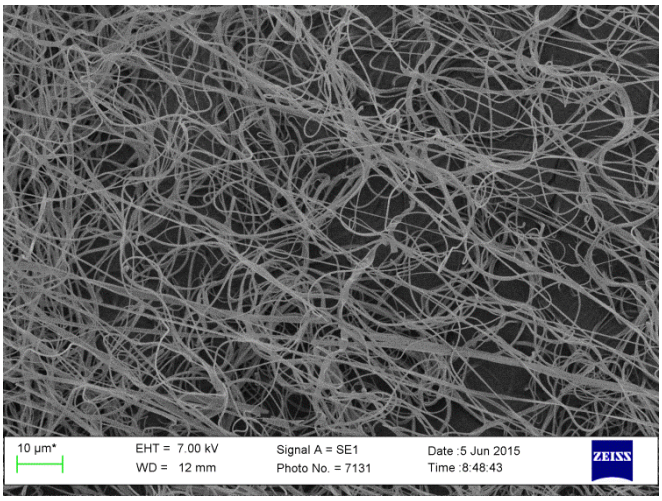

Figure 4.5: SMI qC_8 at 2500× magnification before heat treatment

From Figure 4.4 above, SEM imaging revealed mostly uniform fibre mats. Figure 4.4 d) revealed that after crosslinking of alginate with Ca^{2+}-ions, the nanofibrous structure collapses somewhat. This is expected as the crosslinking process takes place in a solution consisting of 1:5 ethanol:water. Water is a known solvent for alginate and we can thus conclude that the alginate fibres start to dissolve somewhat during the crosslinking

process. The final hydrogel mat however does not seem to be affected by this, as it is still able to absorb water and does not dissolve even when submerged in water for up to 7 days. In Figure 4.4 f) we notice fusion of the nanofibres. The nanofibrous structure does not look fused before heat treatment, as seen in Figure 4.5. This may simply be due to heat treatment that rendered these fibres insoluble in water and organic solvents. It may also be possible that the fibres were not sufficiently dry before heat treatment. It is however difficult to ascribe this phenomenon to crosslinking, as crosslinking takes place on molecular level and can thus not be visualised by means of SEM imaging and therefore we tentatively name it fusion.

Table 4.6: Average fibre diameter of each electrospun polymer and their standard deviation

Fibre mat	Average fibre diameter (nm)	Standard deviation
SMA	310.4	80.2
Uncrosslinked alginate	233.2	70.7
SMI-qC_8	429.1	142.8
SMI-qC_{12}	692.8	173.4

Fibre diameter was determined by taking an average of 100 fibre diameter measurements per sample. The standard deviation was calculated using Microsoft Excel. From Table 4.6 it is interesting to note the average fibre diameters in the sub-micron range. We also note that SMI-qC8 has a smaller fibre diameter than that of SMI-qC12. For both electrospinning solutions the concentration was kept as 28 wt%. During the process of dissolving the polymers, SMI-qC12 took longer to dissolve. It may therefore be possible for the SMI-qC12 solution to be more viscous and therefore producing fibres with a larger diameter. As fibre diameter is also dependent on the applied voltage and distance to the collector plate, the possibility exists that the applied voltage was not sufficiently high enough or the distance to the collector plate not far enough to obtain thinner fibres.

4.6.1. Scanning Electron Microscopy (SEM) characterisation details

Analysis was done on a LEO 1450 VP SEM equipped with a secondary electron detector, variable pressure secondary electron detector, backscattered electron detector, energy dispersive X-ray spectrometer, cathodoluminescence and wave dispersive X-ray spectrometer. Each fibre mat was cut into 0.5 cm × 0.5 cm squares and stuck onto a SEM stub using double sided carbon tape to ensure proper conductivity between the stub and the sample. The samples were sputter-coated with gold under vacuum before the SEM imaging process. Once the SEM images were obtained the images were analysed to determine fibre diameter using SEM Image Studio. An average of 100 fibre diameters per sample were measured. The average fibre diameter and standard deviation were then calculated using Microsoft Excel and summarised in Table 4.6.

4.7. Conclusions

Uniform nanofibres could be produced from synthetic polymers, namely SMA, SMI qC_8 and SMI qC_{12} as well as a natural polymer, namely sodium alginate, using the single needle electrospinning technique as could be confirmed using SEM (Figure 4.4). The fibre diameter of the individual fibres is summarised in Table 4.3. After electrospinning, SMA and alginate could then be successfully crosslinked by either a heat activated crosslinking agent like in the case of SMA or a divalent cation, like in the case of alginate. The crosslinked SMA and alginate fibres were then submerged in PBS over 24 hours in order to determine the absorption ratio of the hydrogels formed when subjected to moisture. It was found that SMA had an average R-value of 8.57 for five 1×1 cm strips submerged in PBS for 24 hours, whilst alginate had an average R-value of 38.4. Absorption behaviour of SMA and alginate in PBS over time was also studied. From Figure 4.2 it was noticed that SMA reached equilibrium absorption at around 45min, whilst in Figure 4.3 it was noticed that alginate reaches equilibrium at around 3-4 h. Bi-layered systems containing qSMI and either SMA or alginate were also electrospun. It was however found that the layers could be removed by simply pulling them apart.

4.8. References

(1) Tan, S.-H.; Inai, R.; Kotaki, M.; Ramakrishna, S. *Polymer (Guildf).* **2005**, *46*, 6128–6134.

(2) Subbiah, T.; Bhat, G.; Tock, R.; Parameswaran, S.; Ramkumar, S. *J. Appl Polym Sci.* **2005**, *2*, 557-569.

(3) Reneker, D. H.; Yarin, A. L. *Polymer.* **2008**, *10*, 2387-2425.

(4) Salles, V.; Seveyrat, L.; Fiorido, T.; Hu, L.; Galineau, J.; Eid, C.; Guiffard, B.; Brioude, A.; Guyomar, D. *In Tech Open.* **2012**.

(5) Uyar, T.; Besenbacher, F. *Polymer.* **2008**, *24*, 5336-5343.

(6) Lee, S. J.; Tatavarty, R.; Gu, M. B. *Biosens. Bioelectron.* **2012**, *1*, 302-307.

(7) Cui, W.; Li, X.; Zhou, S.; Weng, *J. Polym. Degrad. Stab.* **2008**, *3*, 731-738.

(8) Koombhongse, S.; Liu, W.; Reneker, D. H. *J Polym. Sci.* **2001**, *39*, 2598-2606.

(9) Cronje, L. *Surface modification of styrene maleic anhydride nanofibers for efficient capture of Mycobacterium tuberculosis*, PhD Thesis, University of Stellenbosch, South Africa. **2012**.

(10) Prabhakaran, M. P.; Venugopal, J.; Ghasemi-Mobarakeh, L.; Kai, D.; Jin, G.; Ramakrishna, S. *Adv. Polym. Sci*. **2012**, *246*, 21-62.

(11) Yarin, A.; Koombhongse, S.; Reneker, D. *J. Appl. Phys.* **2001**, *9*, 4836-4846

(12) Doshi, J.; Reneker, D. H. *J. Electrostatics* **1995**, *2*, 151-160.

(13) Ding, W.; Wei, S.; Zhu, J.; Chen, X.; Rutman, D. *Macromol. Mater. Eng*. **2010**, *295*, 958–965.

(14) Mitchell, S. B.; Sanders, J. E. *J Biomed Mat Res*. **2006**, 110-120.

(15) Chronakis, I. S. *J. Mater. Process. Technol.* **2005**, *167*, 283–293.

(16) Liu, W.; Thomopoulos, S.; Xia, Y. *Adv. Healthc. Mater.* **2012**, *1*, 10–25.

(17) Willemse, A. C. *Electrospinning bicomponent nanofibres for platinum ion extraction from acidic solutions*, MSc Thesis, University of Stellenbosch, South Africa. **2013**.

(18) Alamein, M. A.; Liu, Q.; Stephens, S.; Skabo, S.; Warnke, F.; Bourke, R.; Heiner, P.; Warnke, P. H. *Adv. Healthcare Mater.* **2012**.

(19) Smit, A. E.; Sanderson, R. D. *Method and apparatus for the production of fine fibres.* **2009**

(20) Chronakis, I. S.; Milosevic, B.; Frenot, A.; Ye, L. *Macromolecules.* **2006**, *1*, 357-361.

(21) Agarwal, S.; Wendorff, J. H.; Greiner, A. *Polymer.* **2008**, *26*, 5603-5621

(22) Frenot, A.; Chronakis, I. S. *Curr. Opin. Colloid Interface Sci.* **2003**, *1*, 64-75.

(23) Kilic, A.; Oruc, F.; Demir, A. *Text. Res. J.* **2008**, *6*, 532-539.

(24) Theron, S.; Yarin, A.; Zussman, E.; Kroll, E. *Polymer.* **2005**, *9*, 2889-2899.

(25) Teo, W.; Ramakrishna, S. *Composites Sci. Technol.* **2009**, *11*, 1804-1817.

(26) Macossay, J.; Marruffo, A.; Rincon, R.; Eubanks, T.; Kuang, A. *Polym. Adv. Technol.* **2007**, *3*, 180-183.

(27) Sohraby, K.; Minoli, D.; Znati, T. *WSN: technology, protocols, and applications;* John Wiley & Sons. **2007**.

(28) Ryu, Y. J.; Kim, H. Y.; Lee, K. H.; Park, H. C.; Lee, D. R. *Eur Polym J.* **2003**, *9*, 1883-1889.

(29) Thompson, C.; Chase, G.; Yarin, A.; Reneker, D. *Polymer*. **2007**, *23*, 6913-6922.

(30) McKee, M. G.; Wilkes, G. L.; Colby, R. H.; Long, T. E. *Macromolecules.* **2004**, *5*, 1760-1767.

(31) Huang, C.; Chen, S.; Lai, C.; Reneker, D. H.; Qiu, H.; Ye, Y.; Hou, H. *Nanotechnology*. **2006**, *6*, 1558-1563.

(32) Deitzel, J. M.; Kleinmeyer, J.; Harris, D.; Tan, N. C. B. *Polym.* **2001**, *42*, 261–272.

(33) Dersch, R.; Steinhart, M.; Boudriot, U.; Greiner, A.; Wendorff, J. *Polym. Adv. Technol*. **2005**, 2-3, 276-282.

(34) Beachley, V.; Katsanevakis, E.; Zhang, N.; Wen, X. *Biomedical Applications of Polymeric Nanofibers;* Springer. **2012**, 171-212.

Chapter 5: Antimicrobial evaluation

5.1. Introduction

In the biological world, a question frequently asked when working with microbes, and probably the most important question, is "Are the microbial cells dead or alive?" In extreme cases, like for example in biological terrorism, the pathogenic viability is of great importance given the possible dire outcome to humans when exposed to a viable organism. The viability of a microbe is thus important in order to determine the risk related to exposure to a pathogenic microbe. Traditionally bacterial viability is determined by plate count[1]. This method however underestimates the real viability of a microbial colony as it only expresses the portion of the colony can undergo cell division in selected culture conditions. There are however three stages of cell viability, namely: viable, nonviable but resuscitable, and nonviable[1]. Sub-degrees of viability of individual cells may also exist due to stress caused by starvation or injury. These sub-degrees would however not be detectable using a plate culture method. One can thus encounter microbes in a viable but nonculturable state and other viable cells that do not reproduce in an environment.

Today various aspects of bacterial vegetative-cell viability can be tested by utilising fluorescent dyes. Common tests include respiratory activity for aerobic and anaerobic bacteria, membrane potential and membrane integrity[1].

This chapter thus presents an antimicrobial evaluation of the electrospun fibres prepared in Chapter 4. The antimicrobial activity of the electrospun fibres was examined against *Staphylococcus aureus*, a Gram-positive bacterium, and *Pseudomonas aeruginosa*, a Gram-negative bacterium. The evaluation utilised fluorescence imaging as well as zone inhibition studies on agar plates.

5.2. Evaluation with Fluorescence Imaging

Fluorescent microscopy has shown to be a rather useful tool in evaluating cell viability in terms of toxicity and antimicrobial activity[2, 3]. The use of different fluorescent dyes that stain target cell constituents, like RNA, DNA and nucleic acids, makes fluorescent imaging a versatile technique. Commercially available kits commonly used to differentiate between viable and nonviable cells are known as "LIVE/DEAD" BacLight Bacterial Viability kits. "LIVE/DEAD" stains are used to determine viability as a function of the membrane integrity of a microbial cell[1, 4]. It is therefore possible to monitor the lysis process by determining the number of intact cells as well as the number of permeable cells at different time points, utilising these commercially available florescent stains[4]. Confocal fluorescence microscopy was thus done on all samples to determine antimicrobial activity of the fibres.

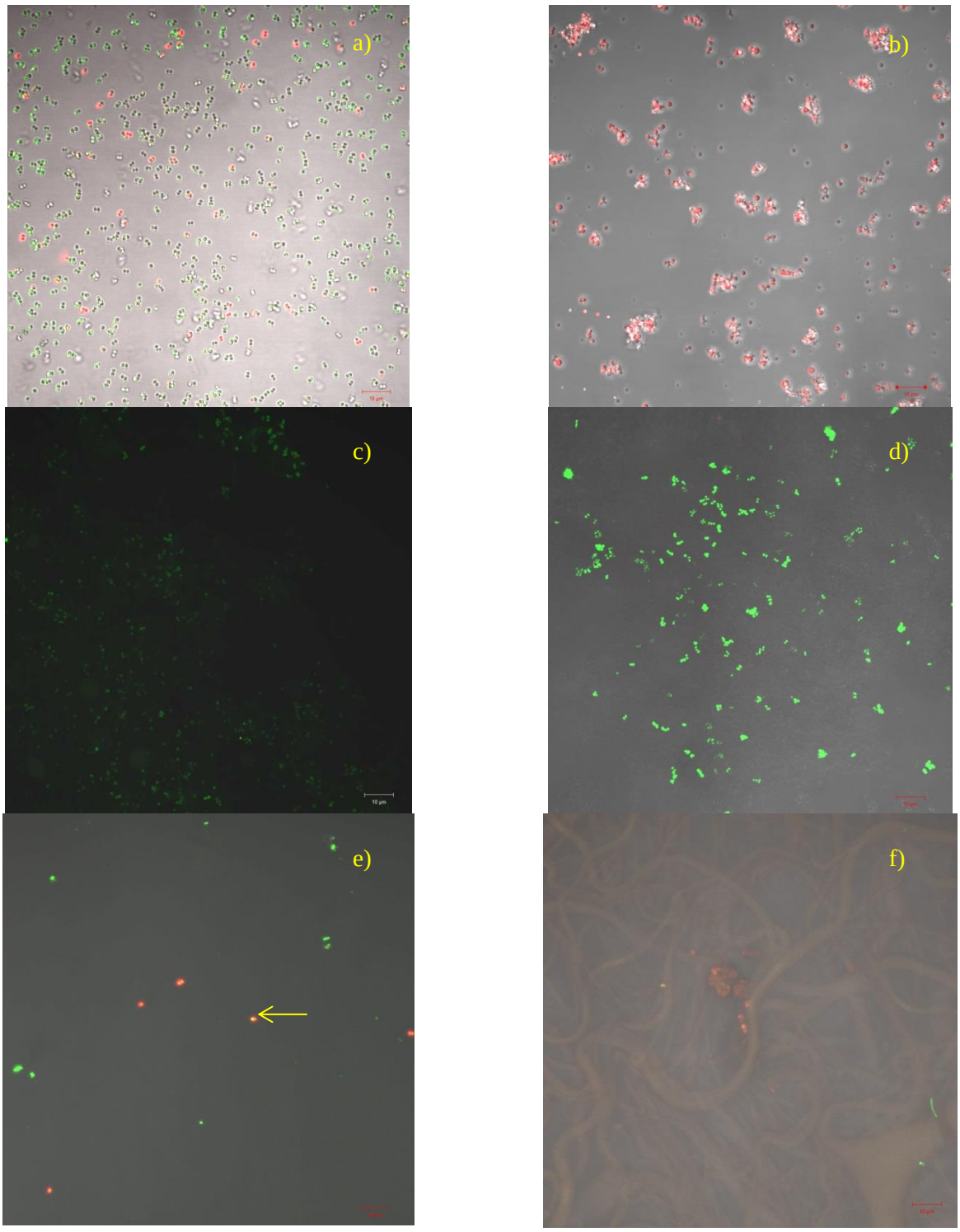

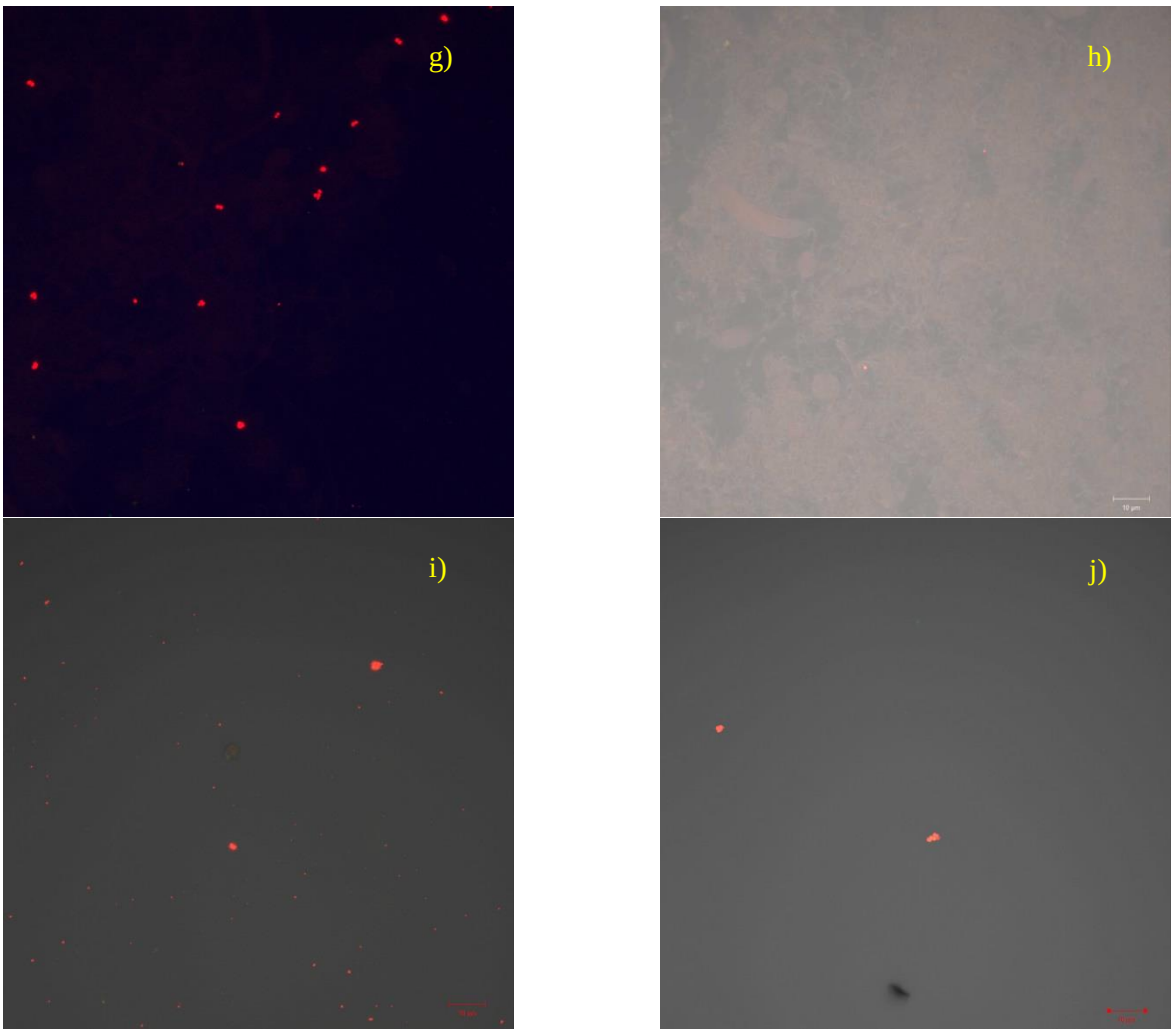

Figure 5.1: Confocal fluorescence imaging of *Staphylococcus aureus* exposed to electrospun fibres: a) Live control, b) Dead control, c) SMA, d) Alginate, e) SMI qC_8, f) SMI qC_{12}, g) SMA and SMI qC_8, h) SMA and SMI qC_{12}, i) Alginate and SMI qC^8, j) Alginate and SMI qC_{12}

Figure 5.1 above shows the fluorescent images of *Staphylococcus aureus* exposed to the different electrospun fibres. The images were taken within 2-4 hours of exposure to the fibres. In the images seen in Figure 5.1 c) and d) we see that neither sodium alginate nor SMA show any antimicrobial activity towards *S. aureus* as the overall majority of organisms are green in colour, indicative of viable cells. In Figure 5.1 e) we see that some of the cells are green, indicating viability, whilst some others are red and orange. The yellow arrow in Figure 5.1 e) points to a cell where one can see a red edge with an orange internal colour. This can be explained as follows: as the cell wall of the organism loses its integrity the red fluorescing PI dye can now enter the cell and stain the internal structures of the cell. The orange colour is thus due to this increase in red fluorescing PI in the internal structures of the organism. In Figure 5.1 f) we see the fibrous structure of the SMI qC_{12} mat. We can see a clump of cells that fluoresces red. This indicates that the cells present on the fibrous mat are nonviable. We can thus conclude that the SMI qC_{12} fibres exhibit greater antimicrobial activity against *S. aureus* as compared to SMI qC_8. This is in agreement with what was found by Bshena[5] in 2012 where he indicated that SMI quaternised with longer aliphatic chains exhibited a greater antimicrobial activity. The same behaviour is seen in Figure 5.1 g)-j).

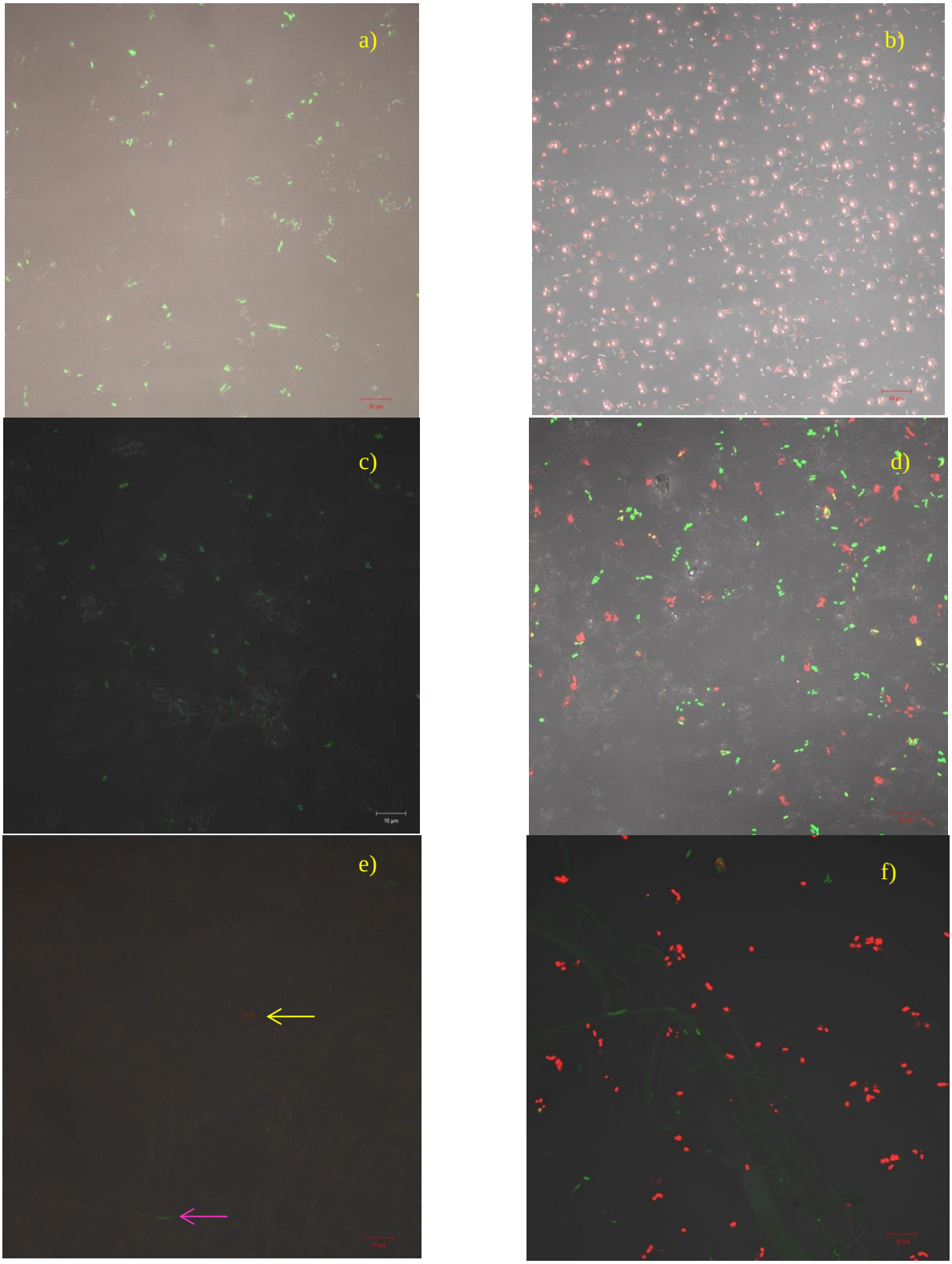

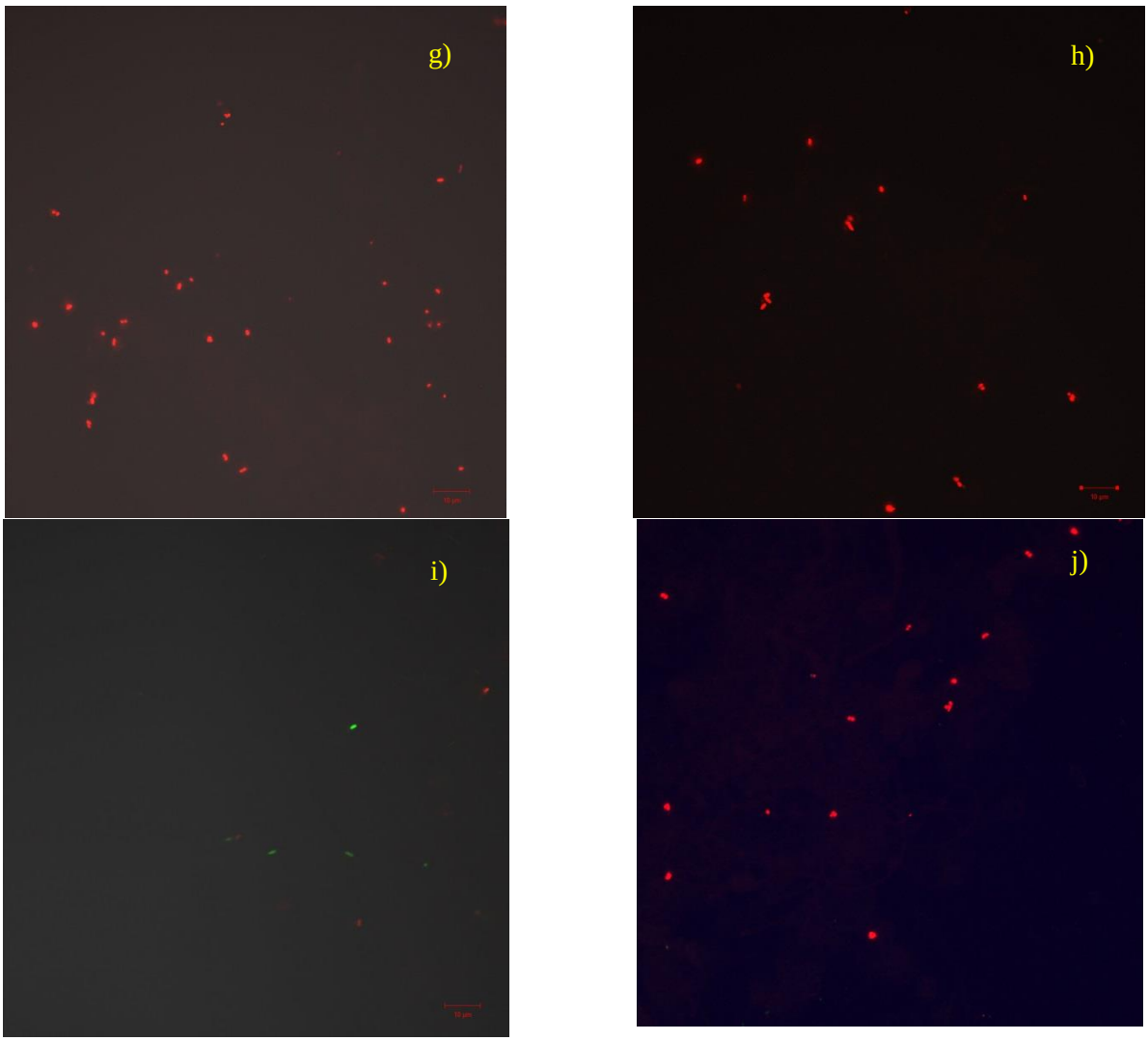

Figure 5.2: Confocal fluorescence imaging of *Pseudomons aeruginosa* exposed to electrospun fibres: a) Live control, b) Dead control, c) SMA, d) alginate, e) SMI qC_8, f) SMI qC_{12}, g) SMA and SMI qC_8, h) SMA and SMI qC_{12}, i) Alginate and SMI qC^8, j) alginate and SMI qC_{12}

Figure 5.2 above shows the fluorescent images of *Pseudomonas aeruginosa* exposed to the different electrospun fibres. The images were taken within 2-4 hours of exposure to the fibres. In the images seen in Figure 5.2 c) we see that all cells present on the SMA are green in colour, indicating that they are still viable. Figure 5.2 d) on the other hand has both red and green cells present on the alginate mat. It is not expected that sodium alginate has any antimicrobial activity towards *P. aeruginosa*. It may however be due to natural cell death, seeing as in a normal colony both viable and nonviable cells are present. It may also be due to the cells not being in a nutrient rich environment anymore. In Figure 5.2 e) towards the bottom of the image the magenta arrow indicates some viable cells on the SMI qC_8 fibre. The yellow arrow in the middle of the image points to a clump of red cells, indicating nonviability. In Figure 5.2 f) we see the fibrous structure of the SMI qC_{12} mat. We also see green viable cells present on the fibres of the SMI qC_{12} mat. Most of the cells however are red, and thus not viable. The same antimicrobial behaviour is seen for SMA and alginate in combination with SMI qC_8 and SMI qC_{12} in Figure 5.2 g)-j).

5.3. Zone inhibition on agar plates

Evaluation of antimicrobial activity by zone inhibition is a common, straight-forward method used in the biological field. Simply put, organisms are grown on growth media and subjected to some kind of antimicrobial agent, whether it is an antibiotic[6, 7] or another microbe[8] that inhibits the growth of a second microbe in the same environment. Microbial growth inhibition can then be observed visually as clear halos

where no growth around the antimicrobial agent will be present. This simple technique is thus a favourable method to also determine the antimicrobial activity of the electrospun fibres prepared in Chapter 4.

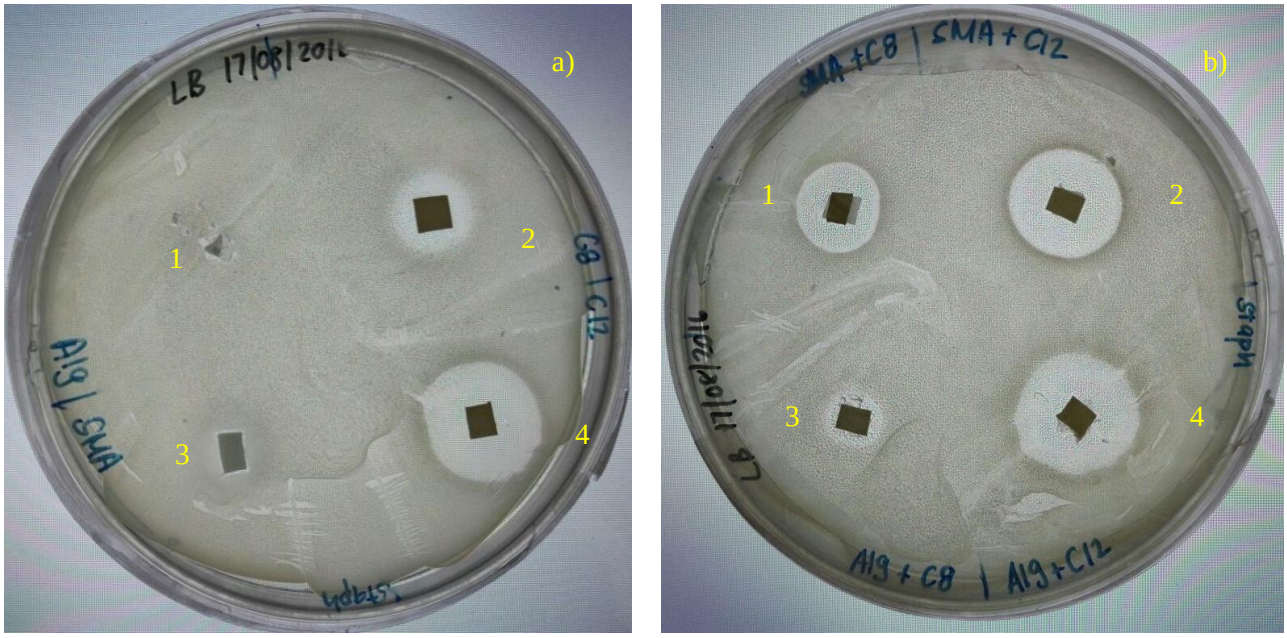

Figure 5.3: Zone inhibition plates of *Staphylococcus aureus*: a) 1: alginate, 2: SMI qC_8, 3: SMA, 4: SMI qC_{12}; b) 1: SMA and SMI qC_8, 2: SMA and SMI qC_{12}, 3: alginate and SMI qC_8, 4: alginate and SMI qC_{12}.

In the top left corner of Figure 5.3 a) we see that alginate does not exhibit a clear zone around the fibres placed onto the agar plate. This is expected as sodium alginate does not exhibit antimicrobial properties. The SMA fibre mat in the bottom left corner of Figure 5.3 a) seems to have a clear zone where no microbial growth is present around it. This is not expected as SMA does not exhibit antimicrobial properties. A possible explanation for this occurrence may be the presence of NaOH on the SMA mat as a 1.5 M NaOH/ethanol solution is used to hydrolyse the SMA nanofibrous mat. In the top right corner of Figure 5.3 a) we see a distinctly clear zone where no microbial growth is present around the SMI qC_8 fibre mat. SMI qC_{12} in the bottom right corner of Figure 5.3 a) exhibits an even larger zone where no microbial growth is present. We can thus say that SMI qC_{12} has a greater antimicrobial effect on *S. aureus* than SMI qC_8, as expected from the work done by Bshena in 2012.

Clear zones where microbial growth is not present can be seen in the case of SMA and SMI qC_8 in the top left corner of Figure 5.3 b), as well as for alginate and SMI qC_8 in the bottom left corner, SMA and SMI qC_{12} in the top right corner and alginate and SMI qC_{12} in the bottom right corner of Figure 5.3 b). Once again the double-layered system containing SMI qC_{12} shows greater antimicrobial activity towards *S. aureus* than those containing SMI qC_8, as indicated by the difference in the size of the clear zones about each fibre mat (the clear zones with no microbial growth of SMI qC_{12} are larger than that of SMI qC_8).

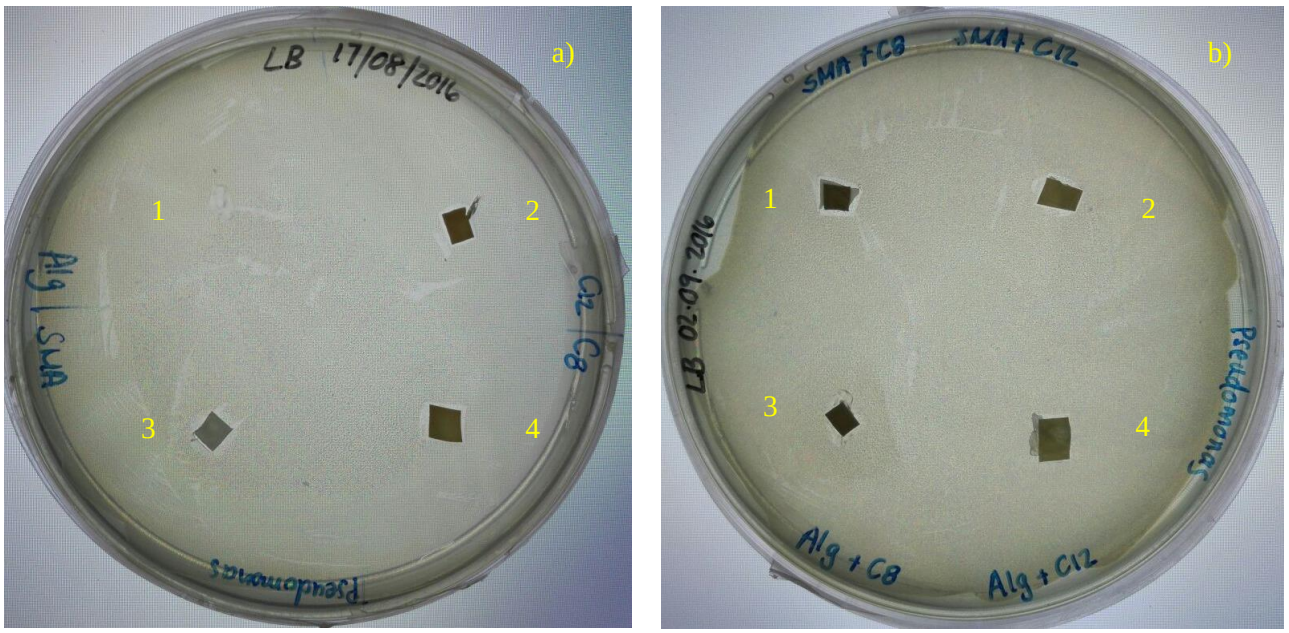

Figure 5.4: Zone inhibition plates of *Pseudomonas aeruginosa*: a) 1: alginate, 2: SMI qC_{12}, 3: SMA, 4: SMI qC_8; b) 1: SMA and SMI qC_8, 2: SMA and SMI qC_{12}, 3: alginate and SMI qC_8, 4: alginate and SMI qC_{12}

Alginate, in the top left corner of Figure 5.4 a), shows no clear zone where no microbial growth takes place around the fibre mat placed onto the agar plate. It is also interesting to note that the fibrous mat formed a hydrogel as seen by the clear colour of the mat and also gel-like consistency upon closer inspection of the agar plate. In the bottom left corner of Figure 5.4 a), it seems like there is a clear zone of no microbial growth around the SMA fibre mat. This is unexpected, but it may be possible that residual NaOH from the 1.5 M NaOH/ethanol solution used to hydrolyse the SMA fibres were present on the fibres and caused the observed clear zone. Though a bit more difficult to see as compared to SMI qC_8 and SMI qC_{12} in Figure 5.3 a), we also notice small zones of inhibited microbial growth about SMI qC_{12} in the top right corner and SMI qC_8 in the bottom right corner of Figure 5.4 a). It is also not clear which of SMI qC_8 and SMI qC_{12} exhibits a greater antimicrobial activity towards *P. aeruginosa* from the aforementioned figure.

Clear zones of antimicrobial growth inhibition are also present in the double layered mats of SMA and SMI qC_8, alginate and SMI qC_8 as well as SMA and qC_{12} as seen in Figure 5.4 b). From the bottom right corner of Figure 5.4 b) however it is unclear whether the alginate and SMI qC_{12} bi-layered mat shows any antimicrobial activity.

5.4. Conclusion

From the confocal images in Figure 5.1, as well as zone inhibition studies we see that both SMI qC_8 and SMI qC_{12} exhibit antimicrobial activity towards *Staphylococcus aureus*. SMI qC_{12} exhibits a greater degree of antimicrobial activity towards *S. aureus* as can be seen from the larger zones of growth inhibition seen in Figure 5.3 a) and b). The bi-layered systems containing either SMA or alginate with SMI qC_{12} also exhibits greater antimicrobial activity towards *S.areaus* than SMA or alginate with SMI qC_8. This is in agreement with what was previously shown by Bshena.

The confocal images for *Pseudomonas aeruginosa* in Figure 5.2 also showed that both SMI qC_8 and SMI qC_{12} exhibited antimicrobial activity towards *P. aeruginosa*. This was also seen for the bi-layered systems containing either SMA or alginate with SMI qC_8 and SMI qC_{12}. It was however difficult to conclude from both the confocal images and the zone inhibition plates which of the two quarternised fibres showed greater antimicrobial activity towards *P. aeruginosa*.

Interestingly it seemed like SMA exhibited antimicrobial activity on both *S. aureus* and *P. aeruginosa* when looking at the zone inhibition plates. This however did not correlate with what was seen in the confocal images and a plausible explanation is the possible presence of residual NaOH on the fibre mats from the hydrolysis procedure which utilises a 1.5 M NaOH/ethanol solution.

5.5. Sample preparation and microscopy

Before any antimicrobial testing was done on the electrospun fibres, the fibre samples were placed in a glass desiccator containing chloroform overnight in order to sterilise the samples and prevent any contamination acquired during the production of the fibres.

5.5.1. Confocal fluorescence imaging

Imaging was done on a Carl Zeiss Confocal LSM 780 Elyra S1 (Figure 5.5) with a SR-SIM superresolution microscope at the Central Analytical Facility at Stellenbosch University.

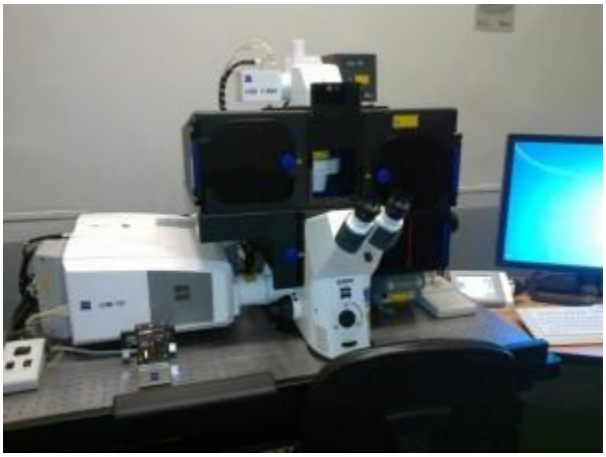

Figure 5.5: Carl Zeiss Confocal LSM 780 Elyra S1 microscope used for fluorescent imaging

For fluorescence imaging, 20 mL Luria-Bertani (LB) media was inoculated with 3-5 colonies of the organism (either *S. aureus* or *P. aeruginosa*) and grown at 37 °C overnight (16 hours) at 150 rpm at an angle. A 200 µL volume of the culture was then transferred to 5 mL of fresh LB media and grown for a further 5 hours in order to ensure that the cells are in its logarithmic growth phase. The culture was then diluted to an optical density (OD) = 0.2 and 10 µL transferred to each of the samples used for imaging.

Staining of the bacteria was done using a "LIVE/DEAD" BacLight Bacterial Viability kit containing Proidium Iodide (PI) and Syto9 dyes. A stock solution of the dyes was made by adding 1µL of each dye to 1000 µL PBS. Staining was then done by adding 100 µL of the dye stock solution to a well in a sample plate containing the fibre mats in individual wells.

5.5.2. Zone inhibition method

Twenty mL LB media was inoculated with 3-5 colonies of the organism (either *S. aureus* or *P. aeruginosa*) and grown at 37 °C overnight (16 hours) at 150 rpm at an angle. The culture was then diluted to an optical density (OD) = 0.2 and 200 µL transferred to each of the agar plates. The plates were incubated overnight at 37 °C after which the plates were inspected for halos, indicating antibacterial growth.

5.6. References

(1) Laflamme, C.; Lavigne, S.; Ho, J.; Duchaine, C. *J Applied Microbiology*, **2004**, *96*, 684-692.

(2) Schiffman, J. D.; Elimelech, M. *ACS Applied Materials & Interfaces* **2011**, *3*, 462-468.

(3) Kang, S.; Pinault, M.; Pfefferle, L. D.; Elimelech, M. *Langmuir* **2007**, *23*, 8670-8673.

(4) Bunthof, C. J.; van Schalkwijk, S.; Meijer, W.; Abee, T.; Hugenholtz, J. *Applied and Environmental Microbiology* **2001**, 4264-4271.

(5) Bshena, O. E. S. *Synthesis of Permanent Non-Leaching Antimicrobial Polymer Nanofibers*, PhD Thesis, University of Stellenbosch, South Africa. **2012**.

(6) Supré, K; Lommelen, K.; De Meulemeester, L. *Veterinary Microbiology*, **2014**, *171*, 374-381.

(7) Bruin, J. P.; Diederen, B. M. W.; Ijzerman, E. P. F.; Den Boer, J. W.; Mouton, J. W. *Diagnostic Microbiology and Infectious Disease*, **2013**, *76* ,339-342.

(8) Bockelmann, W.; Koslowsky, M.; Goerges, S.; Scherer, S.; Franz, C. M. A. P.; Heller, K. J. Food control, **2017**, *17*, 50-56.

Chapter 6: Epilogue

6.1. General conclusions

This thesis focused on the design of a bi-layered wound dressing based on antimicrobial polymer. It has been shown that a moist wound environment is favourable for healing as it increases healing rates. For this reason, a hydrogel was chosen as the first layer of the wound dressing. A hydrogel was then made based on the materials already in use for hydrogel dressings, namely sodium alginate. Though sodium alginate dressings are usually in the form of a sheet, the object of this study was to electrospin both the hydrogel as well as the second antimicrobial layer. A second hydrogel was also introduced in the form of SMA. SMA is an attractive polymer due to its chemical and biological properties, wide availability and low cost. SMA is also the parent molecule from which the polymeric antimicrobial layer was synthesised and then electrospun to achieve the bi-layered wound dressing.

In Chapter 3 the synthesis and characterisation of SMA using conventional free radical chemistry is described. SMA was then successfully modified to yield a SMI precursor, followed by further modification with 2 different alkylhalides, namely 1-bromooctane and 1-bromododecane. During the modification of SMA to yield the SMI precursor, it was found that at lower modifications (30-60 %) of SMA with DMAPA (a compound containing both a primary and tertiary amine) clumping took place. A model study using 1,2-*cis*-cyclohexanedicarboxylic anhydride as model compound was devised in order to better understand this clumping phenomenon and possibly shed some light on the crosslinking of SMI. The model compound was reacted with both DMAPA and TEA. The successful reaction of the model compound with TEA suggests that at lower modifications of SMA with DMAPA intramolecular crosslinking reactions take place with the tertiary amine group of DMAPA, since the primary amine readily reacts with the anhydride residues of SMA. This may also serve as a plausible explanation for the crosslinking of SMI derivatives, like when qSMI fibres are heat treated, rendering them insoluble in water and organic solvents.

Chapter 4 represented the electrospinning process of SMA and its derivatives as well as sodium alginate to obtain nanofibres. SMA and alginate were crosslinked by means of a crosslinking agent in the case of SMA and a divalent cation (Ca^{2+}) in the case of alginate, to yield fibrous hydrogels. The fibrous hydrogels were then subjected to moisture in order to determine their water absorption behaviour over time. It was shown that SMA has a R-value of 8.57 and reaches equilibrium absorption at around 45 minutes of being submerged in PBS. Alginate on the other hand has a R-value of 38.4 and reaches equilibrium absorption at around 3-4 hours of being submerged in PBS. Bi-layered systems of the different qSMI fibres with either SMA or alginate as hydrogel were also produced. The layers seem to have adhered to one another during the electrospinning process, but could be pulled apart.

Chapter 5 described the antimicrobial activity of the fibres and bi-layered systems produced in Chapter 4. The antimicrobial activity was investigated against a Gram-positive bacterium, namely *Staphylococcus aureus*, as well as a Gram-negative bacterium, namely *Pseudomonas aeruginosa*. Fluorescence imagings showed that both SMI qC_8 and SMI qC_{12} as well as the bi-layered systems containing SMI qC_8 and SMI qC_{12} were able to kill the different bacteria. Zone inhibition of the fibres on agar plates was also studied. It was found that SMI qC_{12} and the bi-layered system containing SMI qC_{12} exhibited greater antimicrobial activity against *Staphylococcus aureus* than SMI qC_8 or the bi-layered system containing SMI qC_8. For *Pseudomonas aeruginosa* it was found that both SMI qC_8 and SMI qC_{12} and their bi-layered systems exhibited antimicrobial activity. It was however difficult to determine which of the two antimicrobial polymeric fibres exhibited greater antimicrobial activity against *Pseudomonas aeruginosa*.

6.2. Future recommendations

The encouraging results in terms of antimicrobial activity of SMI qC_{12} against *Stahylococcus aureus* has considerable potential as a wound dressing, considering the widespread occurrence of secondary infection in hospitals due to this organism. Further research in terms of toxicity to human cells is required for wound dressings containing SMI qC_{12}. The production of hydrogels in nanofibrous form is also an advantageous development from this study, as it may minimise problems like adhering to wounds. Further studies in terms of moisture absorption capabilities of the different hydrogels in a different form (like film or sheet) should also be investigated. Although we know that alginate dressings are already in use, hydrogels from SMA should also be evaluated for toxicity and biocompatibility towards mammalian cells. Study into the combined double-layered wound dressing produced in this study should also include investigation towards biocompatibility and toxicity of the wound dressing with mammalian cells.

Acknowledgements

First of all, I would like to acknowledge and thank my supervisor, Prof Bert Klumperman for giving me the opportunity to join his research group. I am grateful for the opportunity to develop my skills under your hand. I would also like to thank Dr Eric van den Dungen for his assistance and patience in helping me develop my research skills as lab assistant during my Undergraduate studies, as well as Dr Rueben Pfukwa for his constant input and guidance.

Thank you to INNOVUS and Stellenbosch University for funding.

I would also like to thank all he helpful analysts at CAF Stellenbosch for their friendly service, Elsa and Jaco for their contribution to my research with NMR spectroscopy, Nadine, Anna and Simba for SEC analysis, Malcolm and Marietjie for LC-MS analysis, Lize for Fluorescence imaging and Angelique and Madeleine at SEM. I also thank Wilma van Rensberg in the BIOPEP group for her efforts in helping me with my antimicrobial studies.

I extend my gratitude to all my colleagues, mentors and friends from Stellenbosch University. A big thank you to all the members of the Klumperman group, especially Lehani, Nusrat, Welmarie and Ingrid. Thank you for kindness and friendship over the years. Lehani, thank you for keeping me sane.I would also like to thank the support staff at Polymer Science: Erinda Cooper, Aneli Fourie, Deon Koen, Calvin Maart, Jim Motsweni and Mienie Jones.

The most special thanks to my family and loved ones for their constant encouragement and support. *Mamma en Pappa, dankie dat julle so baie opgegee het sodat ek myself kon bevorder*. To my partner, Driscoll, thank you for believing in me and pushing me to reach my goals.